

*Geology*  
GJBX-79-139

GJBX-139 '79

**AERIAL RADIOMETRIC AND MAGNETIC SURVEY**  
DICKINSON NATIONAL TOPOGRAPHIC MAP  
SOUTH DAKOTA

**CAUTION**

This is a time release report.  
Do not release any part of this  
publication before

---

PREPARED FOR THE U.S. DEPARTMENT OF ENERGY  
GRAND JUNCTION OFFICE  
GRAND JUNCTION, COLORADO  
UNDER BENDIX FIELD ENGINEERING CORPORATION SUBCONTRACT NO. 78-183-S

GEOLOGICAL SURVEY OF WYOMING

GEOLOGY



**Geodata International, Inc.**  
7035 JOHN W. CARPENTER FRWY.  
DALLAS, TEXAS 75247

**VOL. 1**

metadc958349

## LEGAL NOTICE

This report was prepared as an account of work sponsored by the United States Government. Neither the United States nor the United States Department of Energy, nor any of their employees, nor any of their contractors, subcontractors, or their employees, makes any warranty, express or implied, or assumes any legal liability or responsibility for the accuracy, completeness or usefulness of any information, apparatus, product or process disclosed, or represents that its use would not infringe privately owned rights.

AERIAL RADIOMETRIC AND MAGNETIC SURVEY  
DICKINSON NATIONAL TOPOGRAPHIC MAP  
NORTH DAKOTA

PREPARED FOR THE U.S. DEPARTMENT OF ENERGY

GRAND JUNCTION OFFICE  
GRAND JUNCTION, COLORADO

UNDER BENDIX FIELD ENGINEERING CORPORATION SUBCONTRACT NO. 78-183-S

GEODATA INTERNATIONAL, INC.  
7035 JOHN W. CARPENTER FREEWAY  
DALLAS, TEXAS 75247

## "DICKINSON NATIONAL TOPOGRAPHIC MAP SURVEY"

### ABSTRACT

The results of analyses of the airborne gamma radiation and total magnetic field survey flown for the region identified as the Dickinson National Topographic Map NL13-6 is presented in Volume I and II of this report. The airborne data gathered is reduced by ground computer facilities to yield profile plots of the basic uranium, thorium and potassium equivalent gamma radiation intensities, ratios of these intensities, aircraft altitude above the earth's surface, total gamma ray and earth's magnetic field intensity, correlated as a function of geologic units. The distribution of data within each geologic unit, for all surveyed map lines and tie lines, has been calculated and is included. Two sets of profiled data for each line are included with one set displaying the above-cited data. The second set includes only flight line magnetic field, temperature, pressure, altitude data plus magnetic field data as measured at a base station. A general description of the area, including descriptions of the various geologic units and the corresponding airborne data, is included also.

## TABLE OF CONTENTS

	<u>Page</u>
I. INTRODUCTION	1
A. General	1
1. Area Surveyed	1
2. Summary of the Location, Geology and Physiography of the Dickinson Map Sheet	1
B. Operational Program	4
II. GEODATA COMPUTER AIRBORNE SYSTEM	7
A. General	7
B. Flight Recovery Methods	12
C. Data Reduction	12
D. Data Presentation	17
E. Statistical Analysis Procedures	18
F. Other Corrections	19
III. GEOLOGY OF THE SURVEYED AREA	20
A. Location and General Physiography	20
B. Geology	20
C. Description of the Geologic Map Units	21
D. Radioactive Mineral Prospects in the Map Sheet Area	23
IV. RESULTS OF DATA ANALYSIS	25
A. Geologic Base Map	25
B. National Gamma Ray Map Series (NGRMS)	25
C. Radiometric Stacked Profile Data	25
D. Magnetic Stacked Profile Data	27
E. Magnetic Tapes and Listings	27
F. Statistical Presentation of Data by Geologic Type	27
G. Frequency Distributions of Data for Each Geologic Type	28
H. Microfiche Reproduction of Single Record and Averaged Record Listings	28
I. Altitude and Ground Speed Histograms	28
J. Data Interpretation	28
1. Analysis of the Histograms	28
2. Discussion of the Anomalies	39
3. Summary and Recommendations	45

(TABLE OF CONTENTS CONT'D.)

<u>APPENDIX</u>	<u>TITLE</u>	<u>PAGE</u>
I.	Frequency Distribution of Radiation Data as a Function of Geologic Unit	AI-1
II.	Description of Magnetic Tapes and Listings	AII-1
	A. Description of Magnetic Tapes	AII-1
	B. Description of Listings	AII-13
	Single Record Reduced Data Listings	AII-15
	Averaged Record Data Listings	AII-16
III.	Production Summary	

REFERENCES

LIST OF ILLUSTRATIONS

	<u>Page</u>
Figure 1. Index Map Showing Area Surveyed	2
Figure 2. Dickinson NTMS Indicating Flight Line Location	3
Figure 3. Data Flow Diagram	6
Figure 4. Douglas DC-3S	8
Figure 5. System Block Diagram	9
Figure 6. Geodata Computer Airborne System	10
Figure 7. Typical End-of-Flight Line Spectral Plot	11
Figure 8. Computer Presentation of Typical Map Line	13
Figure 9. Typical Map Line Showing Statistical Deviations	13
Table 1. Geologic Unit Average Value as a Function of Map Line for $^{208}\text{Tl}$	29
Table 2. Geologic Unit Average Value as a Function of Map Line for $^{214}\text{Bi}$	30
Table 3. Geologic Unit Average Value as a Function of Map Line for $^4\text{K}$	31
Table 4. Geologic Unit Average Value as a Function of Map Line $^{214}\text{Bi}/^{208}\text{Tl}$	32
Table 5. Geologic Unit Average Value as a Function of Map Line for $^{214}\text{Bi}/^4\text{K}$	33
Table 6. Geologic Unit Average Value as a Function of Map Line for $^{208}\text{Tl}/^4\text{K}$	34
Table 7. Mean ( $\bar{X}$ ) and Standard Deviation $\sigma$ for Each Geologic Type	35
Table 8. Radioactivity Histograms for Geologic Map Units with Non-Unimodal Form. Recommended Splits for Histograms based on $^{208}\text{Tl}$ data.	36
Table 9. Radioactivity Anomalies Listed by Flight Line and Geologic Map Dickinson Map Sheet.	40
Table 10. Radioactivity Anomalies Occurring in the Geologic Map Units of the Dickinson Map Sheet.	41

(List of Illustrations Cont'd.)

Page

Table 11.	Statistical Summary of Radioactivity Anomalies	42
Table AIII-1	Test Line Results	AIII-2
Table AIII-2	Average Speed and Altitude Determined from Data of Appendix II	AIII-3
Table AIII-3	Diurnal Corrections to Map Line Data	AIII-4



SECTION I.  
INTRODUCTION

A. GENERAL

1. Area Surveyed

Geodata International, Inc., Dallas, Texas, conducted an airborne gamma ray and total magnetic field survey of an area in North Dakota defined by the Dickinson National Topographic Map Sheet as outlined on Figure 1. This survey was performed from a fixed-wing aircraft, using a computer-controlled, large-volume radiation detector system to detect the upward emanating gamma radiation flux from the surface materials. Each map line was flown in an east-west direction with line lengths of 97 miles; each tie line was flown in a north-south direction with line lengths of 69.0 miles. Map lines and tie lines are located as shown in Figure 2.

The Dickinson NTMS report is separated into two volumes; Volume I giving the description of the program and results, and Volume II presenting the flight line profile data and statistical analysis results.

2. Summary of the Location, Geology and Physiography of the Dickinson Map Sheet

The area represented by the Dickinson Quadrangle is located in southwestern North Dakota and is bounded by latitudes  $46^{\circ}$  to  $47^{\circ}$  north and longitudes  $102^{\circ}$  to  $104^{\circ}$  west. The area is located north of the Black Hills in the unglaciated portion of the Missouri Plateau section of the Great Plains Province.

The geology and geological structures of the area are relatively simple. The western portion of the area has a dominant northwest-trending fold belt. The northcentral portion has a dominant northeast-trending fold belt. The exposed rocks in the area range from upper Cretaceous to recent sediments. The Cretaceous strata were involved in the Laramide Orogeny and were laid down in the intervening basin resulting from the gradual raising of the Rocky Mountains to the west. Cenozoic times saw several periods of regional uplift, erosion and volcanic activity. Quaternary units are represented as thin deposits along streams.

The upper Cretaceous, Paleocene and Eocene formations contain uranium-bearing lignites. The most extensive and highest grade lignites occur in the Tongue River member of the Paleocene Fort Union Formation. The Oligocene and Miocene tuffaceous formations are considered to be source rocks for the uranium.

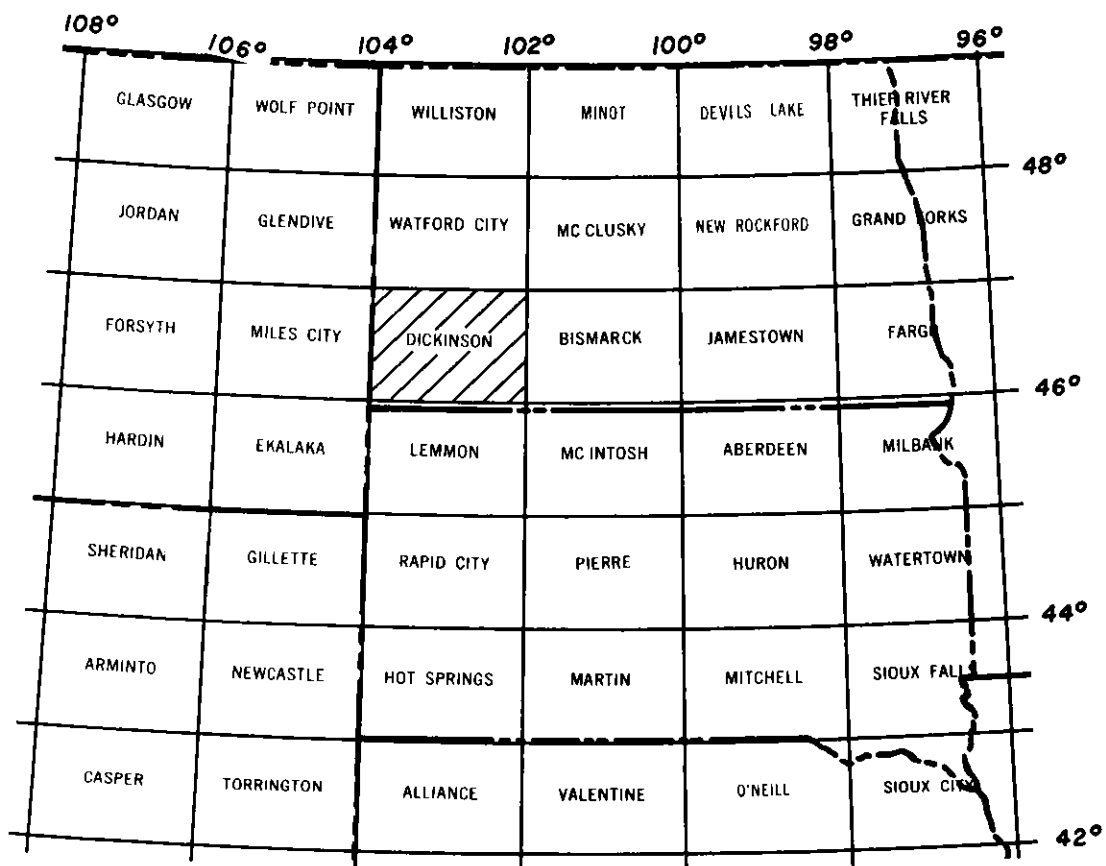


Fig. 1. Index Map Showing Area Surveyed

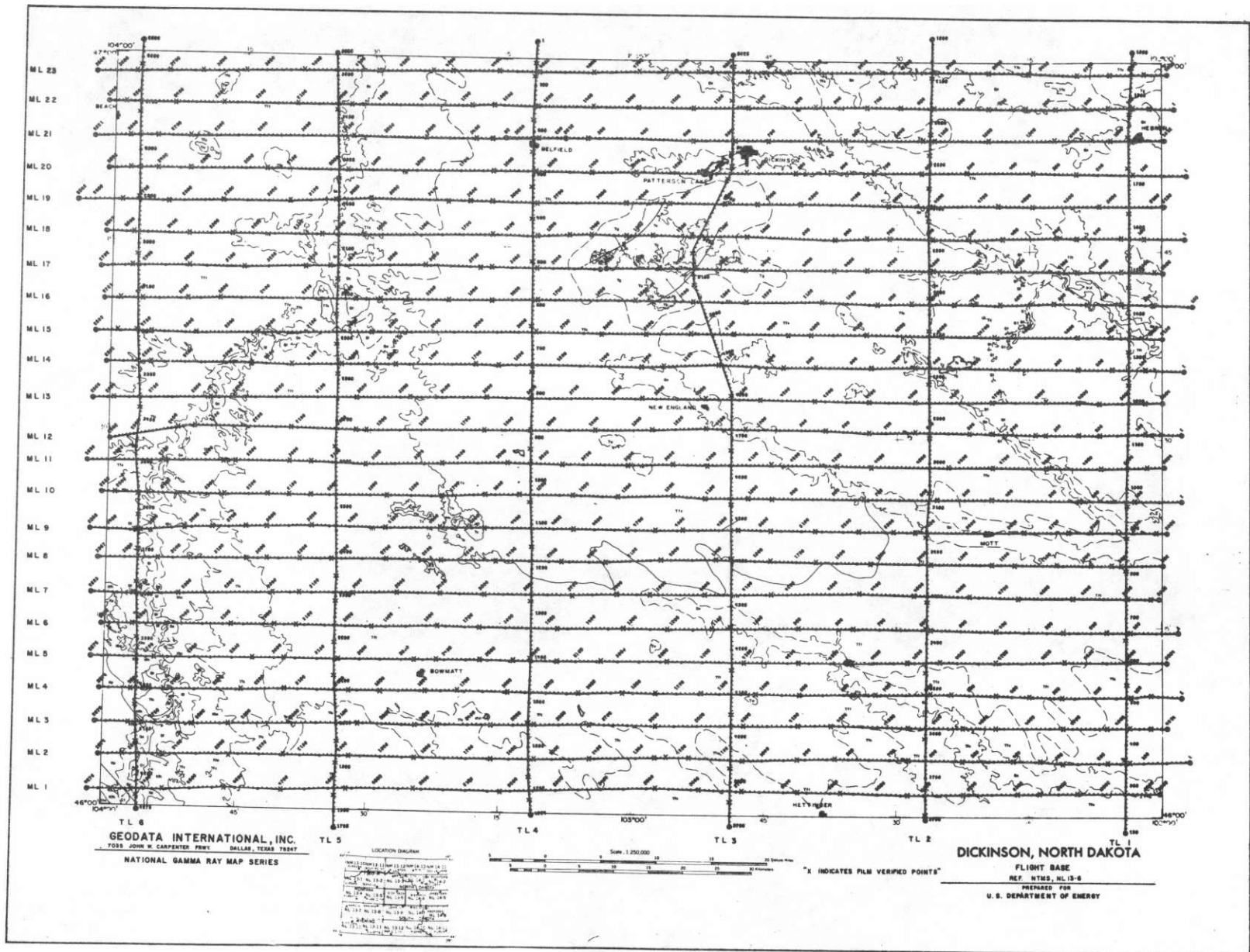


Fig. 2. NTMS Indicating Flight Line Location

## B. OPERATIONAL PROGRAM

The airborne data gathered were reduced using ground-based computer facilities to give the basic uranium, thorium and potassium equivalent gamma radiation intensities, ratios of these intensities, aircraft altitude above the earth's surface, total gamma ray and earth's magnetic field intensity, correlated as a function of geologic units indicated from the developed geologic map. Results of analyses of these field data are presented as profile plots of the gamma radiation and earth's magnetic field. The surveyed area of Figure 1, which indicates latitude/longitude position, has been based according to the National Topographic Map Series (NTMS) which covers the United States with 1<sup>0</sup> latitude/2<sup>0</sup> longitude sheets. The topographic maps have a scale of approximately 1 inch = 4 miles. Each final base map is an overlay of the NTMS base map from which certain geographic data have been transposed, and includes the available geologic data. Each final anomaly map has the surveyed flight lines superpositioned with the standard deviations of each fifth data point relative to the average value within each geologic unit as determined for each NTMS map. These anomaly maps are identified as National Gamma Ray Map Series maps (NGRMS).

Computer profile plots of the gamma radiation and magnetic data have been created for all surveyed map lines and tie lines. Each line has indicated on the profiled line the location of each geologic type as a function of record number. The distribution of data within each geologic unit has been calculated and is included. The scale of the profile data in this final report is 1:500,000 and the scale of the NGRMS is both 1:250,000 and 1:500,000. Volume II of the final report containing the 1:500,000 profile data also contains the flight line map, geologic base of the pertinent NTMS and the NGRMS maps indicating the standard deviations at the scale of 1:500,000. Two sets of profiled data for each line flown are included with the first set displaying magnetic field, gamma radiation and other data. The second set includes only magnetic field, temperature, pressure, altitude data, and magnetic field data as measured at a base station. Each set contains the flight line location relative to the geologic map. All data have been located giving latitude and longitude positions in fractional degrees as made possible from visual spotting, photographic recording of the aircraft location, and from doppler navigation guidance of the aircraft and recording of location each second on magnetic tape. Data have been acquired and processed according to the data flow shown in Figure 3.

The magnetic data tapes containing (1) raw data, (2) the single record reduced data, (3) the statistical analysis data, and (4) the magnetic field data, are converted to the EBCDIC format and retained for filing within the USDOE permanent data bank.

The final report includes a general geologic description of the area, including descriptions of the various geologic units and correlates the airborne data to the geologic units as provided by the geologic maps. Also included is a frequency distribution study of the data as a function of the geologic units encountered over the NTMS area including the tie line data.

This report also contains a discussion of the area surveyed, and includes all single record reduced data and averaged record data listings on MICROFICHE.

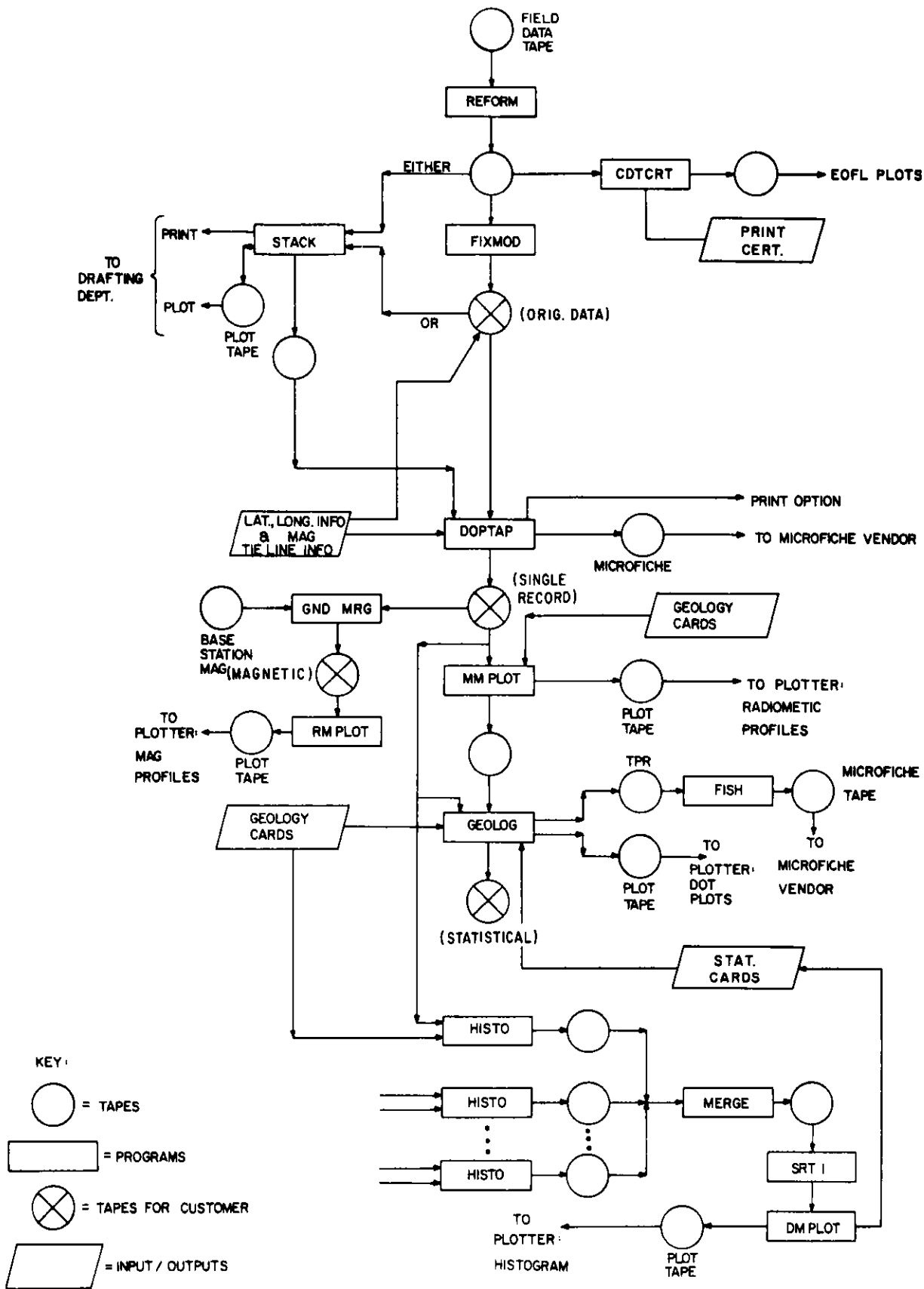


FIGURE 3. DATA FLOW DIAGRAM

## SECTION II

### GEODATA COMPUTER AIRBORNE SYSTEM

#### A. GENERAL

The Geodata Computer Airborne System (GCAS) is mounted in a Douglas Super DC-3 shown in Figure 4. The functional block diagram is shown in Figure 5 and the airborne system is presented in Figure 6. Nine (9) 11½" dia. by 4" thick NaI(Tl) detectors are used to measure the spectral gamma ray intensity at an aircraft elevation of about 400 feet above the earth's surface. Eight (8) of these nine (9) detectors are positioned to measure the gamma rays from the earth's surface (from  $4\pi$  solid angle). The ninth detector is mounted, partially shielded, to monitor  $^{214}\text{Bi}$  radiation incoming from the upper  $2\pi$  solid angle.

Each detector has a volume of 415.5 cubic inches. Eight detectors give a total volume for measurement of  $4\pi$  solid angle data of 3324 cubic inches, or a  $V/v = 23.7$  at an aircraft speed of 140 mph ( $V =$  detector volume, in.<sup>3</sup>;  $v =$  aircraft speed, mph).

The system block diagram of Figure 5 shows the control center of the system to be the NOVA computer. The 8-detector data are accumulated for each one-second data integration period in a manner giving no dead-time for read-out onto magnetic tapes. Two magnetic tape recorders are used, one recording total spectral data and computer results (LDT), and the other only the computer results (CDT). Digital-to-analog conversion of the resultant intensities, their ratios and magnetic data are plotted onto multitrack paper as data are gathered allowing immediate examination for anomalous data. A third section of the computer core gathers spectral radiation data and continues to sum each second's data until the end of the flight line (EOFL), Figure 7. The spectral data from the single detector are accumulated each 9 seconds. The computer uses data from the shielded detector to determine the concentration of the atmospheric  $^{214}\text{Bi}$  which allows calculation of the surface-emanated  $^{214}\text{Bi}$  values before altitude corrections. The computer then corrects all data to a constant aircraft altitude above the surface of 400 feet. A highly accurate radar altimeter, the Collins ALT-50 system, makes 8 measurements/second and gives from the computer the average of these eight readings. Automatic digital gain calibration of the 8-detector and 1-detector system is accomplished by stabilizing on the  $^{40}\text{K}$  photopeak data.

A proton precession magnetometer having a 0.25 gamma readout resolution and less than a 1.0 gamma noise envelope is also sampled once per second providing a measurement of the total intensity of the earth's magnetic field. The sensor is carried as a "bird" on a 100 feet cable to minimize the magnetic effects of the aircraft, (Figure 4). Digitizing of doppler navigation cross-track and along-track analog data allows position information to be recorded each second. This Bendix DRA - 12C system has a  $\pm 100$ th/nautical mile accuracy. A permanent record of flight location is also made using 35mm film which records a continuous recoverable track with 20% overlap/frame at an elevation of 400 feet. Any two 6-digit numbers are displayed during flight; one allows the navigator to observe the record

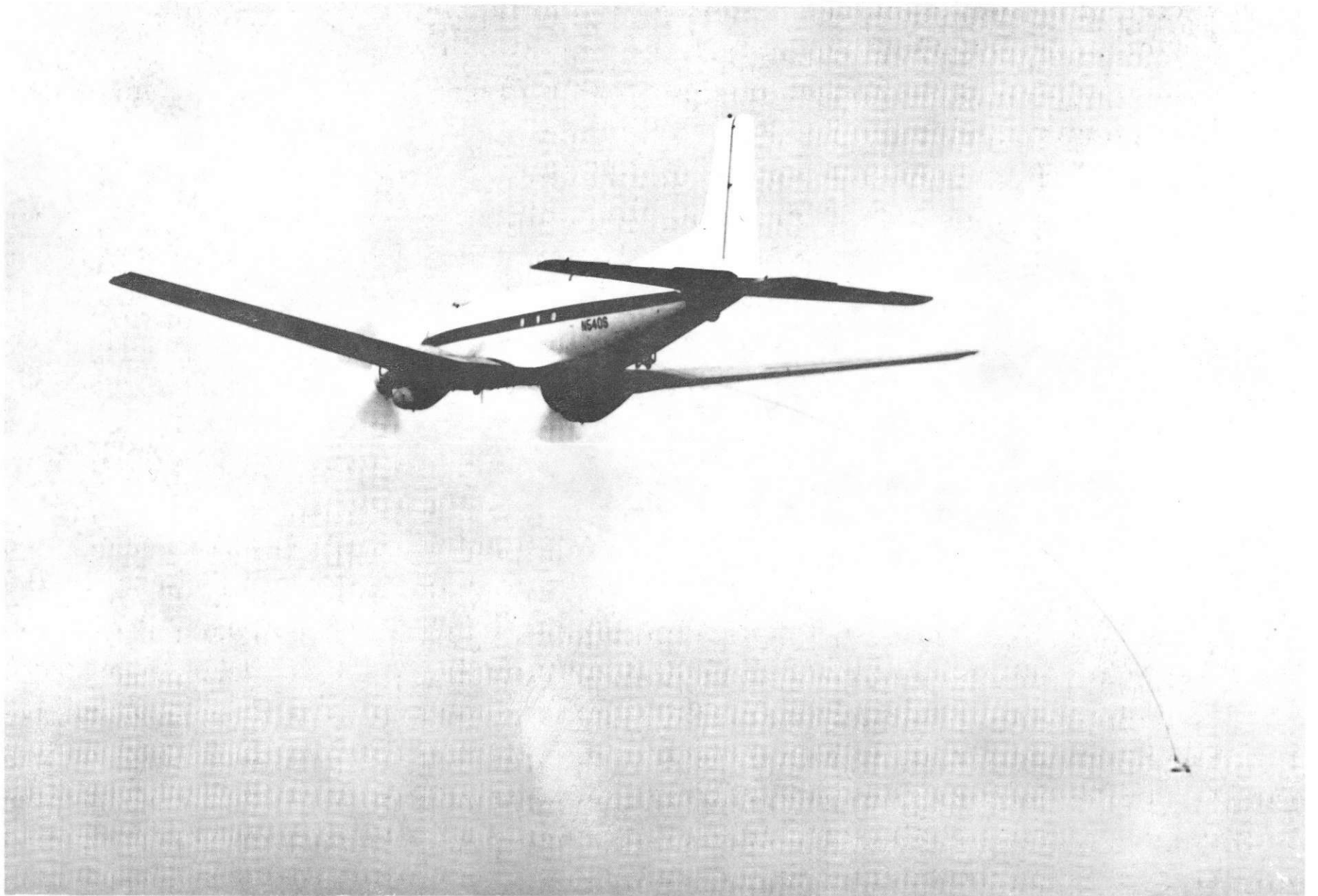


Figure 4. Douglas DC-3S



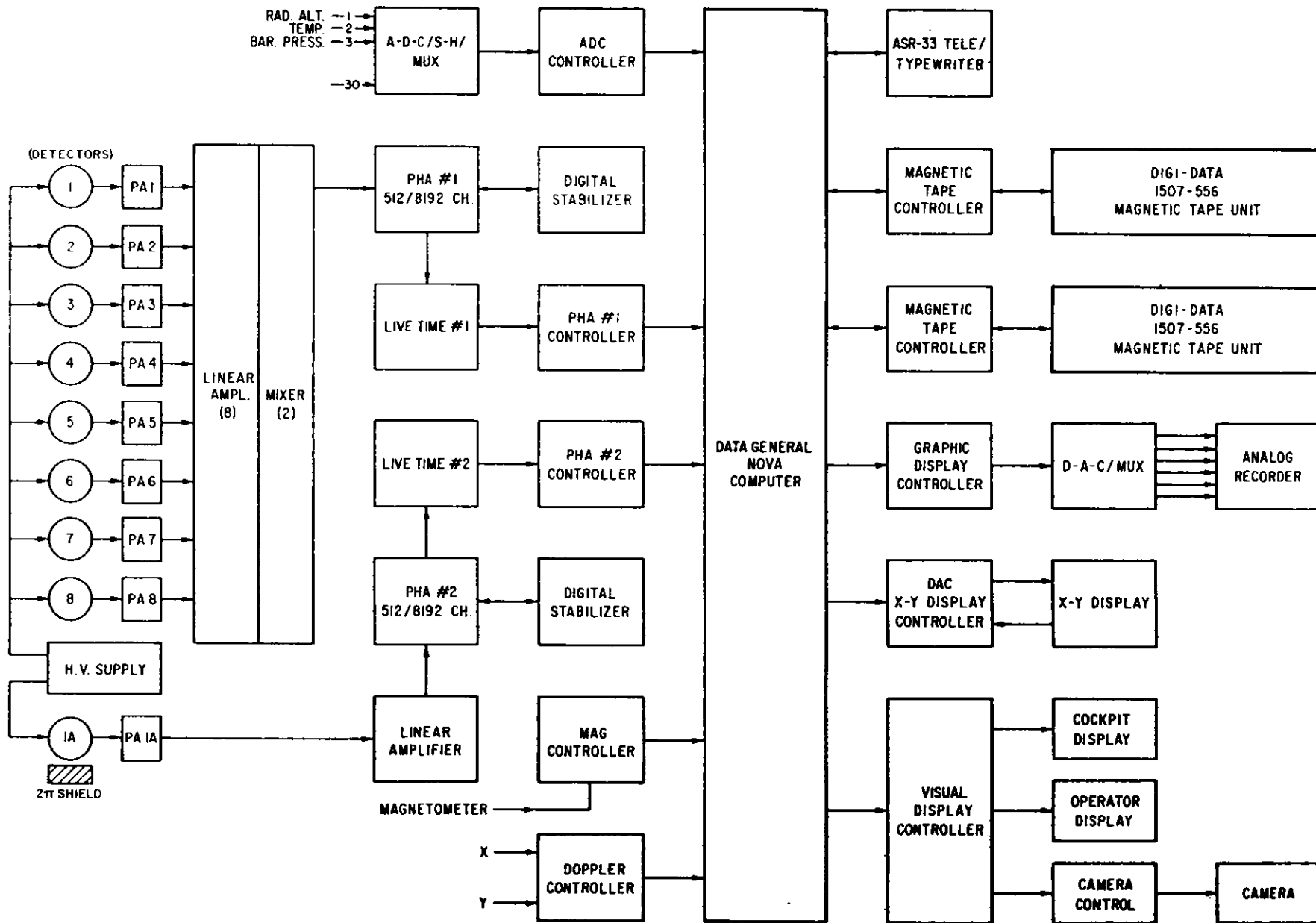


Figure 5. - System Block Diagram

(TABLE 9. Cont'd.)

	$^{214}\text{Bi}$	$^{208}\text{Tl}$	$^{214}\text{Bi}/^{208}\text{Tl}$
TL5	Tfc, 1945-1955, Tft, 2215-2225, 2260-2275	Tft, 2200-2215, 2250-2265, 2270-2285, 2305-2365, 2475-2490, 2500-2520, 2610-2630, 2715-2745, 2755-2760, 2830-2840; Qa, 2850-2875, 2905-2915, 3050-3065; Qt, 3065-3105; Qa, 3200-3210	Tfc, 1910-1915, 1950-1975; Qa(2760-2770), (2810-2820) (3230-3250)
TL6		Qa, 4250-4235, 4125-4105; Kfh(4060-4050), (3975-3965) Kfh, 4065-4040; Tft, 3265-3235; 3135-3120, 3095-3080, 3015-3005, 2960-2935, 2885-2870, 2760-2745, 2715-2700	Khc(3875-3865); Tft(3070-3050), (2960-2940), (2810-2785), (2680-2665)

(....) denotes negative anomaly

TABLE 10. Radioactivity etc.

Geologic Unit	Number	%	Number	%	Number	%	Number	%
<u>Quaternary</u>								
Qa	12	9.0	11	6.2	14	12.8	(10)	(15.6)
Qt	0	0	3	1.7	1	0.9	(1)	(1.6)
<u>Tertiary</u>								
Tw	0	0	1	0.6	0	0	(0)	(0)
Tb	0	0	1	0.6	0	0	(1)	(1.6)
Tc	1	0.8	0	0	1	0.9	(3)	(1.6)
Tg	6	4.5	5	2.8	2	1.8	(1)	(6)
Tfs	44	33.1	62	35.0	34	31.2	(5)	(7.8)
Tft	41	30.8	66	37.3	30	27.5	(23)	(35.9)
Tfc	21	15.8	23	13.0	21	19.3	(16)	(25.0)
<u>Mesozic</u>								
Khc	6	4.5	3	1.7	3	2.8	(2)	(1.2)
Kfh	1	0.8	1	0.6	3	2.8	(2)	(0)
Kp	1	0.8	1	0.6	0	0	(0)	(0)
Total	133	100.1	177	100.1	109	100.0	(64)	(100.0)

\* ML-17, ML-8, WA and anomalies near towns omitted from this table.

(....) denotes negative anomaly

TABLE 11. Statical Summary of Radioactivity Anomalies

<u>Total Samples</u>	$^{214}\text{Bi}$	$^{208}\text{Tl}$	$^{214}\text{Bi}/$	$^{208}\text{Tl}$
Number of Anomalies	133	177	109	(64)
Number of Geologic Units	9	11*	9	(9)
<u>Quaternary Samples</u>				
Number of Anomalies	12	11	14	(10)
Number of Geologic Units	1	2	2	(2)
<u>Tertiary Samples</u>				
Number of Anomalies	113	158	88	(49)
Number of Geologic Units	5	6*	5	(6)
<u>Mesozic Samples</u>				
Number of Anomalies	8	5	6	(4)
Number of Geologic Units	3	3	2	(2)

\* The unit TW belongs to either Tb or Tc.

(....) denotes negative anomaly

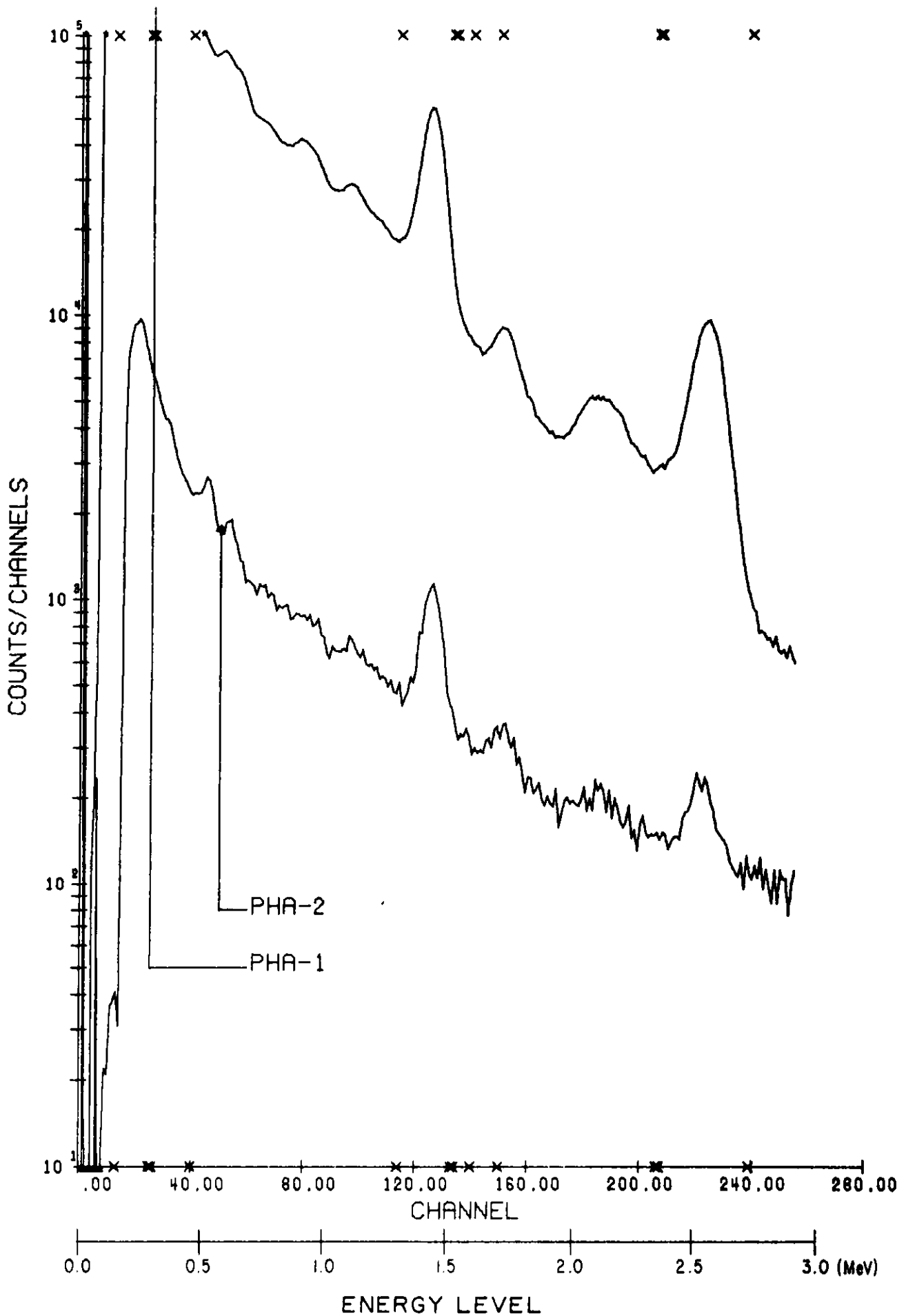


Figure 7. Typical End-of-Flight Line Spectral Plot

number-of-the-day along the flight line and the second allows the GCAS operator to observe any computer number desired.

The attenuation of gamma radiation is calculated using equations accounting for air density and uses experimentally-determined values for attenuation coefficients. The energy region from 3-6 MeV is used to allow cosmic events to be removed from the data in the energy range 0-3 MeV. Energy resolution from the  $^{137}\text{Cs}$  662.0 KeV photopeak was 9.0% or better for each detector.

The GCAS equipment has 3 basic operating modes: (1) CALIBRATE, which allows proper gain calibration of the radiation detectors to be set; (2) OPERATE, which allows data to be received, reduced and recorded, and (3) PLAYBACK, which allows the operator to examine the newly acquired data.

## B. FLIGHT RECOVERY METHODS

Doppler navigation system data have been used to locate the flight line positions. These doppler lines have been positioned and verified by many locations determined by photography and/or navigator visual position location as a function of displayed record numbers. These data are computer plotted giving the flight path as a line of dots, each dot representing every fifth record locations, and each "circle" represents every 50th record location. Figure 8 indicates the computer plot of a typical map line. These data are then transferred to form the flight line base shown in Figure 2. Location points used to position the flight line at least every 10 miles are shown on the flight line map as an "X" through each point.

## C. DATA REDUCTION

The processing flow chart representative of the work performed for this survey is shown in Figure 3. The original field data tapes contain the various tag words,  $4\pi$  spectral and  $2\pi$  spectral data for each one second along the flight line. The REFORM program sums the proper energy intervals of the spectra for each second and produces a trailer record for each line which contains the accumulated  $4\pi$  and  $2\pi$  spectra for the line. The CDTCRT is a data certification program which is run immediately upon receipt of the field data tapes and produces the EOFL spectral plots, Figure 7. The program identification and function is given below:

<u>PROGRAM</u>	<u>FUNCTION</u>
REFORM	Produce energy group sums and EOFL spectra
FIXMOD	Primary processing for matrix reduction, BIAIR computation, live times, background and altitude correction.
STACK	Flight path recovery to produce plots of actual paths at a scale of 1:250,000
DOPTAP	Single record processing with latitude/longitude, IGRF and single point statistical adequacy computation. Produces microfiche.
MMPLT	Averaged record processing with averaged statistical adequacy computation. Produces radiometric stacked profiles plot tapes.

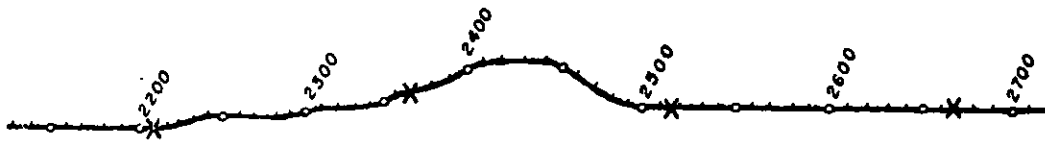


Figure 8. Computer Presentation of Typical Map Line

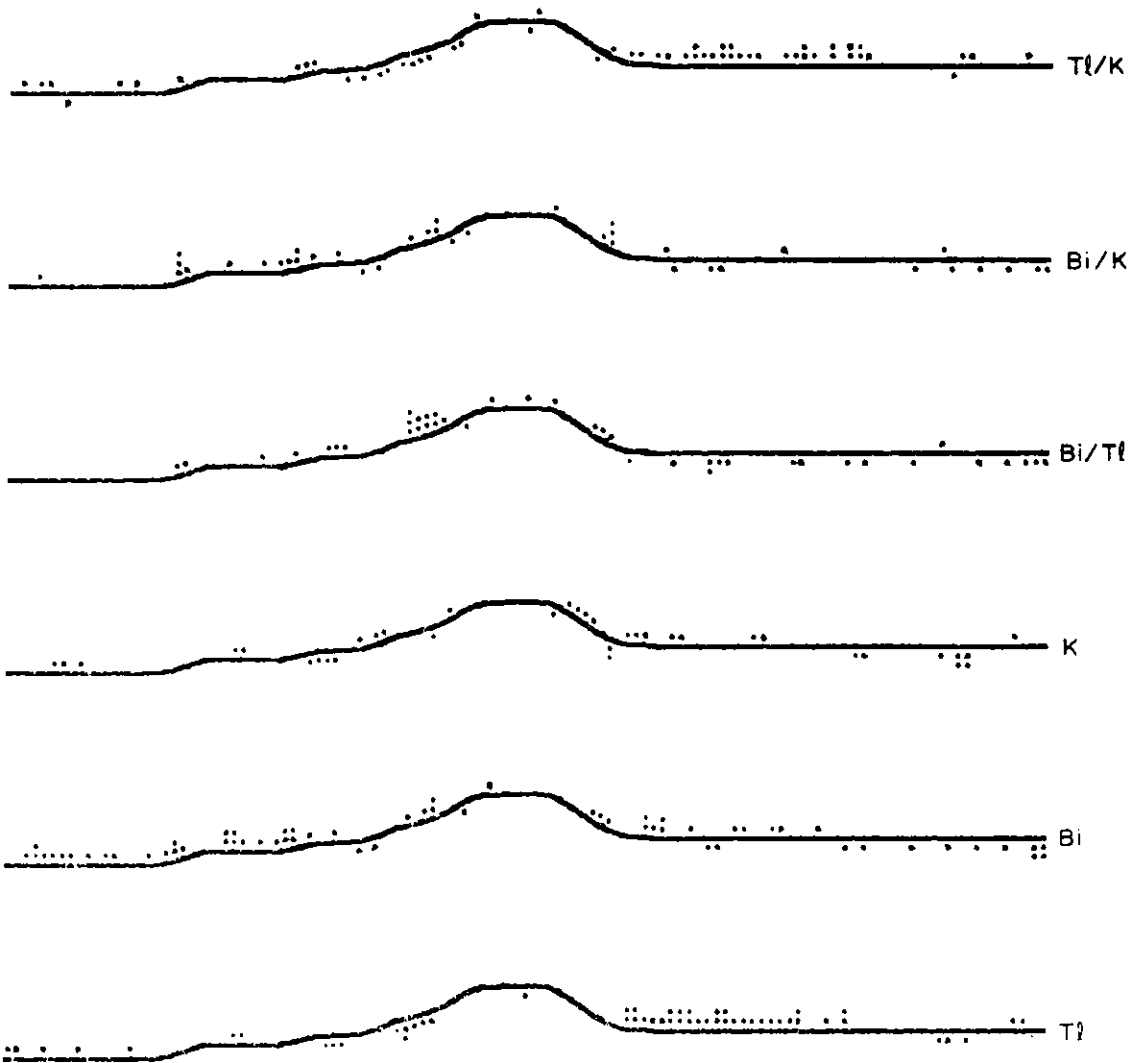


Figure 9. Typical Map Line Showing Statistical Deviations

GNDMRG Merges aircraft magnetometer and ground magnetometer in proper time sequence and transfers temperature, pressure and altitude information

RMPLT Produces tapes for magnetometer stacked profile plots

GEOLOG Produces averaged value microfiche with geology and plot tape for standard deviation "dot plots" related to geologic type

HISTO,MERGE and SRT1 Programs preliminary to obtaining the histograms as a function of geologic type for the entire area

DMPLOT Produces plot tape for the area histograms

As stated in the above list of program functions, the FIXMOD program performs the primary processes for determining the reported eTh, eU and K counting rate associated with the earth's surface as measured at 400 feet above the surface. For this reason, the analytical work of this program is described in more detail below.

Each one second of  $4\pi$  spectral data is summed by the REFORM program according to the following energy intervals:

Cosmic:	3.0	MeV and greater
$^{208}\text{Tl}$ photopeak:	2.410	to 2.796 MeV
$^{214}\text{Bi}$ photopeak:	1.05	to 1.322 plus 1.638 to 2.410 MeV
$^4\text{K}$ photopeak:	1.322	to 1.638 MeV

In general, these raw sums contain counts not only from ground sources, but also from aircraft background and atmospheric radioactivity. To determine the counts in the energy intervals which are caused only by the isotope associated with the interval, a  $4 \times 4$  matrix method is used. This matrix may be formed through the use of a standard cosmic spectrum, plus the Grand Junction Test Pad determinations of  $\alpha$ ,  $\beta$ ,  $\gamma$ , f and g, or from four standard spectra representing respectively cosmic, thorium, uranium and potassium pure spectra at a 400 foot altitude.

This matrix multiplication is represented by:

$$\begin{bmatrix} A_{11} & A_{12} & A_{13} & A_{14} \\ A_{21} & A_{22} & A_{23} & A_{24} \\ A_{31} & A_{32} & A_{33} & A_{34} \\ A_{41} & A_{42} & A_{43} & A_{44} \end{bmatrix} \cdot \begin{bmatrix} \text{COS} \\ \text{TL} \\ \text{BI} \\ \text{K} \end{bmatrix} = \begin{bmatrix} \text{MCOS} \\ \text{MTL} \\ \text{MBI} \\ \text{MK} \end{bmatrix}$$



where the  $A_{ij}$  are the elements of the  $4 \times 4$  matrix; the column matrix on the left represents the four raw data sums and the column matrix on the right is the counts in each energy interval caused only by the indicated isotope. These matrix result counts are for the measured live time. To obtain the counts per second, it is necessary to divide by the live time, LTC1, thus:

$$\begin{aligned} \text{MCOS/LTC1} &= \text{COS1} \\ \text{MTL/LTC1} &= \text{TL1} \\ \text{MBI/LTC1} &= \text{BI1} \\ \text{MK/LTC1} &= \text{K1} \end{aligned}$$

The TL1, BI1 and K1 counts per second contain the aircraft associated backgrounds caused by thorium, uranium and  $^4\text{K}$ . Geodata has determined these backgrounds for this installation to be 6.83 counts per second in the  $^{208}\text{Tl}$  energy interval due to background  $^{208}\text{Tl}$ , 6.60 counts per second in the  $^{214}\text{Bi}$  energy intervals due to background  $^{214}\text{Bi}$  and 28.30 counts per second in the  $^4\text{K}$  interval due to background  $^4\text{K}$ . For this work, the background counting rates were determined by high altitude flights free from atmospheric  $^{214}\text{Bi}$ . The backgrounds are checked during the survey by observing counting rates over large water bodies under the flight path.

These backgrounds are subtracted from the above determined count rate values

$$\overline{\text{TL1}} = \text{TL1} - 6.83$$

$$\overline{\text{BI1}} = \text{BI1} - 6.60$$

$$\overline{\text{K1}} = \text{K1} - 28.30$$

The  $\overline{\text{BI1}}$  value contains counts caused by atmospheric  $^{214}\text{Bi}$  which must be subtracted before altitude correction is applied. The  $2\pi$  crystal data are used to determine the magnitude of the count to be subtracted. Since the predominant variable source affecting the  $2\pi$  crystal is the atmospheric  $^{214}\text{Bi}$ , it is possible to utilize most of the spectrum in the BIAIR determination, and thereby produce some improvement in the statistical error. The energy range used for the  $2\pi$  crystal is from 1.05 to 2.79 MeV. Within this range the aircraft background has been determined as 8.22 counts per second and the  $4\pi$  cosmic count greater than 3.0 MeV must be multiplied by .1967 to determine the cosmic count in the 1.05 to 2.79 MeV range for the  $2\pi$  system.

The atmospheric  $^{214}\text{Bi}$  (BIAIR) associated with the unshielded detector array is determined using the shielded detector by the relation:

$$\text{BIAIR} = \frac{G(X) \cdot \left[ \text{VC} - .1967 \text{COS1} - 8.22 - (k_1(h)\overline{\text{TL1}}) \right]}{(1 - k_2 G(X))}$$

where:  $G(X)$  is the relationship between the  $4\pi$  and  $2\pi$  detector measurement solid angle and the column change of the detector arrays.

VC is the total count,  $2\pi$ , ch (91-239), c/s; COS 1 is the  $4\pi$  cosmic count, greater than 3.0 MeV c/s;  $k_1, k_2$ , are constant factors correcting for the penetration/spill of the surface emanated radiation.

$\overline{T}_{21}, \overline{BII}, \overline{KI}$  are results of data reduction,  $4\pi$ , c/s

The final  $^{214}\text{Bi}$  counting rate caused by surface sources is then

$$\text{BISUR} = \overline{BII} - \text{BIAIR}$$

The quantities  $\overline{T}_{21}, \text{BISUR}$  and  $\overline{KI}$  are then corrected to an equivalent counting rate at 400 feet through the equations indicated below:

$$\text{TLS} = \overline{T}_{21} \cdot e^{-\mu_1(400 - \frac{\rho}{\rho_0} x)}$$

$$\text{BIS} = \text{BISUR} \cdot e^{-\mu_2(400 - \frac{\rho}{\rho_0} x)}$$

$$\text{KS} = \overline{KI} \cdot e^{-\mu_3(400 - \frac{\rho}{\rho_0} x)}$$

$$\text{TC (total count)} = (\overline{TC} - 337 - S \cdot \text{BIAIR}) e^{-\mu_4(400 - \frac{\rho}{\rho_0} x)}$$

where  $\overline{TC}$  = live time corrected total count, channel 35 → 239, and  
 $S = 17.5$ , the ratio of Bi spectral data, region channel 35 → 239/  
 channel 143 → 159

where:

TLS, BIS, KS = respective counting rates at 400 feet caused by surface sources

$\rho_0$  = air density at standard temperature and pressure

$\rho$  = air density

$\mu_1, \mu_2, \mu_3, \mu_4$  = respective linear attenuation coefficients

$x$  = aircraft height above the surface in feet

Following data reduction, average values for each radiation variable and variable ratios are plotted for each flight line to demonstrate the consistency of average values and that a smooth flow of results continues from day to day and from start to finish of each day. Quality control on the eU (BIAIR) in the atmosphere is also monitored through examination of data acquired over water with the requirement being that near-zero intensities should exist.

Each profile has a latitude or longitude degree line to give accurate surface location of all data.

Diurnal variations of the magnetic field base station intensity are measured and applied to the field data. Any heading errors have previously been removed from all data. The magnetic field data are then IGRF corrected to give the residual magnetic field.

#### D. DATA PRESENTATION

The surveyed area was positioned geographically to completely cover the specific National Topographic Map. Each topographic map has been used as the flight base and sufficient geographical and 15' location information has been shown. The flight line pattern has been superpositioned onto these created base maps where the standard deviation levels for each independent variable and each ratio of these variables have been plotted (NGRMS) based on the data contained within the total map area. Every fifth data point along each map line has its standard deviation value shown at the location of that value. Therefore, there are six NGRMS sheets which indicate the location and magnitude of anomalous data, Figure 9.

The multivariable map line profile, which represents all variables as a function of their latitude and longitude location for each line, is presented at a scale of 1:500,000. Each profile presents:

1. Aircraft altitude above the surface
2. eTh ( $^{208}\text{Tl}$  from  $^{232}\text{Th}$  decay series)
3. eU ( $^{214}\text{Bi}$  from  $^{238}\text{U}$  decay series)
4. K ( $^4\text{K}$  from natural potassium)
5. BIAIR (atmospheric  $^{214}\text{Bi}$ )
6. Residual magnetic field
7. Gross count (greater than 400 keV)
8. eU/eTh ( $^{214}\text{Bi}/^{208}\text{Tl}$ ) ratio
9. eU/K ( $^{214}\text{Bi}/^4\text{K}$ ) ratio
10. eTh/K ( $^{208}\text{Tl}/^4\text{K}$ ) ratio
11. Geologic data including aircraft flight path

The residual magnetic field map line profile, which represents five variables as a function of their latitude and longitude location for each line, plus geologic data at a scale of 1:500,000 is presented as:

1. Aircraft altitude
2. Atmospheric temperature
3. Atmospheric pressure
4. Residual magnetic field data
5. Magnetic field base line station data
6. Geological data including aircraft flight path

The output of these various computations supplies, beyond two profile sets, the following data:

- o Histograms of the radiation data distribution within each geologic unit.
- o Histograms of the average velocity distribution for each one-second record for each map and tie line.
- o Histograms of the average altitude distribution for each one-second record for each map and tie line.
- o Tables giving the average radiation concentration of each geologic unit for each flight line.
- o Average radiation concentration for each variable as a function of flight line, including the atmospheric  $^{214}\text{Bi}$ .
- o Set of maps showing the standard deviation data as a function of location and radiation variable.

These types of presentation will be explained in this report.

#### E. STATISTICAL ANALYSIS PROCEDURES

It is necessary to exclude from the statistical analysis all variables which have too low a counting rate to be statistically valid, and data which were obtained at altitudes above 1000 feet. To this end, a statistical adequacy test was run on all data for each data record. If a given value of  $T_{\ell}$ ,  $B_i$  or  $K$  failed the test, that variable value and any ratio value associated with it were not used in the statistical determinations of mean and standard deviation values. In addition, such values are indicated on the radiometric profiles by a vertical (tic) mark along the base line for the variable, and are flagged in the single record and averaged record listings (microfiche). The ratio values are set to zero in the Radiometric Profile Plots. The flags in the listings appear under the heading AKUT for altitude,  $^{40}\text{K}$ ,  $^{214}\text{Bi}$  and  $^{208}\text{Tl}$  respectively. The flags are zero for statistically valid data and one for rejected data in the case of  $K$ ,  $U$  and  $T$ . For altitude ( $A$ ) a zero indicates altitudes to 700 feet; a one (1) indicates altitudes between 700 and 1000 feet, and a two (2) indicates altitudes above 1000 feet.

The tests used to reject data were as follows:

$$(1) \quad \overline{T_{\ell}I} < 1.5 \sqrt{T_{\ell w} - \overline{T_{\ell}I}} = 1.5 \sigma T$$

$$(2) \quad \text{BISUR} < 1.5 \sqrt{B_{iw} - \text{BISUR}} = 1.5 \sigma B$$

$$(3) \quad \overline{KI} < 1.5 \sqrt{K_w - \overline{KI}} = 1.5 \sigma K$$

where the "w" subscript refers to the respective window counting rates from the raw data and  $\overline{T_{\ell}I}$ , BISUR and  $\overline{KI}$  have previously been defined. If any of the above inequalities were true, the associated variable was flagged and that value was rejected in all statistical determinations.

The values of the radicals in the above equations which are indicated as  $\sigma_T$ ,  $\sigma_B$ ,  $\sigma_K$  and the barred values were calculated on the basis of a single record value for determining flags in the single record listings and on the basis of the 7-point weighted values for determining flags in the averaged records listings.

The mean value and standard deviations were calculated assuming the data to have a normal distribution within a geologic type. The equation used in determining the variance is:

$$\sigma^2 = \frac{1}{N-1} \left[ \sum_{i=1}^N x_i^2 - N\bar{x}^2 \right]$$

where N is the number of statistically valid samples for a given geologic type,  $x_i$  is the value of the variable for sample number i, and  $\bar{x}$  is the mean value of the variable for the geologic type. Values from the entire survey of the area are used in these computations.

#### F. OTHER CORRECTIONS

The magnetic heading correction for aircraft and equipment used in this survey were determined by flying a predetermined path at the survey altitude in first an east to west direction, then in a west to east direction. The same procedure is used on a north-south path. Based on these data, the heading corrections are:

West to east travel: +3.56 gammas  
 East to west travel: -3.56 gammas  
 North to south travel: -1.0 gammas  
 South to north travel: +1.0 gammas

Lake Mead data reduction give the following altitude relationships:

$$T_{\theta S} = 182 e^{-.002019x}$$

$$B_{iS} = 71 e^{-.002161x}$$

$$KS = 810 e^{-.002719x}$$

$$TC = \bar{TC} e^{-.00194x}$$

where x represents the aircraft altitude above the surface corrected to one atmosphere pressure at 0°C.

The system sensitivities at 400 feet for DC-3S N540S are:

$$S_{T_{\theta}} = 7.02 \text{ c/s/ppm eTh}$$

$$S_{B_i} = 11.33 \text{ c/s/ppm eU (narrow window)}$$

$$S_K = 107.91 \text{ c/s/percent K (narrow window)}$$

## SECTION III.

### GEOLOGY OF THE SURVEYED AREA

#### A. LOCATION AND GENERAL PHYSIOGRAPHY

An aerial radiometric survey was conducted over an area depicted by the Dickinson Quadrangle on a scale of 1:250,000 (N.T.M.S.). The surveyed area is located in southwestern North Dakota, and is bounded by latitudes 46° to 47° north and longitudes 102° to 104° west (Denson, et al, 1959). The area includes all of Hettinger and Stark counties, the major portions of Bowman and Adams counties, and the southern half of Golden Valley and Billings. It also includes a very small portion of the southernmost part of Dunn and Mercer, and a small part of the western portion of Morton and Grant Counties.

The area is located north of the Black Hills in the unglaciated portion of the Missouri Plateau section of the Great Plains Province (Fenneman, 1946). The rolling prairie is broken by small areas of badlands and by many steep-walled buttes and mesas; notably Medicine Pole Hills, Sentinel Buttes, Buillion Butte, H.T. Butte, Chalky Buttes and Rainy Buttes (Moore, et al, 1959). The regional drainage pattern is generally easterly, except in the far western portion of the quadrangle where the Little Missouri River flows from south to north (Denson, et al, 1959). The buttes stand 300-500 feet above the surrounding country. Low sandy hills and broad sandy flats border the rivers.

#### B. GEOLOGY

The area lies north of the Black Hills uplift in the south-central portion of the Williston Basin. The western portion of the area has a dominant northwest-trending fold belt typified by the Cedar Creek anticline. The northcentral portion of the area has a northeast-trending structure which may be influenced by orogenic folding to the north as typified by the Nesson anticline (Collier, 1918). In general, the strike of the rocks is NW and the regional dip is 10-40 feet per mile to the NE (Denson, et al, 1959). The Fox Hills sandstone has a well-defined northwest strike with a dip of 35° to the northeast.

The geology of the region has been compiled from the studies of Winchester, et al (1916), Bauer (1924), Hares (1928), Fenneman (1946), Baker (1952), Hansen (1954), Denson and Gill (1955), King and Young (1955), Denson, et al (1959), Moore, et al (1959), Gill (1962) and Trimble (1979). The exposed rocks in the area range from upper Cretaceous to recent sediments. The Cretaceous formations consist of the Pierre Shale (Kp), the Fox Hills (Kfh) and the Hell Creek (Khc). The Cretaceous strata were involved in the Laramide Orogeny and were laid down in the intervening basin resulting from the gradual raising of the Rocky Mountains to the west.

The Paleocene Fort Union formation unconformably overlies the Cretaceous strata and consists of the undifferentiated Ludlow and Cannonball members (Tfc), the Tongue River Member (Tft), and the Sentinal Butte Member (Tfs), and was deposited on the Cretaceous rocks. The Golden Valley Formation (Tg) was laid down in early Eocene. The Eocene was also a time of marked regional uplift and erosion. Oligocene was a time of deposition of the White River Group (Tw), consisting of the Brule Member (Tb) and the Chadron Member (Tc). The early Miocene was a time of regional uplift, peneplanation and development of steep-sided canyons and landslides (Gill, 1962). It was also the time of deposition of the Arikaree Formation (Ta) which unconformably overlies the White River Group. The Quaternary was a time of continued erosion and deposition of fluvial terrace deposits (Qt) and alluvium (Qa).

### C. DESCRIPTION OF THE GEOLOGIC MAP UNITS

A brief description of the exposed geological units in the Dickinson Quadrangle are given based on the work of the Tertiary Committee of North Dakota Geological Society (1954), Denson and Gill (1955), Moore, et al (1959) and from the geological map compiled by the Martel Laboratories, Inc.

#### Mesozoic

##### Cretaceous

Kp: Pierre Shale Formation

The Pierre Shale Formation is the oldest formation exposed in the area. It is a marine, dark-grey to brownish-black, sandy shale and siltstone containing large limestone concretions and thin beds of bentonite. The formation is exposed in the southwestern portion of the area.

Kfh: Fox Hills Formation

The Fox Hills Formation is a marine, greyish-white to brown, fine-grained, cross-bedded sandstone that crops-out in the southwestern portion of the area.

Khc: Hell Creek Formation

The Hell Creek Formation is a heterogeneous fresh to brackish-water, dark-grey to grey, cross-bedded, bentonitic claystone and shale with grey-brown to yellow, medium-grained, sandstone lenses. It contains many concretions and thin lenses of iron carbonate (siderite). The uppermost 100 feet of the unit contains thin lenses of lignite which may be uranium-bearing. Locally, carnotite occurs in the sandstone in the Long Pine Hills of Eastern Montana.

#### Cenozoic

##### Tertiary

Fort Union Formation

Tfc: Ludlow and Cannonball Member, Undifferentiated

The undifferentiated Ludlow and Cannonball members crop-out in the southern and western portion of the area, and consist of an upper unit of thick-bedded sandstone, grey to buff, calcareous or ferruginous, with alternating beds of yellow to buff clay and silty limestone with a lower unit of sandstone. Grey to buff, olive-green and chocolate-colored bentonitic claystone layers contain lignite. Iron cemented sandstone concretions are also present.

Tft: Tongue River Member

The Tongue River Member is approximately 600 feet thick, and covers a major part of the southern and western portion of the area. It is a massive white, light-grey to tan sandstone, siltstone and shale that contains many lenticular beds of grey orthoquartzite and thick, persistent beds of lignite.

Tfs: Sentinel Butte Shale Member

The Sentinel Butte Shale Member varies from 250 to 550 feet in thickness, and has the largest areal exposure of any of the strata in the area. The upper 50-90 feet of the unit is composed of a yellow-grey, very fine to medium-grained, massive, cross-bedded sandstone with interbedded uranium-bearing lignites.

### Eocene

Tg: Golden Valley Formation

The Golden Valley Formation consists of greyish-orange to yellow sandstone and siltstone. The lower 45 feet of the unit consists of purplish-grey to white kaolinitic clay and siltstone. The unit contains a few thin lenticular beds of lignite and carbonaceous shale. Original thickness is unknown due to post-Eocene erosion; the maximum thickness is 175 feet in the type area.

### Oligocene

Tw: White River Group

Tc: Chadron Formation

The Chadron Formation is approximately 170 feet thick, and is a white to dark-grey bentonitic and light-grey tuffaceous claystone, siltstone and sandstone, with local limestone beds. The basal unit consists of coarse-grained tuffaceous conglomeratic sandstone.

Tb: Brule Formation

The Brule Formation is at least 70 feet thick, and is a massive buff to pinkish-tan, tuffaceous siltstone and sandstone. Abundant vertebrate remains occur near its base.



## Miocene

### Ta: Arikaree Formation

The Arikaree Formation is a massive, greenish-white to ash-grey, very fine-grained, tuffaceous sandstone and siltstone with a few thin beds of orthoquartzite, dolomite and volcanic ash. The Arikaree Formation is dominantly of aeolian origin.

## Quaternary

### Qt: Terrace Deposits

The Terrace deposits consist of silt, sand and a small amount of gravel.

### Qa: Alluvium

The Alluvium consist of silt, sand, clay and a small amount of gravel.

## D. RADIOACTIVE MINERAL PROSPECTS IN THE MAP SHEET AREA

Known uranium occurrences in the surveyed area are associated with lignites and their enclosing strata. Uranium-bearing lignites occur at many horizons, principally in the Fort Union Formation in the Medicine Pole Hills, Bullion Butte area, Sentinel Butte area, and Chalky Butte area (Zeller and Schopf, 1959; Gill, et al, 1959). There are at least 27 million tons of lignite averaging 2.3 feet in thickness with an average uranium content of 0.013% in these areas.

In the Medicine Pole Hills, a widespread persistent lignite bed, the Harmon lignite bed, underlies most of the area. It contains 2.8 million short tons of lignite with an average uranium content of 0.006%. In the Bullion Butte area, there are two uranium-bearing lignites. The Nunn lignite bed is the most radioactive, and is 3 to 12 feet thick, averaging 4.8 feet, and averaging 0.007% uranium, with the highest content being 0.036%. The Nunn lignite bed is about 400 feet stratigraphically above the base of the Sentinel Butte Member. In the Sentinel Butte area, there are five uranium-bearing lignites near the top of the Sentinel Butte Member. There are about 5 million tons of lignite in these beds that average 0.007% uranium over a vertical distance of 2.5 feet.

In the Chalky Butte area, the Chalky Butte lignite bed occurs in the northern part of the area, and the Slide Butte lignite bed underlies most of the area. The Chalky Butte lignite bed contains about 5 million short tons of lignite with an average of 0.008% uranium over a 2 foot vertical distance. The Slide Butte lignite averages 2 feet in thickness, and is 80 feet stratigraphically below the Chalky Butte lignite and 70 feet above the base of the Sentinel Butte Member. It is stratigraphically the highest lignite bed at HT and Slide Buttes, and contains 2.5 million

short tons of lignite with an average of Slide Buttes it averages 0.024% uranium.

All of the uranium-bearing deposits are stratigraphically near the unconformity at the base of the Oligocene, and bear no apparent relationship to the age of the formation in which they occur. The White River Group and the Arikaree Formation contain appreciable amounts of volcanic ash which is considered to be the source material for the uranium in the underlying lignites. The lignite beds having the most uranium are highest in the stratigraphic section with the highest uranium concentrations at the top of thick lignite beds. Where the lignites are not more than 2.5 feet thick, the lower part of the lignite may contain higher uranium contents than the upper part. This inverse relationship may have resulted from uranium-bearing ground-water moving laterally along the base of thin and fractured lignite beds, which normally overlie impervious underclays. Core samples indicate that only the stratigraphically highest lignite bed beneath the unconformity at the base of the Chadron Formation contains appreciable quantities of uranium. The data indicate that the uranium in the lignite is of secondary origin, having been leached from the unconformably overlying tuffaceous White River Group and the Arikaree Formation.

## SECTION IV

### RESULTS OF DATA ANALYSIS

#### A. GEOLOGIC BASE MAP

The Dickinson geologic base map is produced to the scale of the NTMS with the geologic data obtained from the Dickinson 1:250,000 map sheet supplied by Bendix Field Engineering Corporation. The base map is presented in Volume II of this report without the superpositioned flight lines at a scale of 1:500,000, and at a scale of 1:250,000 as a separate sheet.

#### B. NATIONAL GAMMA RAY MAP SERIES (NGRMS)

The geologic base has been photographically screened to allow emphasis of the flight line locations and of the information regarding data analysis. These maps are used as the base for presenting statistical information on the six variables:

- \*  $^{208}\text{Tl}$
- \*  $^{214}\text{Bi}$
- \*  $^4\text{K}$
- \*  $^{214}\text{Bi}/^{208}\text{Tl}$  Ratio
- \*  $^{214}\text{Bi}/^4\text{K}$  Ratio
- \*  $^{208}\text{Tl}/^4\text{K}$  Ratio

The six NGRMS sheets are presented in Volume II of this report at a scale of 1:500,000 and as separate sheets at a scale of 1:250,000.

The statistical information is summarized on these maps through the utilization of one, two or three dots above or below the flight line at every fifth data point. One dot above the line indicates that the counting rate or ratio value at that point is between  $1\sigma$  and  $2\sigma$  greater than the mean value for that geologic type where  $\sigma$  (sigma) is a measure of the spread of the data about the mean assuming a gaussian shaped distribution. The mean and  $\sigma$  values are determined for each geologic type based on all flight line data from the area, as is discussed further in Part F below. Two dots indicate values between  $2\sigma$  and  $3\sigma$ , and three dots show values greater than  $3\sigma$ . Dots below the line indicate counting rate or ratio values which are less than the mean value by 1, 2 or  $3\sigma$  in the same manner.

#### C. RADIOMETRIC STACKED PROFILE DATA

The profiles of all Map Lines and Tie Lines are presented in Volume II of this report at a scale of 1:500,000 and at a scale of 1:250,000 as separate sheets.

The same vertical scale is used for a given variable for all map lines, but the vertical scale changes to fit the specific variable plotted. The scales used for each variable are:

1. Altitude  
100 feet/division, aircraft altitude above the surface;  
no averaging.
2. T<sub>ℓ</sub> (<sup>208</sup>T<sub>ℓ</sub>)  
10 counts/second/division (c/s/div). Seven seconds of data  
are averaged with weighting of 1:2:3:4:3:2:1 and the  
average value plotted at the center of the group of 7.
3. Bi (<sup>214</sup>Bi)  
5 c/s/div; 7-second weighted average as for T<sub>ℓ</sub>.
4. K (<sup>40</sup>K)  
30 c/s/div; 7-second weighted average as for T<sub>ℓ</sub>.
5. BiAir  
10 c/s/div; 95-second non-weighted average.
6. Residual Magnetic Field (RMAG)  
20 gammas/division; the residual magnetic field is the total  
magnetic field as measured by a proton precession magnetometer  
from which has been subtracted the International Geomagnetic  
Reference Field (Stassinapoulous; NSSDC-72-12).
7. Total Count, 400 KeV to 2.80 MeV (GC)  
250 c/s/div; no averaging
8. <sup>214</sup>Bi/<sup>208</sup>T<sub>ℓ</sub> Ratio (Bi/T<sub>ℓ</sub>)  
0.1 /division; 7-second weighted averaging as for T<sub>ℓ</sub>
9. <sup>214</sup>Bi/<sup>40</sup>K Ratio (Bi/K)  
.03 /division; 7-second weighted averaging as for T<sub>ℓ</sub>.
10. <sup>208</sup>T<sub>ℓ</sub>/<sup>40</sup>K Ratio (T<sub>ℓ</sub>/K)  
.05 /division; 7-second weighted averaging as for T<sub>ℓ</sub>.
11. Geology  
The surface geology along the flight line, with a width of  
about six miles, is displayed above the profiles and the  
flight path is superimposed.

#### D. MAGNETIC STACKED PROFILE DATA

For each map line and tie line, a magnetic multiple-parameter stacked profile is produced at a scale of 1:500,000 in Volume II of this report, and at a scale of 1:250,000 as separate sheets. The same vertical scale is used for a given variable for all map lines, but the vertical scale varies to fit the specific variable plotted. The scales used for each variable are:

1. Altitude

100 feet/division; aircraft altitude above the surface; no averaging.

2. Temperature

1 degree celsius/division; no averaging.

3. Barometric Pressure

0.25 inches mercury/division; no averaging

4. Base Station - Magnetic Field

5 gammas/division; no averaging

5. Residual Magnetic Field

10 gammas/division; no averaging.

#### E. MAGNETIC TAPES AND LISTINGS

The description of the magnetic tapes and their listings is presented in Appendix II.

#### F. STATISTICAL PRESENTATION OF DATA BY GEOLOGIC TYPE

After the flight lines are superimposed on the geologic base, it is possible to select the record numbers associated with each geologic type existing below the aircraft as it travels along the flight path. This information is used as input to various programs to produce interpretation information based on the statistical variations within the geologic types existing in the area.

The first group of data in the averaged output microfiche listing gives the computed mean and standard deviation for all six radiometric variables for each geologic type. These values were computed on the basis of the data from individual flight lines.

The listing for the averaged output (microfiche) gives the mean value and the magnitude of the deviations from the mean for each averaged radiometric record along the entire flight line. The deviation

from the mean is indicated by integers in the "rank" column of the listing. The integers one, two, or three with no preceding sign indicate one, two, or three sigma and greater deviations above the mean value. If the integers are preceded by a minus sign, the deviations are below the mean.

Tables 1-6 list the mean values for each geologic type based on the data from a single line rather than from the entire area.

#### G. FREQUENCY DISTRIBUTIONS OF DATA FOR EACH GEOLOGIC TYPE

The six radiation variables were grouped according to geologic type, and presented in the form of frequency distribution plots. These plots, which show the number of occurrences at a specific magnitude as a function of the magnitude, are included in Appendix I of Volume I. Data from all map lines and tie lines were used to determine these distributions. Statistically invalid values, as determined according to Section III, Part D above, were not used in producing the distributions. The mean and standard deviations for each geologic type encountered in the Lemmon quadrangle are presented in Table 7 for easy reference.

#### H. MICROFICHE REPRODUCTION OF SINGLE RECORD AND AVERAGED RECORD LISTINGS

The output listings of the single point non-averaged and averaged computer programs have been reproduced on MICROFICHE, and are included in Volume I of this report. A 7-point weighted average was used to produce the listing of the six radiation variables. An example of both the single point and averaged listings is included in Appendix II for reference.

#### I. ALTITUDE AND GROUND SPEED HISTOGRAMS

A histogram of the ground speed and altitude of the aircraft for each map line and tie line is included in Appendix III. When lines pass over cities requiring an increase in altitude, these lines may reflect a double distribution in altitude.

##### 1. Analysis of the Histograms

Radioactivity data for the various geologic units is presented as a series of histograms (Appendix I) with values in counts per second (c/s) plotted against frequency of events and summarized in Table 8. A histogram should approximate a Gaussian distribution if the geologic unit is represented by facies of similar kind and geochemical content. Bimodal or polymodal distributions for the  $^{214}\text{Bi}$ ,  $^{208}\text{Tl}$  and  $^{40}\text{K}$  values may indicate variation in geologic or geochemical content, or large scale variations in hydrologic regimes of the soils.

	KPH	KHC	KP	QA	QT	TA	TB	TC	TFC	TFS	TFT	TG	TW
ML 1	37	39	39	41					43		45		
ML 2	36	35	51	42	38				41		45		
ML 3	40	35	50	42	38				44		46		53
ML 4	34	37	40	36	35				39		42		
ML 5	34	35	38	40	34				39		42		
ML 6	35	34	38	39	35				40		43		
ML 7	34	38		32	34				39		42		
ML 8		38		36					42	28	38		
ML 9		37		37	34			41	40	39	40		
ML10		39		33				44	41	38	42		
ML11		41		36					39	39	43		36
ML12				34	34				39	38	45		
ML13				38					37	37	43		
ML14				39	36			35	42	40	42	44	
ML15				41	42			34		40	43	44	
ML16				38	43		50	50		38	44	42	45
ML17				32	43		38	41		34	38	35	
ML18				39				41		38	42	34	
ML19				39				39		40	42	39	
ML20				35						38	42		
ML21				38						38	41	33	
ML22				39						39	43		
ML23				38					47	39	41	43	
TL 1				37					39	41	41	45	
TL 2				38					43	40	41	35	
TL 3				36				45	42	39	41	41	
TL 4									41	41	46		
TL 5				43	48				39		46		
TL 6	40	39	49	43	41				44		47		

Table 1. Geologic Unit Average Value as a Function of Map Line for  $^{208}\text{Tl}$  (Counts/Second)

	KFH	KHC	KP	QA	QT	TA	TB	TC	TFC	TFS	TFT	TG	TW
ML 1	18	17	15	20					20		22		
ML 2	18	17	24	19	19				20		23		
ML 3	21	16	21	22	17				21		25		35
ML 4	17	23	18	27	21				25		28		
ML 5	20	20	21	26	24				25		27		
ML 6	20	23	19	26	22				23		26		
ML 7	23	26		25	25				21		24		
ML 8		30		35					33	20	28		
ML 9		29		26	27			14	30	20	27		
ML10		23		25				27	21	23	26		
ML11		28		20					23	21	23		21
ML12				19	19				20	21	21		
ML13				21					19	18	21		
ML14				20	19			20	20	19	20	22	
ML15				20	22			33		19	20	23	
ML16				26	20		21	19		21	23	23	17
ML17				35	43		33	34		36	40	33	
ML18				19				18		18	20	13	
ML19				20				21		18	21	22	
ML20				19						19	24		
ML21				20						23	24	19	
ML22				20						19	20		
ML23				20					22	22	20	24	
TL 1				29					25	27	30	33	
TL 2				28					28	27	26	26	
TL 3				28				31	27	28	28	35	
TL 4									23	29	28		
TL 5				23	23				24		25		
TL 6	16	20	19	24	22				20		21		

Table 2. Geologic Unit Average Value as a Function of Map Line for  $^{214}\text{Bi}$  (Counts/Second)



	KPH	KHC	KP	QA	QT	TA	TB	TC	TFC	TFS	TFT	TG	TW
ML 1	135	130	140	142					147		149		
ML 2	135	131	149	138	138				142		151		
ML 3	130	129	145	131	131				144		152		163
ML 4	136	124	132	132	128				130		146		
ML 5	130	129	113	141	130				133		144		
ML 6	128	125	131	139	120				133		146		
ML 7	120	125		113	128				138		139		
ML 8		120		110					135	108	130		
ML 9		118		125	119			164	128	131	133		
ML10		122		112				127	120	128	136		
ML11		119		124					121	126	138		120
ML12				122	113				127	127	139		
ML13				127					121	126	138		
ML14				131	131			115	125	130	134	124	
ML15				134	139			89		125	138	125	
ML16				120	134		143	149		114	133	114	106
ML17				95	112		102	90		97	105	84	
ML18				126				104		118	133	77	
ML19				133				61		129	132	122	
ML20				119						126	136		
ML21				126						127	132	107	
ML22				128						130	137		
ML23				129					127	128	128	128	
TL 1				126					133	127	131	126	
TL 2				126					139	124	134	117	
TL 3				118				95	142	124	137	117	
TL 4									123	131	152		
TL 5				131	144				138		142		
TL 6	141	132	136	141	143				136		151		

Table 3. Geologic Unit Average Value as a Function of Map Line for  $^{40}\text{K}$  (Counts/Second)

	KFH	KHC	KP	QA	QT	TA	TB	TC	TFC	TFS	TFT	TG	TW
ML 1	50	46	39	50					47		49		
ML 2	49	49	46	45	50				49		51		
ML 3	54	46	42	54	46				49		56		66
ML 4	53	61	46	74	61				65		68		
ML 5	62	59	55	67	70				65		64		
ML 6	57	69	53	68	64				59		60		
ML 7	67	69		89	76				53		59		
ML 8		80		96					78	74	74		
ML 9		77		70	79			35	76	53	66		
ML10		61		75				62	52	63	63		
ML11		68		56					60	56	56		60
ML12				57	58				54	55	48		
ML13				55					52	50	49		
ML14				51	52			58	48	48	50	50	
ML15				50	52			95		49	49	52	
ML16				70	49		44	37		57	54	56	39
ML17				109	102		86	83		106	105	96	
ML18				51				45		49	49	37	
ML19				53				53		48	52	57	
ML20				55						50	57		
ML21				54						27	59	62	
ML22				54						49	47		
ML23				53					47	58	51	56	
TL 1				80					65	66	73	75	
TL 2				76					64	69	65	74	
TL 3				79				69	64	71	68	85	
TL 4									58	73	61		
TL 5				53	47				63		54		
TL 6	40	52	40	58	54				47		45		

Table 4. Geologic Unit Average Value as a Function of Map Line for  $^{214}\text{Bi}/^{208}\text{Tl}$  (Times 100)

	KPH	KHC	KP	QA	QT	TA	TB	TC	TFC	TFS	TFT	TG	TW
ML 1	134	136	113	149					139		147		
ML 2	133	134	162	137	141				143		151		
ML 3	166	125	146	176	136				150		168		217
ML 4	132	187	138	206	168				198		198		
ML 5	161	162	190	190	187				196		190		
ML 6	157	188	150	194	191				180		179		
ML 7	194	213		269	200				152		177		
ML 8		258		319					245	188	217		
ML 9		246		214	227			88	240	160	203		
ML10		196		225				222	179	188	198		
ML11		237		166					192	170	173		183
ML12				162	173				165	166	158		
ML13				166					163	148	156		
ML14				156	146			182	164	148	157	179	
ML15				153	159			367		160	153	185	
ML16				225	155		154	128		195	180	215	166
ML17				373	390		328	390		377	384	400	
ML18				158				189		158	155	169	
ML19				154				362		147	166	183	
ML20				166						153	180		
ML21				162						183	188	194	
ML22				165						148	152		
ML23				157					176	177	163	188	
TL 1				236					195	217	231	268	
TL 2				229					204	225	204	221	
TL 3				244				350	193	229	205	303	
TL 4									195	228	186		
TL 5				177	158				178		176		
TL 6	114	155	144	177	155				152		143		

Table 5. Geologic Unit Average Value as a Function of Map Line  $^{21}\text{Bi}/^{40}\text{K}$  (Times 1000)

	KFH	KHC	KP	QA	QT	TA	TB	TC	TFC	TFS	TFT	TG	TW
ML 1	273	298	284	295					296		298		
ML 2	272	273	347	308	281				294		299		
ML 3	310	270	351	325	295				310		302		327
ML 4	251	304	304	278	278				306		292		
ML 5	263	276	342	286	265				299		298		
ML 6	277	274	292	285	295				307		298		
ML 7	290	307		292	268				286		302		
ML 8		324		332					315	256	293		
ML 9		319		303	288			253	316	300	306		
ML10		321		299				348	345	302	314		
ML11		347		296					323	309	313		306
ML12				281	301				310	304	327		
ML13				305					312	299	316		
ML14				304	280			305	337	310	317	357	
ML15				308	303			390		328	313	355	
ML16				324	320		351	341		339	334	378	428
ML17				343	382		382	470		357	368	419	
ML18				311				417		323	318	455	
ML19				295				665		308	319	324	
ML20				303						306	313		
ML21				303						305	317	313	
ML22				311						305	320		
ML23				300					372	311	321	336	
TL 1				297					301	328	316	358	
TL 2				302					314	325	312	300	
TL 3				312				504	301	322	305	357	
TL 4									339	318	307		
TL 5				331	333				290		328		
TL 6	285	297	359	308	286				323		316		

Table 6. Geologic Unit Average Value as a Function of Map Line  $200T_L/10^3K$  (Times 1000)

T $\lambda$		B $i$		K		B $i$ /T $\lambda$		B $i$ /K		T $\lambda$ /K		NO. EVENTS	GEOL. UNIT
$\sigma$	$\bar{X}$	$\sigma$	$\bar{X}$	$\sigma$	$\bar{X}$	$\sigma$	$\bar{X}$	$\sigma$	$\bar{X}$	$\sigma$	$\bar{X}$		
5.3870	37.0	4.3335	19.0	10.6542	134.5	0.1559	0.5264	0.0400	0.1431	0.0425	0.2764	499.0	KFH
4.7630	38.1	5.9911	22.7	10.3732	127.0	0.1663	0.6017	0.0572	0.1814	0.0411	0.3010	1545.0	KHC
7.6401	46.4	4.8772	20.6	13.6274	139.6	0.1091	0.4510	0.0348	0.1480	0.0486	0.3326	294.0	KP
5.9876	38.6	5.9621	23.5	15.6905	127.0	0.2077	0.6270	0.0670	0.1901	0.0395	0.3050	5064.0	QA
5.3991	40.1	5.3902	22.5	11.9003	134.8	0.1633	0.5718	0.0509	0.1689	0.0375	0.2979	556.0	QT
6.8967	45.3	7.3041	26.5	24.3793	125.9	0.2391	0.6168	0.0980	0.2274	0.0438	0.3647	91.0	TB
6.9633	42.1	8.7353	24.2	32.4889	103.4	0.2032	0.5798	0.1323	0.2643	0.1546	0.4461	455.0	TC
5.5588	41.8	5.4322	22.3	15.0079	138.4	0.1503	0.5415	0.0473	0.1636	0.0427	0.3044	7736.0	TFC
6.0128	38.9	6.9442	22.2	15.4626	124.9	0.2299	0.5655	0.0687	0.1818	0.0430	0.3128	24571.0	TFS
6.2297	43.0	6.7321	25.6	17.3871	138.9	0.1919	0.6082	0.0606	0.1877	0.0385	0.3109	24738.0	TFT
7.2961	38.6	8.8007	25.8	23.4874	107.2	0.2442	0.6800	0.1060	0.2509	0.0756	0.3701	1809.0	TG
6.7273	40.3	6.3735	22.3	19.5513	121.5	0.1449	0.5616	0.0380	0.1826	0.0714	0.3379	76.0	TW
6.7497	40.1	9.4709	30.2	18.6962	124.8	0.2959	0.7817	0.0919	0.2493	0.0348	0.3219	133.0	WTR
7.9236	39.4	8.1207	25.8	21.7386	127.2	0.3705	0.6005	0.0951	0.2036	0.0917	0.3120	1497.0	ZWA

TABLE 7. Mean ( $\bar{X}$ ) and Standard Deviation  $\sigma$  for Each Geologic Type.

TABLE 8. Radioactivity Histograms for Geologic Map Units with Non-Unimodal Form. Recommended Splits for Histograms based on  $^{208}\text{Tl}$  data.

<u>Geologic Unit</u>	<u>No. of Events</u>	<u>Recommended Split C/S</u>
Qa	5064	None
Qt	556	None
Tw	76	39
Tb	91	None
Tc	455	26
Tg	1809	None
Tf <sup>2</sup>	24571	None
Tft	24738	None
Tfc	7736	None
Khc	1545	None
Kfh	499	None
Kp	294	31

Kp: Pierre Shale Formation

The Pierre Shale Formation is represented by 294 events and 0.4% of the total events.  $^{40}\text{K}$  and  $^{214}\text{Bi}$  are unimodal with modes at 130 c/s and 18 c/s, respectively.  $^{208}\text{Tl}$  is polymodal, with major modes at 41 c/s and 52 c/s, and a critical parameter of 31 c/s. Determination of other critical parameters is not plausible.

Kfh: Fox Hills Formation

The Fox Hills Formation is represented by 499 events and 0.7% of the total events. The  $^{40}\text{K}$ ,  $^{214}\text{Bi}$  and  $^{208}\text{Tl}$  histograms are unimodal, with modes at 130 c/s, 18 c/s and 35 c/s, respectively. All three distributions are slightly negatively skewed.

Khc: Hell Creek Formation

The Hell Creek Formation is represented by 1,545 events and 2.3% of the total events. The  $^{40}\text{K}$ ,  $^{214}\text{Bi}$  and  $^{208}\text{Tl}$  histograms are unimodal distributions, with modes at 128 c/s, 22 c/s and 38 c/s, respectively.  $^{214}\text{Bi}$  is positively skewed.

Tfc: Cannonball and Ludlow Members, Undifferentiated, of the Fort Union Formation

The Cannonball and Ludlow members, undifferentiated, is the third most extensive unit, and is represented by 7,736 events and 11.5% of the total events. The  $^{40}\text{K}$ ,  $^{214}\text{Bi}$  and  $^{208}\text{Tl}$  histograms are unimodal distributions, with modes at 138 c/s, 22 c/s and 41 c/s, respectively.  $^{214}\text{Bi}$  is positively skewed or is bimodal with a second mode at 47 c/s, with a critical parameter of 43 c/s.

Tft: Tongue River Member of the Fort Union Formation

The Tongue River Member is the most extensive unit represented by 24,738 events and 36.7% of the total events.  $^{40}\text{K}$  and  $^{214}\text{Bi}$  are unimodal with modes at 142 c/s and 27 c/s, respectively.  $^{214}\text{Bi}$  is slightly positively skewed.  $^{208}\text{Tl}$  is bimodal with modes at 43 c/s and 18 c/s. However, separation of the overlapping tails of the distribution is not plausible.

Tfs: Sentinel Butte Shale Member of the Fort Union Formation

The Sentinel Butte Shale Member is the second most extensive unit represented by 24,571 events and 36.4% of the total events. The  $^{40}\text{K}$  and  $^{214}\text{Bi}$  histograms are unimodal distributions, with modes at 125 c/s and 22 c/s respectively.  $^{214}\text{Bi}$  is slightly positively skewed.  $^{40}\text{K}$  is negatively skewed.  $^{208}\text{Tl}$  is bimodal with a prominent mode at 40 c/s. However, separation of the overlapping tails of the distribution is not plausible.

Tg: Golden River Formation

The Golden River Formation is represented by 1,809 events and 2.7% of the total events.  $^{40}\text{K}$  and  $^{214}\text{Bi}$  are polymodal with prominent modes at 125 c/s and 25 c/s, respectively. However, separation of the overlapping tails of the distributions is not plausible.  $^{208}\text{Tl}$  is unimodal and slightly negatively skewed with a mode at 40 c/s.

Tc: Chadron Formation of the White River Group

The Chadron Formation is represented by 455 events and 0.7% of the total events.  $^{40}\text{K}$  is polymodal with a prominent mode at 100 c/s. However, separation of the overlapping tails of the distribution is not plausible.  $^{214}\text{Bi}$  and  $^{208}\text{Tl}$  are bimodal with prominent modes at 15 c/s and 45 c/s, respectively. However, separation of the overlapping tails of the  $^{214}\text{Bi}$  distribution is not plausible. The critical parameter for  $^{208}\text{Tl}$  is at 26 c/s.

Tb: Brule Formation of the White River Group

The Brule Formation is represented by 91 events and 0.1% of the total events.  $^{40}\text{K}$  is either bimodal with a critical parameter at 125 c/s, or it is polymodal with modes at 95 c/s, 105 c/s, 115 c/s and 130 c/s.  $^{214}\text{Bi}$  is bimodal with modes at 19 c/s and 33 c/s. Separation of the overlapping tails of the  $^{214}\text{Bi}$  distributions is not plausible.  $^{208}\text{Tl}$  is either bimodal or polymodal with modes at 42 c/s and 52 c/s. However, critical parameters cannot be determined.

Tw: White River Group

The White River Group which was not differentiated into the Brule and the Chadron formations is represented by only 76 events and 0.1% of the total events.  $^{40}\text{K}$ ,  $^{214}\text{Bi}$  and  $^{208}\text{Tl}$  are polymodal with prominent modes at 105 c/s, 20 c/s and 36 c/s, respectively. The critical parameter of  $^{40}\text{K}$ ,  $^{214}\text{Bi}$  and  $^{208}\text{Tl}$  are 145 c/s, 30 c/s and 39 c/s, respectively.

Qt: Terrace Deposits

The Terrace deposits are represented by 556 events and 0.8% of the total events.  $^{40}\text{K}$  and  $^{208}\text{Tl}$  are unimodal with modes at 135 c/s and 40 c/s, respectively.  $^{208}\text{Tl}$  is negatively skewed.  $^{214}\text{Bi}$  is polymodal with prominent modes at 24 c/s and 19 c/s. The critical parameters are at 31 c/s and 36 c/s.  $^{214}\text{Bi}$  and  $^{208}\text{Tl}$  are positively skewed.  $^{214}\text{Bi}$  has a few high values.  $^{40}\text{K}$  is negatively skewed or possibly bimodal.

Qa: Alluvium

The alluvium is represented by 5,064 events and 7.5% of the total events.  $^{40}\text{K}$ ,  $^{214}\text{Bi}$  and  $^{208}\text{Tl}$  are unimodal, with modes at 127 c/s, 23 c/s and 38 c/s, respectively.



## 2. Discussion of the Anomalies

### Introduction

Anomalous  $^{214}\text{Bi}$  and  $^{208}\text{Tl}$  amounts and anomalous  $^{214}\text{Bi}/^{208}\text{Tl}$  values were analyzed for the geologic units of the Dickinson Airborne Radiometric Maps. A radioactivity anomaly is considered to be: 1) a cluster of three or more values of one-standard deviation or greater that was visually distinguishable on the map; 2) a juxtaposition of two or more two-standard deviations; or 3) one or more three-standard deviation values. Only positive anomalies were considered for  $^{214}\text{Bi}$  and  $^{208}\text{Tl}$  amounts (Tables 9 and 10), but both positive and negative anomalies were considered for the  $^{214}\text{Bi}/^{208}\text{Tl}$  values (Tables 9 and 10). The  $^{214}\text{Bi}$ ,  $^{208}\text{Tl}$  and  $^{214}\text{Bi}/^{208}\text{Tl}$  anomalies based on the above three criteria were taken from the flight lines, and the lines shown in Figures 1, 2 and 3, and are tabulated in Tables 10 and 11. However, ML8 and ML17 have an unusually large number of anomalies that do not appear to reflect local geology. Therefore, they were omitted from the statistical treatment of the data. Also omitted were data near small towns.

A total of 12 geologic units showed anomalous values: Qa, Qt, Tw, Tab, Tc, Tg, Tfs, Tft, Tfc, Khc, Kfh and Kp. The percentage of anomalies by unit is given in Table 10, and summarized for each time period, Quaternary, Tertiary and Mesozoic, in Table 11. Three units of the Fort Union Formation, Tfs, Tft and Tfc, have about 80% of all the anomalous values.

Table 11 shows that the positive ratio anomalies were less numerous than those for  $^{214}\text{Bi}$ . 37% of the ratio anomalies were of the negative type. There were more positive  $^{208}\text{Tl}$  anomalies than  $^{214}\text{Bi}$  anomalies. The number of geological units with anomalies was the same for  $^{214}\text{Bi}$  and the positive and negative ratio anomaly, with  $^{208}\text{Tl}$  having the highest number.

### Relationship of Radioactivity Anomalies to Geologic Units

#### Introduction

$^{214}\text{Bi}$  anomalies are sparse but concentrated in the southwest, south and southeast portions of the area. Positive  $^{214}\text{Bi}/^{208}\text{Tl}$  anomalies show a similar pattern. The negative  $^{214}\text{Bi}/^{208}\text{Tl}$  anomalies are concentrated in the southern, northwestern and northeastern portion of the area.

Quaternary Geologic Units: Qt and Qa

$^{214}\text{Bi}$  and  $^{214}\text{Bi}/^{208}\text{Tl}$  Anomalies

Approximately 9% of all  $^{214}\text{Bi}$  anomalies, 13% of the positive ratio anomalies and 16% of the negative ratio anomalies occur in Quaternary units, 100% of these occur in the unit Qa for  $^{214}\text{Bi}$ , 93% for the

TABLE 9. Summary of Anomalies

	$^{214}\text{Bi}$	$^{208}\text{Tl}$	$^{214}\text{Bi}/^{208}\text{Tl}$
ML23	Tfs,4435-4440,4450-4490	Tfs,4375-4410,5015-5025 5780-5800,5810-5835	Tft(3650-3670),(3700-3715) (3770-3780),(3880-3895); Tfs,4435-4490,4535-4550; Qa,4775-4785;Qa(5125-5140) (5535-5550)
ML22	Tfs,1510-1490	Tfs,1720-1705,1665-1650 1640-1620,1590-1570; 1565,1540;Qa,120-105; Tfs,90-75	Tft(2505-2490),(2420-2405) (2395-2370),(2255-2240), (2235-2220);Tfs(1625-1600) 1510-1490;Qa(915-905); Tfs,880-870(785-770)
ML21	Tft,3265-3290;Tfs, 3530-3565	Tfs,3445-3455,3490-3500	Tft,3265-3290;Qa(1390- 1400);Tfs,890-915,630-670
ML20	Tfs,275-270	Tft,2505-2490;Tfs,1615- 1600,1595-1565,1510- 1500,1475-1460,1445- 1420,1385-1370,1350- 1335,280-265	
ML19		Tfs,3600-3620,3720-3730 4880-4895,4965-4980	Tg(3880-3890);Tc(3955- 3965);Tft(4895-4905)
ML18	Tfs,1940-1925	Tfs,Qa,2055;Tfs,1925- 1910;Tc,1250-1235;Tg, 1190-1175	Tft(2325-2290);Tfs,1940- 1925;Tc(1225-1210)
ML17	Tft,2815-2930,2950- 3175,3185-3255,3265- 3320;Qa,3320-3355;Tfs, 3355-3370;Tft,3370- 3615;Tfs,3615-3935; Tg,3935-3960;3975- 3990,4060-4080,4085- 4100,4120-4140;Tc, 4170-4195;Tg,4300- 4365;Tfs,4475-4525; 4530-4650,4700-4525 4750-4760,4770-4780, 4785-4880;Qa,4880- 4905;Tc,4905-4990,Qa, 5020;Tfs,5020-5045;Qa, 5045-5060,5100-5140; Tft,5165-5185;Tfs, 5190-5220,5240-5270		Tft,2815-2955,2965-3085, 3095-3200,3205-3280,3290- 3320;Qa,3320-3355;Qt, 3355-3370;Qa,3370-3380; Tft,3380-3430,3435-3615; Tfs,3615-3670,3680-3800, 3810-3865,3880-3935;Tg, 3935-3970,3975-3990,4150- 4160;Tc,4170-4190;Tg,4250- 4255,4280-4295,4320-4350, 4360-4375;Tfs,4455-4465, 4480-4510,4520-4535,4545- 4690,4700-4720,4740-4760, 4770-4780,4800-4850,4860- 4870,4890-4900,4915-4990; Qa,4990-5020;Tfs,5020-5045 Tft,5045-5060,5140-5145, 5170-5185;Tfs,5195-5220; 5230-5270;Tft,5290-5345

(TABLE 9. Cont'd.)

	$^{214}\text{Bi}$	$^{208}\text{Tl}$	$^{214}\text{Bi}/^{208}\text{Tl}$
ML16	Tft,2050-2040;Tfs,2040-1975;Qa,410-400;WA400-370;Qa,370-350	Tft,2675-2635;Tfs,2280-2265,155-1540;Tg,1540-1495,1485-1470;Tb,1460-1450	Tft(2675-2655);Tfs,2050-1985;Tb(1460-1445);Tfs,1055;Qa,410-400;WA,400-385
ML15	Tfs,3510-3915,3535-3565,4500-4530	Tft,2720-2740;Qt,3045-3055,3260-3275;Qa,3325-3340;Tfs,3750-3785;3920-3935;Tg,4045-4075;Tfs,4975-4990	Tft(2725-2750)(2905-2915)Qt(3265-3275)Qa(3325-3340);Tfs,3510-3520,3535-3575,(3775-3795),4515-4530;WA(5100-5130)
ML14		Tfs,1810-1795,1705-1665,1510-1490,1435-1420,1415-1390;Tg,1060-1035;Tfs,950-940,885-870,840-805,535-520,410-395,280-265	Tft(2335-2325)
ML13		Tft,2970-2995,3115-3125;Tfs,3755-3765;3850-3860,3930-3960,4070-4080,4200-4215,4410-4420	
ML12	Tfs,1780-1765,1735-1725,1415-1400,690-680	Tft,1925-1895,1875-1865,1720-1705,735-720,175-155	Tfs,1775-1770,1735-1725,1415-1410,690-670,(180-165)
ML11	Tfc,2590-2600	Tft,2855-2865,3020-3035,3100-3110;Tfs,3945-3955,4660-4675,4945-4960	Qa,2730-2745;Tfc(2835-2850);Tfs,3500-3510,3525-3545,3605-3625
ML10	Tft,2160-2145,2110-2075;Tfs,1695-1680;Qa,695-685;Tfs,435-395,365-340	Khc,2360-2350,2340-2335;Tfc,2280-2275;Tft,1915-1900;Tfs,1185-1170,85-65	Tft,2160-2145,2110-2090;Tfs,1690-1680,735-725;Qa,695-670;Tfs(605-595);Tfs,455-445,350-335,265-255;Tft,190-180
ML9	Khc,3400-3410,3420-3440;Qa,3475-3490;Khc,3515-3525;3530-3545;Tfc,3570-3620,3645-3660;Tft,3720-3740,3825-3840,3885-3900,3950-3965,4085-4100;Qa,5535-5560	Tft,3925-3955,4045-4055;Tfs,5015-5035	Khc,3400-3410,3420-3440;Qa,3475-3490;Tfc,3570-3610,3645-3655;Tft,4085-4100;Tc(4295-4310)Qa,5540-5560

(TABLE 9. Cont'd.)

	$^{214}\text{Bi}$	$^{208}\text{Tl}$	$^{214}\text{Bi}/^{208}\text{Tl}$
ML8	Qa,3255-3220;Khc,3220-3170,3160-3150;Tfc,3125-3115,3110-3050,3040-3030 Tft,2995-2970,2900-2870,2855-2820,2715-2700,2695-2680,2560-2530,2490-2465; Tfs,2320-2305,2290-2275,2270-2250,2220-2205,1530-1500;Tft,1050-1035,840-800	Khc,3175-3155;Tft,3000-2980,2295-2765,2730-2715	Khc,3270-3255;Qa,3255-3230;Khc,3210-3195,3185-3175,3160-3150;Tfc,3135-3120,3105-3050;Tft,2900-2885,2855-2845,2550-2535;Tfs,2505-2485;Tft,2475-2460,2445-2420;Tfs,2405-2390,2320-2310;Tft,2165-2150,2135-2125;Tfs,2085-2070,1965-1950;Tft,1925-1910;Tfs,1820-1805,1780-1760,1695-1685,1530-1500;Tft,1350-1335,1315-1305,1185-1175,1050-1030,865-805
ML7	Kfh,2650-2660;khc,2805-2835;Tft,3065-3075,4510-4525,4540-4555	Khc,2825-2835;Tft,3085-3100,3205-3225	Kfh,2650-2660;Qt,2670-2685;Qa,3860-3875;Tft,4750-4770
ML6	Tfc,2390-2370,2245-2230; Tft,2120-2015,1265-1255	Tft,2160-2135,2025-2010 1885-1870,1860-1835, 1825-1815,1685-1670, 1605-1585,1415-1400, 1215-1200,1080-1065, 670-655,465-445	Kfh,2550-2540,Khc,2495-2470;Qa,2435-2430;Tfc,2245-2230;Tft,2110-2030,1265-1255,250-240
ML5	Kfh,2720-2735;Tfc,2820-2845,2855-2865;Tft,3050-3120,3960-3985,4040-4050,4550-4570,4740-4750	Tft,3355-3365,3570-3580 3605-3620;Qa,4145-4155; Tft,4180-4200,4265-4275	Kfh,2720-2735;Tfc,2820-2865;Tft,3050-3085,3090-3120,3940-3990,4040-4050,4530-4540,4765-4775
ML4	Tft,2150-2140,1640-1615,1525-1505,1460-1370,1260-1250,1235-1220,980-960,870-840;Tfc,770-760;Qa,720-705;Tfc,600-570,555-530,520-495	Tft,2055-2035,1780-1730 905-895,885-860	Tfc,2460-2450;Tft,2010-1990,1630-1615,1560-1550,1525-1500,1455-1370,1260-1250,1235-1225,985-960;Tfc,775-760;Qa,715-705;Tfc,600-590,580-570,495-485
ML3	Tft,3005-3015;Tfc,3385-3410;Tft,3445-3490,3925-3940,3980-3995,4130-4150	Tw,2995-3010;Tfc,3030-3040,3375-3385,3425-3440;Tft,3500-3585;Tfc,3670-3695;Tft,3750-3765,3780-3830,3840-3865,4285-4310;Tfc,4310-4345 4705-4715,4765-4785	Tfc,3400-3410;Tft,3450-3465,3480-3490,(3495-3515),(3520-3540),(3545-3570);Tft,3980-3990,4095-4105,4130-4145;Tfc(4445-4460)

(TABLE 9. Cont'd.)

	$^{214}\text{Bi}$	$^{208}\text{Tl}$	$^{214}\text{Bi}/^{208}\text{Tl}$
ML2	Kp, 2550-2530; Tfc, 1660-1615; Tft, 980-970, 960-920	Qa, 2525-2490; Tfc, 2250-2235, 2225-225, 2085-2055, 1095-1075; Tft, 1035-995, 835-780; Tfc, 220-210	Tfc(2205-2190), (2185-2170); Tfc, 1660-1650, 1640-1615; Tft(1145-1125); Tft, 940-930, Tfc(735-725); Tft, (660-650); Tfc(535-525); Qa(445-435); Tfc(225-210)
ML1	Tfc, 4910-4920; 5740-5750	Kp, 4395-4405; Tfc, 4735-4780, 5200-5210, 5650-5660, 5675-5690; Tft, 5825-5835, 5865-5840; Tfc, 5890-5910, 5995-6015, 6030-6080; Tft, 6210-6220, Tfc, 6220-6240	Khc(4515-4525); Tfc(4655-4670), (4765-4785), (4810-4825); Tfc, 4910-4920, (4985-4995), (5045-5055), (5275-5285); Tfc, 5740-5750; Tfc(6035-6050), (6200-6220), (6235-6250)
TL1	Qa, 300-310, 320-330; Tfc, 330-350, Tft, 710-725; Qa, 915-925; Tft, 1280-1300, Tfs, 1335-1340; Tft, 1400-1420, 1535-1550; Tft, 1400-1420, 1535-1550; Tfs, 1650-1680, 1735-1740; Qa, 1800-1815; Tfs, 1865-1880, 1925-1945	Tfs, 1025-1040, 1065-1080, 1480-1490, Tg, 1895-1905	Tfc, 200-245, 330-345; Qa, 320-330; Tfs, 690-725, 760-790; Qa, 910-920; Tft, 1275-1295; Tfs, 1660-1675; Qa, 1840-1860
TL2	Tfc, 3775-3760, 3495-3475; Qa, 3135-3110; Tfs, 3040-3025, 2950-2935, 2605-2595; Qa, 2570-2550; Tfs, 2515-2495; Qa, 2450-2415; Tfs, 2380-2365, 2340-2330, 2305-2290, 2280-2265	Tfc, 3780-3755; Tfs, 2415-2405, Qa, 2080-2070	Tfc, 3570-3555, 3495-3480; Qa, 3140-3115; Tfs, 3090; Qa, 2570-2550; Tfs, 2515-2500; Qa, 2435-2420; Tfs, 2370-2355
TL3	Tfc, 3875-3895, 3910-3935; Tft, 4175-4195; Tfs, 4755-4775, 4830-4840, 4850-4875; Tg, 4900-4910, 4925-4945, 4975-4990; Tfs, 4990-5045; Tg, 5045-5055; 5095-5115; Tc, 5215-5240; Tg, 5285-5305	Tfs, 4890-5005	Tft, 4170-4195; Qa, 4700-4740; Tg, 4900-4910; Tfs, 5005-5025, 5095-5110; Tc, 5220-5235; Tg, 5280-5305; Tfs, 5400-5420; Qa, (5535-5545)
TL4	Tfs, 1175-1145, 1135-1105, 1095-1060, 1045-975, 965-920, 910-895, 730-720, 675-655, 645-635, 620-600, 240-180; 135-40	Tfc, 1585-1575; Tft, 1455-1440, 1400-1345; Tfs, 1055-1035, 270-245, 205-195, 190-165	Tfs, 1070-1060, 965-950, 235-220, 135-70

(TABLE 9. Cont'd.)

	$^{214}\text{Bi}$	$^{208}\text{Tl}$	$^{214}\text{Bi}/^{208}\text{Tl}$
TL5	Tfc,1945-1955,Tft,2215-2225,2260-2275	Tft,2200-2215,2250-2265,2270-2285,2305-2365,2475-2490,2500-2520,2610-2630,2715-2745,2755-2760,2830-2840;Qa,2850-2875,2905-2915,3050-3065;Qt,3065-3105;Qa,3200-3210	Tfc,1910-1915,1950-1975;Qa(2760-2770),(2810-2820)(3230-3250)
TL6		Qa,4250-4235,4125-4105;Kfh(4060-4050),(3975-3965)Kfh,4065-4040;Tft,3265-3235;3135-3120,3095-3080,3015-3005,2960-2935,2885-2870,2760-2745,2715-2700	Khc(3875-3865);Tft(3070-3050),(2960-2940),(2810-2785),(2680-2665)

(....) denotes negative anomaly

TABLE 10. Radioactivity etc.

Geologic Unit	Number	%	Number	%	Number	%	Number	%
<u>Quaternary</u>								
Qa	12	9.0	11	6.2	14	12.8	(10)	(15.6)
Qt	0	0	3	1.7	1	0.9	(1)	(1.6)
<u>Tertiary</u>								
Tw	0	0	1	0.6	0	0	(0)	(0)
Tb	0	0	1	0.6	0	0	(1)	(1.6)
Tc	1	0.8	0	0	1	0.9	(3)	(1.6)
Tg	6	4.5	5	2.8	2	1.8	(1)	(6)
Tfs	44	33.1	62	35.0	34	31.2	(5)	(7.8)
Tft	41	30.8	66	37.3	30	27.5	(23)	(35.9)
Tfc	21	15.8	23	13.0	21	19.3	(16)	(25.0)
<u>Mesozic</u>								
Khc	6	4.5	3	1.7	3	2.8	(2)	(1.2)
Kfh	1	0.8	1	0.6	3	2.8	(2)	(0)
Kp	1	0.8	1	0.6	0	0	(0)	(0)
Total	133	100.1	177	100.1	109	100.0	(64)	(100.0)

\* ML-17, ML-8, WA and anomalies near towns omitted from this table.

(....) denotes negative anomaly

TABLE 11. Statical Summary of Radioactivity Anomalies

<u>Total Samples</u>	$^{214}_{\text{Bi}}$	$^{208}_{\text{Tl}}$	$^{214}_{\text{Bi}}/^{208}_{\text{Tl}}$
Number of Anomalies	133	177	109 (64)
Number of Geologic Units	9	11*	9 (9)
<u>Quaternary Samples</u>			
Number of Anomalies	12	11	14 (10)
Number of Geologic Units	1	2	2 (2)
<u>Tertiary Samples</u>			
Number of Anomalies	113	158	88 (49)
Number of Geologic Units	5	6*	5 (6)
<u>Mesozic Samples</u>			
Number of Anomalies	8	5	6 (4)
Number of Geologic Units	3	3	2 (2)

\* The unit TW belongs to either Tb or Tc.

(.....) denotes negative anomaly



positive  $^{214}\text{Bi}/^{208}\text{Tl}$  and 9% for the negative  $^{214}\text{Bi}/^{208}\text{Tl}$ . There are nine instances where positive  $^{214}\text{Bi}/^{208}\text{Tl}$  anomalies and  $^{214}\text{Bi}$  anomalies coincide. They occur at ML4, stations 705-715; ML9, stations 3475-3490; ML10, stations 685-695; ML16, stations 400-410; TL5, stations 3230-3245; TL1, stations 320-330, 912-920; and TL2, stations 3140-3115, 2570-2550, and 2435-2420. They all occur in the unit Qa.

#### $^{208}\text{Tl}$ Anomalies

Approximately 6% of all  $^{208}\text{Tl}$  anomalies occur in Quaternary units with 79% of these in the unit Qa. There is no coincidence between  $^{214}\text{Bi}$  and  $^{208}\text{Tl}$  in the Quaternary units.

Tertiary Geologic Units: Tw,Tc,Ts,Tfs,Tft and Tfc

#### $^{214}\text{Bi}$ and $^{214}\text{Bi}/^{208}\text{Tl}$ Anomalies

Approximately 80% of all  $^{214}\text{Bi}$  anomalies, 78% of the positive  $^{214}\text{Bi}/^{208}\text{Tl}$  anomalies and 69% of the negative  $^{214}\text{Bi}/^{208}\text{Tl}$  anomalies occur in Tertiary units. Approximately 36% of these occur in the unit Tft for  $^{214}\text{Bi}$ , 34% for the positive  $^{214}\text{Bi}/^{208}\text{Tl}$  and 47% for the negative  $^{214}\text{Bi}/^{208}\text{Tl}$ . Approximately 39% of these occur in the unit Tfs for  $^{214}\text{Bi}$ , 39% for the positive  $^{214}\text{Bi}/^{208}\text{Tl}$  and 10% for the negative  $^{214}\text{Bi}/^{208}\text{Tl}$ . Approximately 19% of these occur in the unit Tfc for  $^{214}\text{Bi}$ , 15% for the positive  $^{214}\text{Bi}/^{208}\text{Tl}$  anomalies in the unit Tfs coincide or overlap with positive  $^{214}\text{Bi}$  values. Approximately 69% of the positive  $^{214}\text{Bi}/^{208}\text{Tl}$  anomalies in the unit Tft coincide or overlap with  $^{214}\text{Bi}$  values. 67% of the positive  $^{214}\text{Bi}/^{208}\text{Tl}$  anomalies in the unit Tfc coincide or overlap with positive  $^{214}\text{Bi}$  values. 100% of the positive  $^{214}\text{Bi}/^{208}\text{Tl}$  anomalies in the units Tg and Tc coincide or overlap with positive  $^{214}\text{Bi}$  values.

Positive  $^{214}\text{Bi}/^{208}\text{Tl}$  anomalies that coincide with or overlap positive  $^{214}\text{Bi}$  anomalies occur in the unit Tfc at ML1, stations 4910-4920, 5740-5750; ML2, stations 1650-1660, 1615-1640, 930-940; ML3, stations 3400-3410; ML4, stations 705-715, 600-590, 570-580 and near 485-495; ML5, stations 2820-2845; ML6, stations 2230-2245; ML9, stations 3570-3610, 3645-3655. TL2, stations 3495-3480; TL3, stations 5220-5235; and TL5, stations 1950-1975. Those that occur in the unit Tft are at ML3, stations 3450-3465, 3480-3490, 4095-4105, 4130-4150 and 5980-5990; ML4, stations 1615-1630, 1505-1525, 1370-1455, 1250-1260, 1225-1235, and 960-985; ML5, stations 3050-3085, 3940-3990, 4040-4050 and near 4765-4775; ML6, stations 2030-2110; ML21, stations 3265-3290; TL1, stations 1275-1295; and TL3, stations 4170-4195. Those that occur in the unit Tfs are at ML10, stations 1680-1690 and 335-350; ML12, stations 1770-1785, 1725-1735, 1410-1415 and 670-690; ML15, stations 3510-3520, 3535-3575, 4515-4530; ML16, stations 1985-2050; ML18, stations 1940-1925; ML22, stations 1490-1510; ML23, stations 4435-4490 and 4535-4550; TL1, stations 1660-1675; TL2, stations 2515-2500 and 2370-2355; TL3, stations 5005-5025 and 5095-5110; and TL4, stations 1070-1060, 965-950 and 235-220. Positive  $^{214}\text{Bi}/^{208}\text{Tl}$  anomalies that coincide with or overlap positive  $^{214}\text{Bi}$  anomalies occur in the unit Tc at TL2, stations 5220-5235, and in the unit Tg at ML3, stations 4900-4910 and 5280-5305.

## $^{208}\text{Tl}$ Anomalies

Approximately 85% of all  $^{208}\text{Tl}$  anomalies occur in Tertiary units with 39% in the unit Tfs, 42% in the unit Tft and 15% in the unit Tfc. Only 6% of the  $^{208}\text{Tl}$  and  $^{214}\text{Bi}$  anomalies coincide. It seems that  $^{208}\text{Tl}$  and  $^{214}\text{Bi}$  suffered strong differentiation in this area. The examples where they overlap are in unit Tft at ML6, stations 2015-2120; ML9, stations 3940-3960; and TL5, stations 2270-2285; in unit Tfs at ML20, stations 270-275; TL2, stations 3750-3780 and near stations 2400-2415; TL4 near stations 1015-1055 and 200-210, and stations 165-190.

Mesozoic Geologic Units: Khc, Kfa and Kp

## $^{214}\text{Bi}$ and $^{214}\text{Bi}/^{208}\text{Tl}$ Anomalies

Approximately 6% of all  $^{214}\text{Bi}$  anomalies, 6% of the positive  $^{214}\text{Bi}/^{208}\text{Tl}$  anomalies and 6% of the negative  $^{214}\text{Bi}/^{208}\text{Tl}$  anomalies occur in Mesozoic units. Approximately 75% of these occur in the unit Khc for  $^{214}\text{Bi}$ , 50% for the positive  $^{214}\text{Bi}/^{208}\text{Tl}$  and 50% for the negative  $^{214}\text{Bi}/^{208}\text{Tl}$ . There is only one anomaly for  $^{214}\text{Bi}$  in units Kfh and Kp, and no positive or negative ratio anomalies in unit Kp. 50% of the positive  $^{214}\text{Bi}/^{208}\text{Tl}$  anomalies in the unit Khc coincide or overlap with positive  $^{214}\text{Bi}$  values. 40% of the positive  $^{214}\text{Bi}/^{208}\text{Tl}$  anomalies in the unit Kfh coincide or overlap with positive  $^{214}\text{Bi}$  values.

Positive  $^{214}\text{Bi}/^{208}\text{Tl}$  anomalies that coincide with or overlap positive  $^{214}\text{Bi}$  anomalies occur in the unit Kfh at ML7, stations 2650-2660. Those in the unit Khc occur at ML9, stations 3400-3410 and 3420-3440.

## $^{208}\text{Tl}$ Anomalies

Only approximately 2% of all  $^{208}\text{Tl}$  anomalies occur in Mesozoic units, with 60% of these in the unit Khc. Only 20% of the  $^{208}\text{Tl}$  and  $^{214}\text{Bi}$  anomalies coincide or overlap. The one example of coincidence occurs in the unit Khc at ML7, stations 2825-2835.

## Cultural Features

There are several cultural features such as small towns, lignite mining and a reservoir that might effect the radiometric data on the Dickinson Quadrangle. There are positive  $^{214}\text{Bi}$  anomalies just north of the small town of Belfield on ML21, stations 3530-3565 and TL4; stations 240-180; in the small town of Mott, stations 5535-5560; in the reservoir on the eastern edge of the quadrangle at ML16, stations 370-400; and west of the small town of Hebron, TL1, stations 1800-1815. There are positive  $^{208}\text{Tl}$  anomalies both north and south of the town of Belfield.

There are positive  $^{214}\text{Bi}/^{208}\text{Tl}$  anomalies in the town of Mott, ML9, stations 5540-5560; in the reservoir at ML16, stations 385-400;

just north of the town of Dickinson at ML21, stations 630-670; just west of the town of Dickinson at TL3, stations 5400-5420; and in the town of Belfield, TL3, stations 235-220. Negative  $^{214}\text{Bi}/^{208}\text{Tl}$  anomalies occur on ML15, stations 5100-5130 associated with the reservoir; on ML3, stations 5400-5420; and just west of the town of Dickinson, and on TL4, stations 220-235, just west of the town of Belfield.

All of the potentially culturally related anomalies are included in the general listing of anomalies in Table 9, but, except for the positive anomaly in the reservoir, were not used in the statistical calculations.

### 3. Summary and Recommendations

The distribution of radioactivity anomalies in the Dickinson Quadrangle is disperse and uneven.  $^{214}\text{Bi}$  anomalies and the positive  $^{214}\text{Bi}/^{208}\text{Tl}$  anomalies show similar patterns with concentrations in the southern and west-northcentral portion of the area. The negative  $^{214}\text{Bi}/^{208}\text{Tl}$  anomalies are concentrated primarily in the southern, northwestern and northeastern portion of the area. The lower part of the Tongue River Member contains 67% of these coincidence stations.

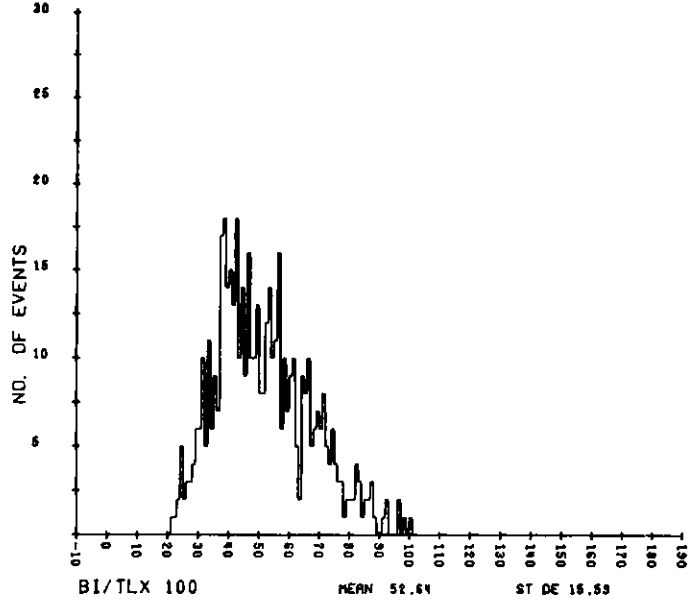
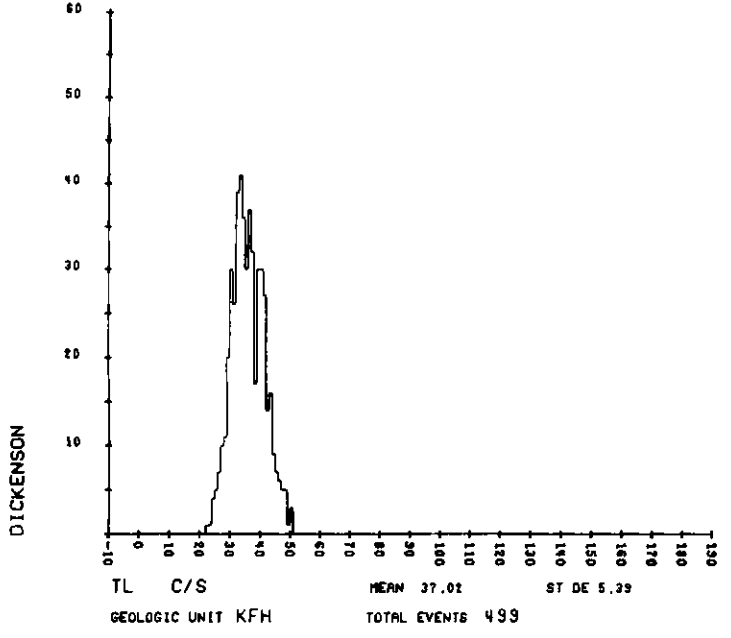
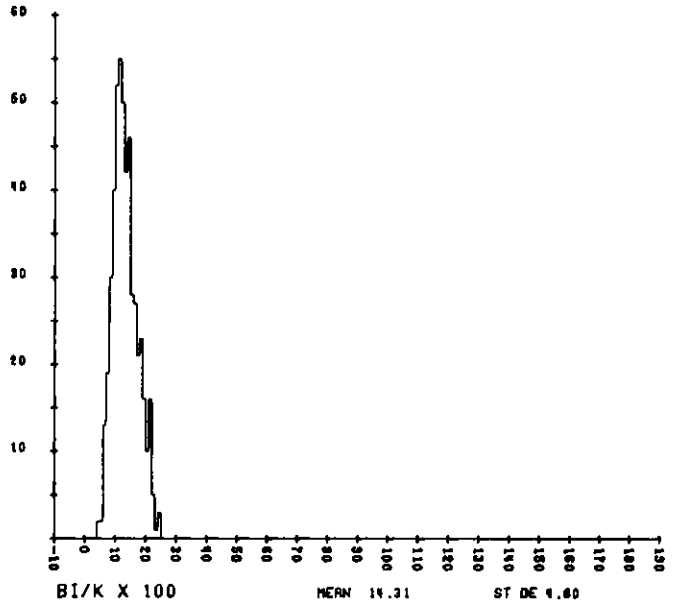
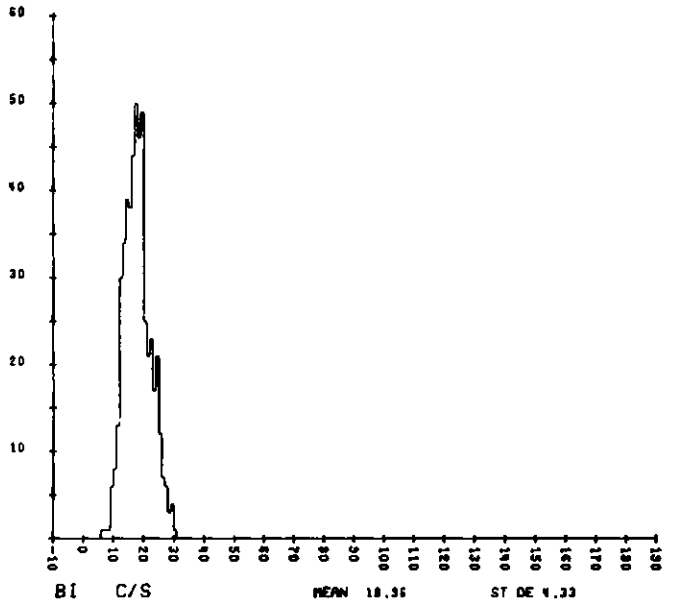
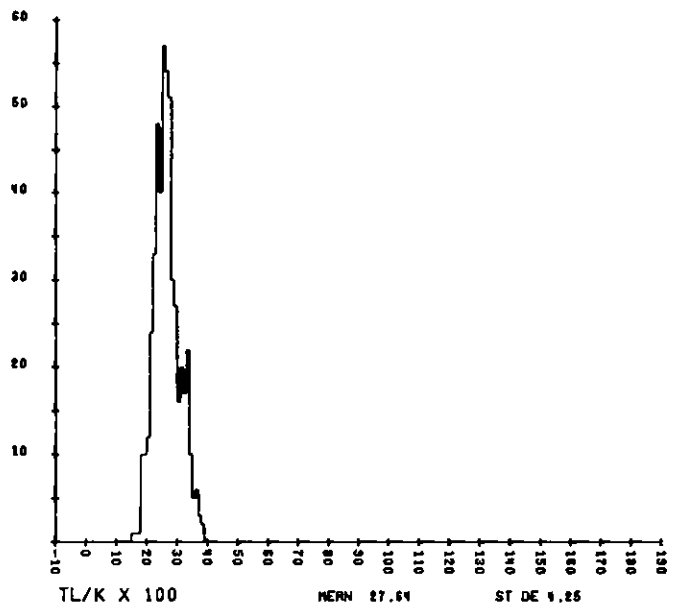
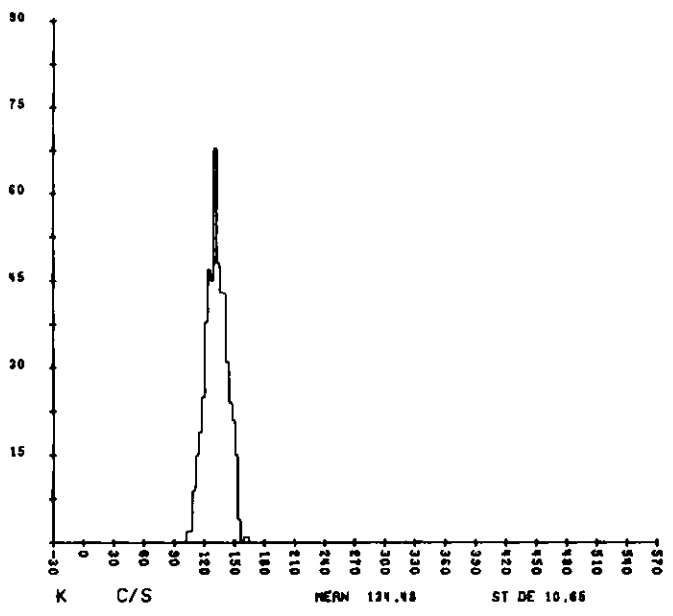
A total of 12 geologic units showed anomalous values: Qa, Tw, Tb, Tc, Tg, Tfs, Tft, Tfc, Khc, Kfh and Kp. When the number of anomalies per unit is normalized against the number of times the unit was encountered in flight, there is little statistical difference between units. However, unit Khc has a significantly higher concentration of  $^{214}\text{Bi}$  anomalies than the other units; and the Cannonball Member of the Fort Union Formation and the alluvium unit have significantly higher numbers of negative  $^{214}\text{Bi}/^{208}\text{Tl}$  anomalies than the other units.

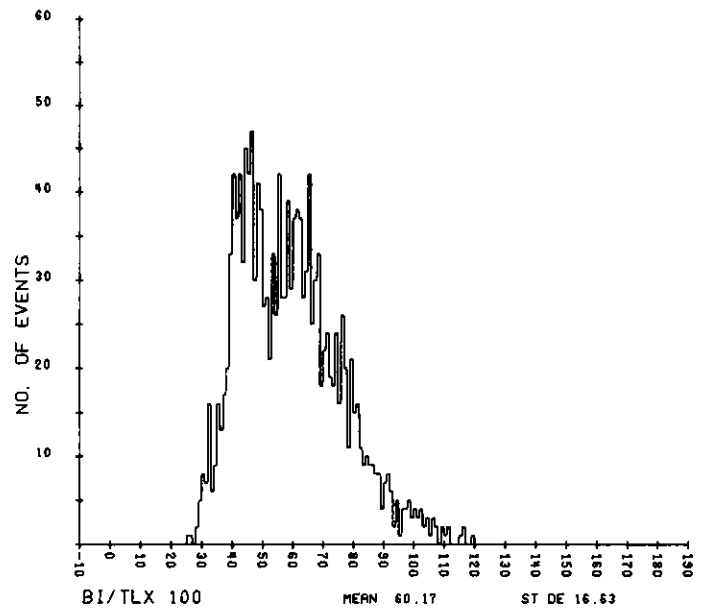
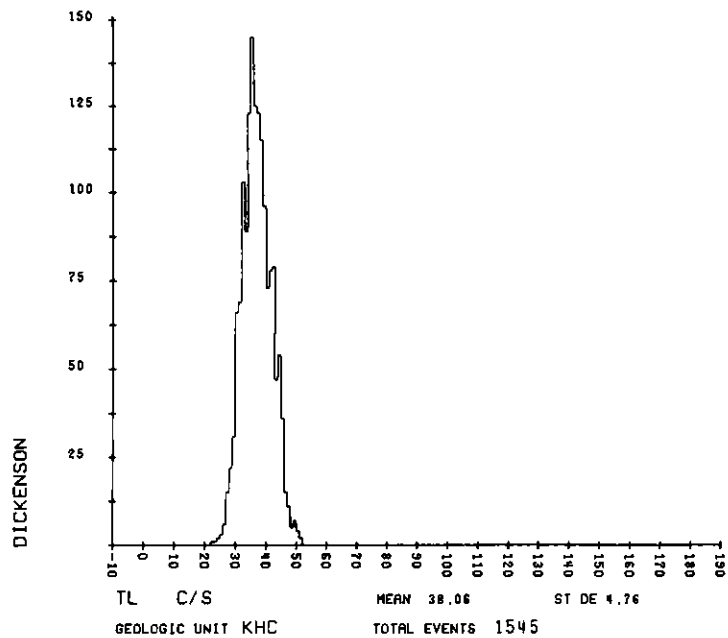
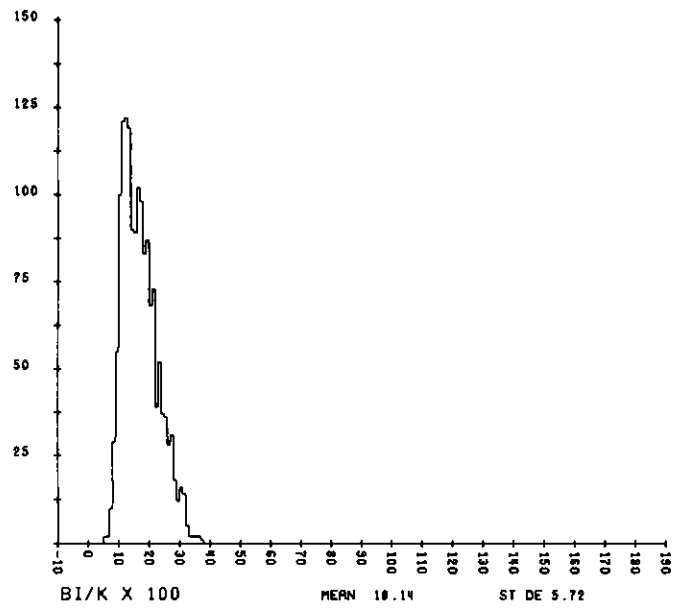
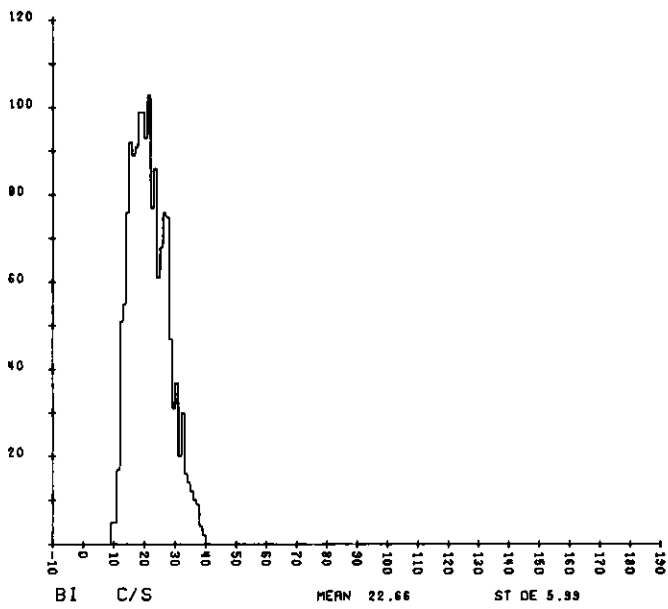
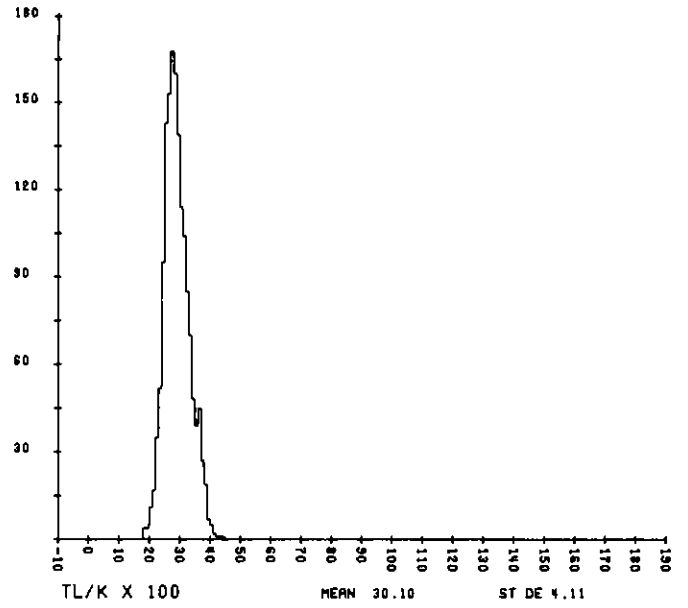
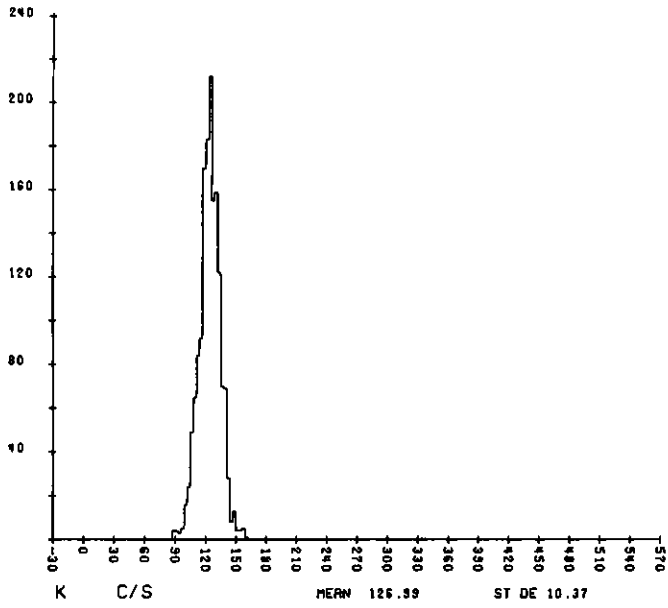
Some radioactive anomalies appear to be associated with known outcrops of uranium-bearing lignites such as in Medicine Pole Hills and Bullion Butte areas, but there are numerous other anomalies, especially in the Fort Union Formation that bear no obvious relationship to the uranium-bearing lignites. This may be a reflection of near-surface water movements or, possibly, epigenetic mineralization.

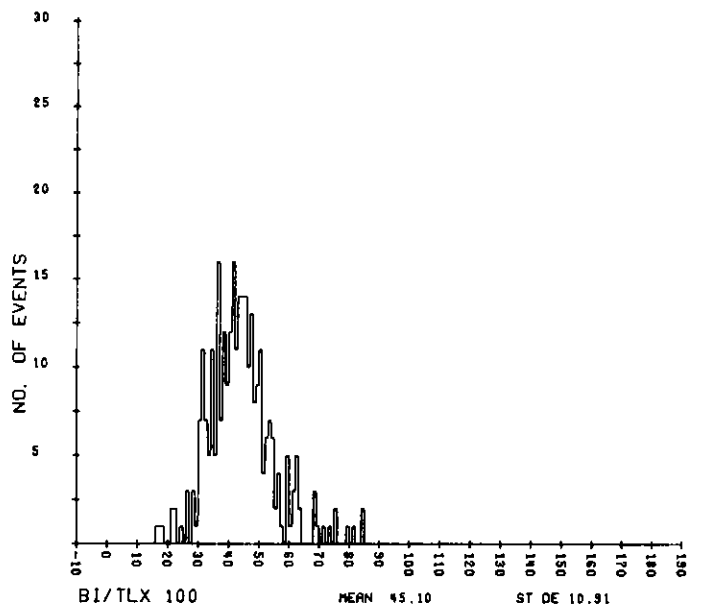
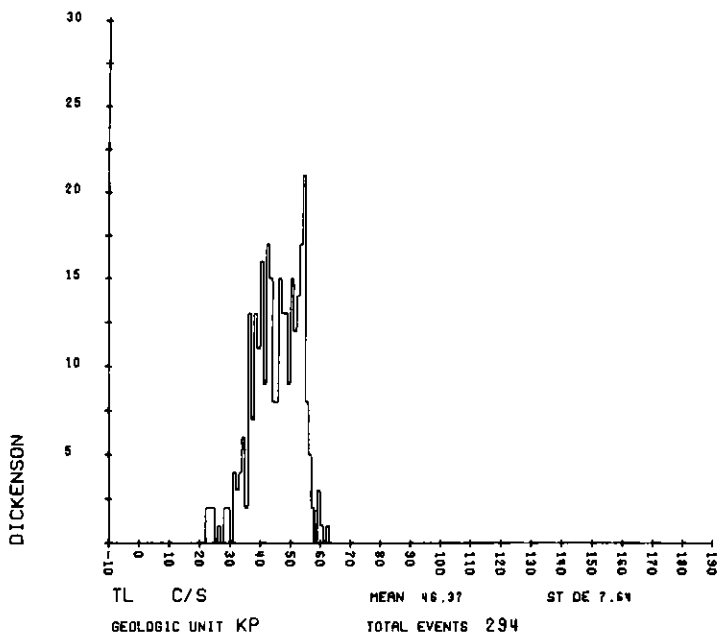
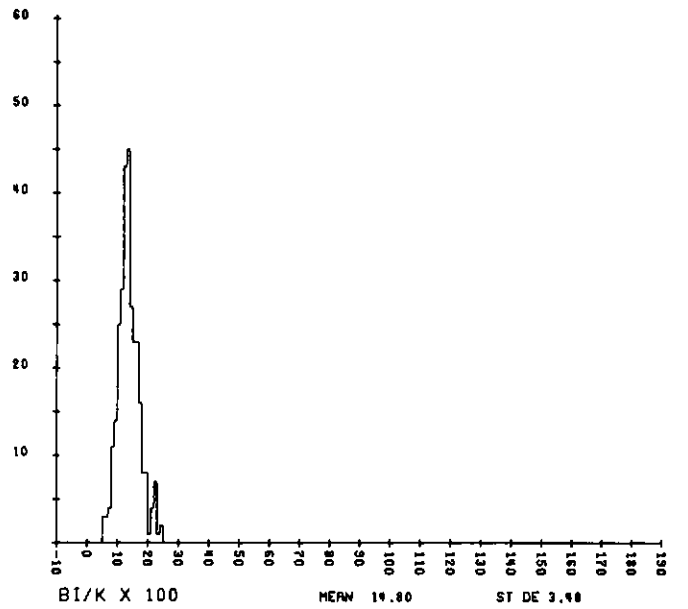
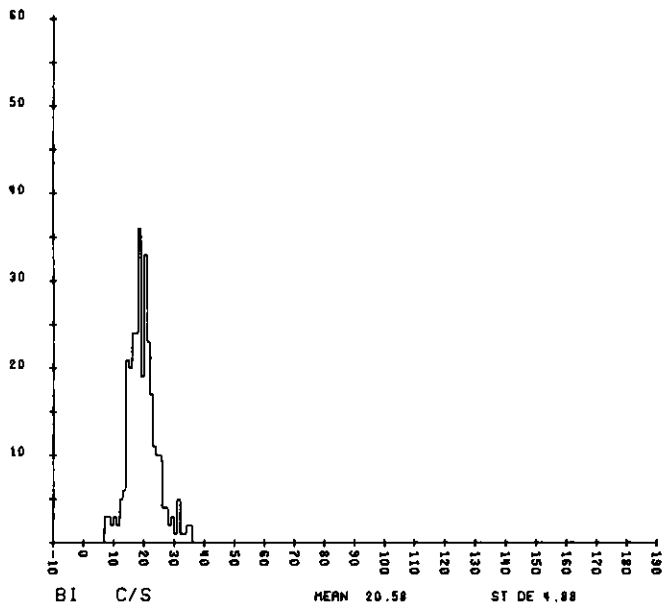
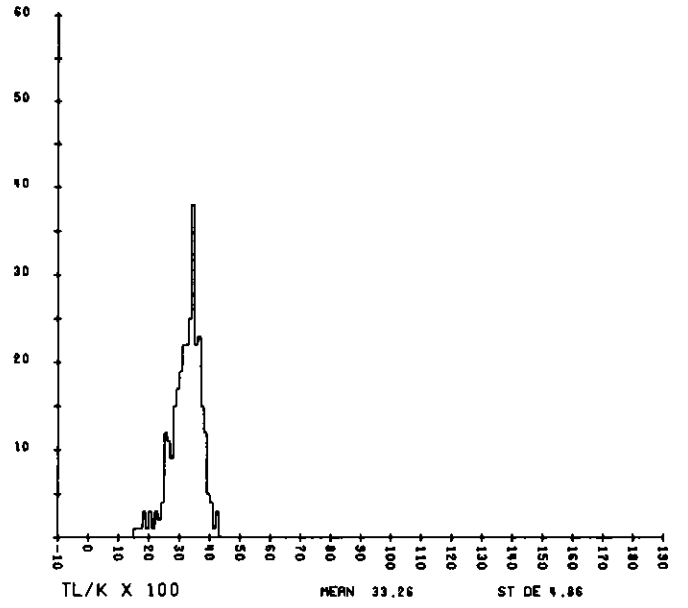
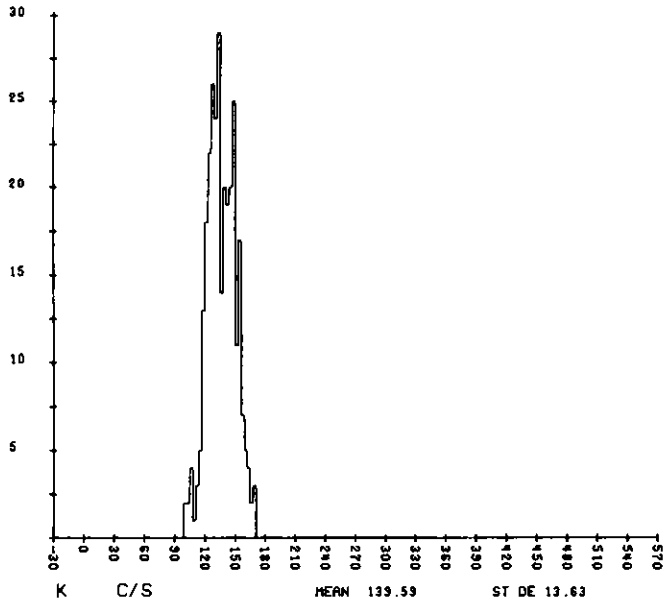
APPENDIX I

FREQUENCY DISTRIBUTION OF RADIATION DATA

AS A FUNCTION OF GEOLOGIC UNIT

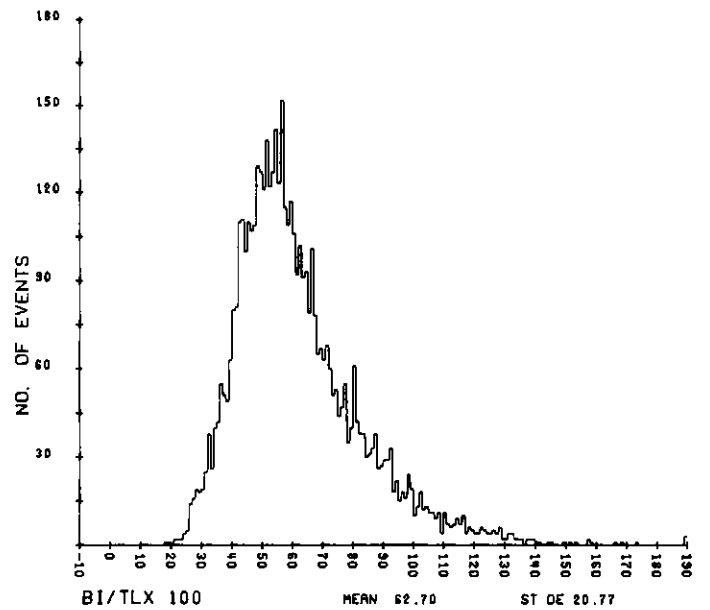
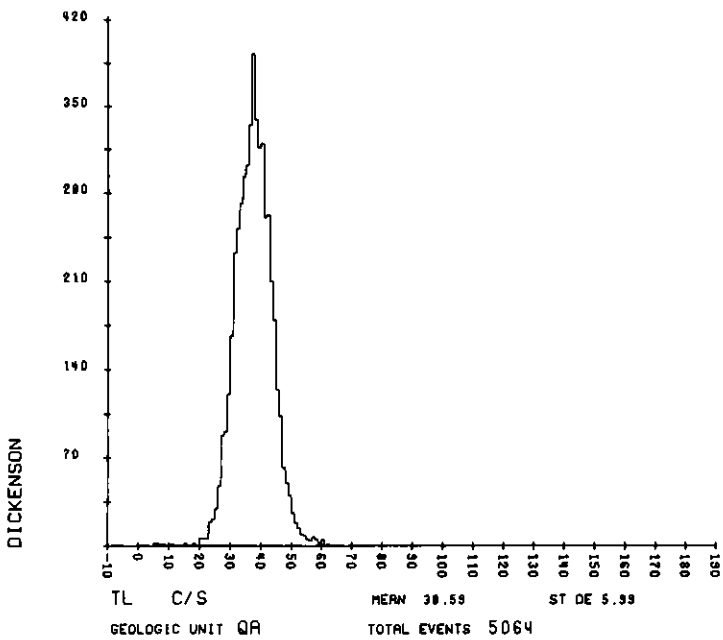
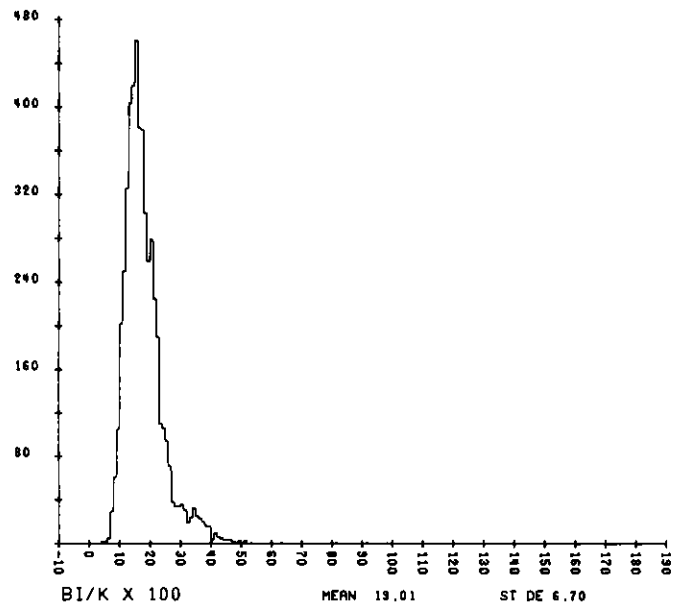
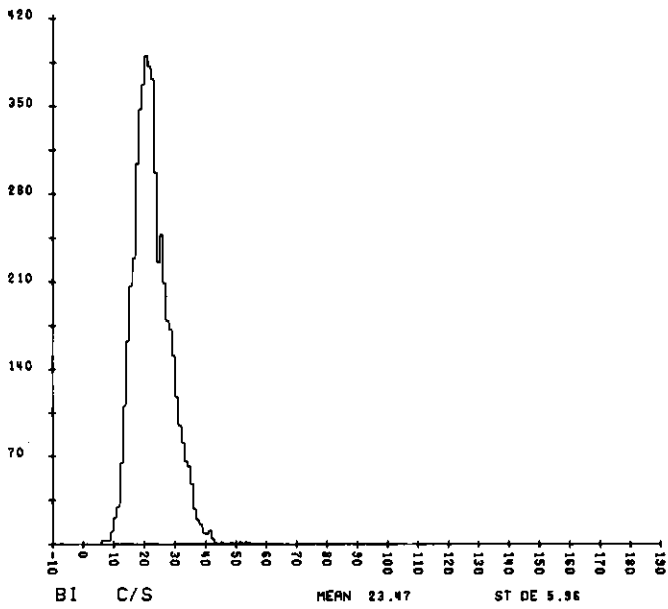
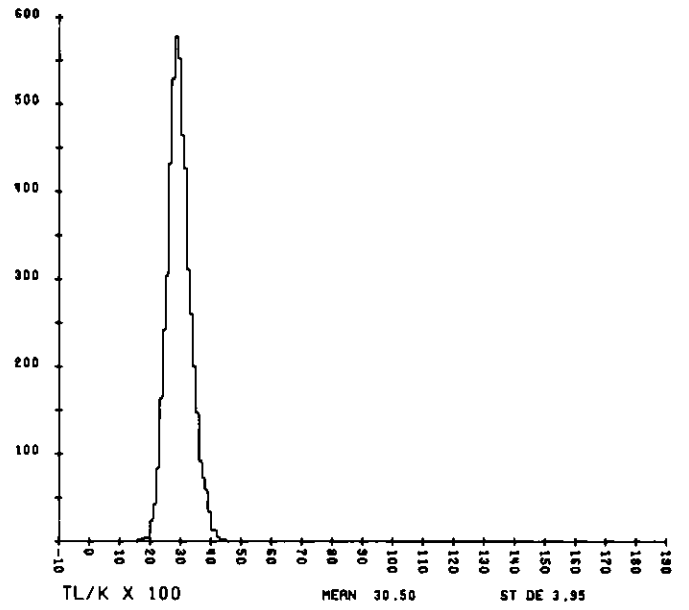
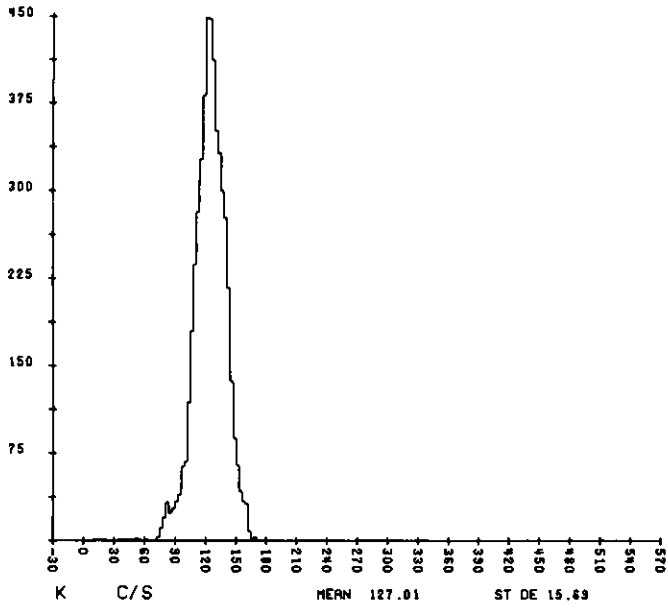




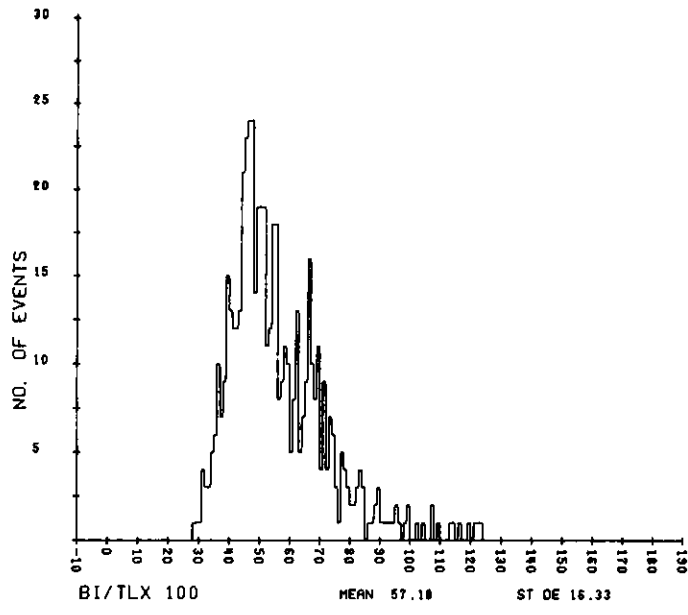
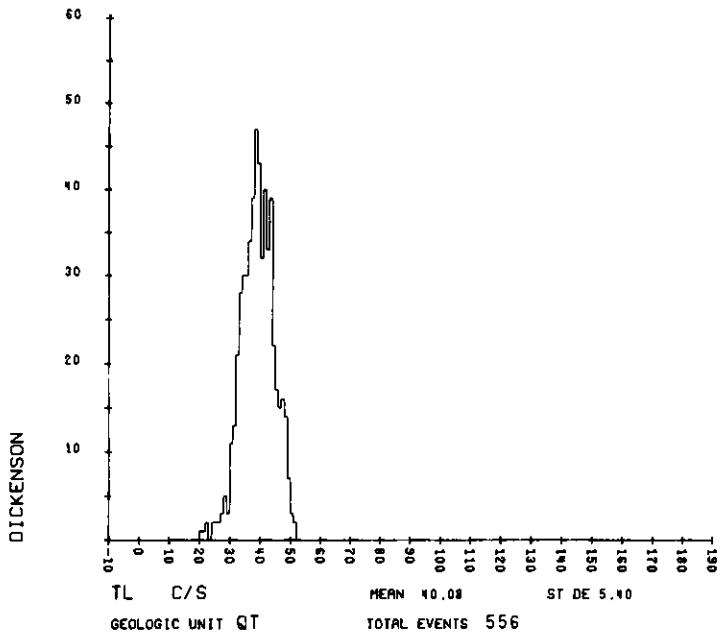
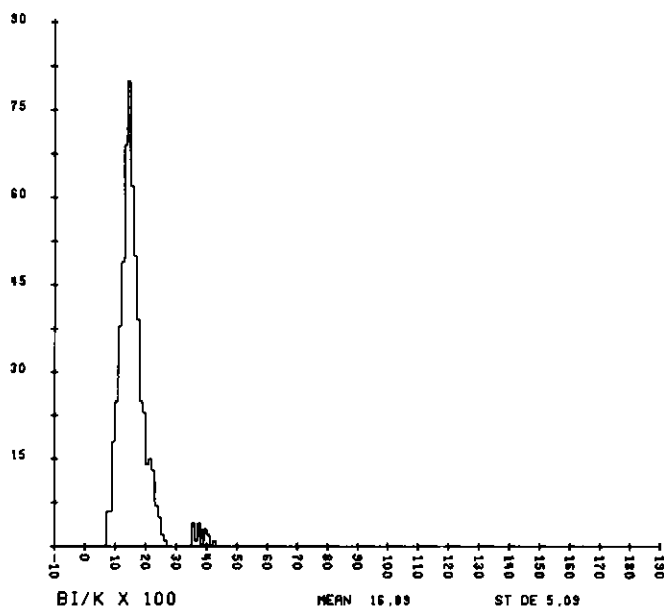
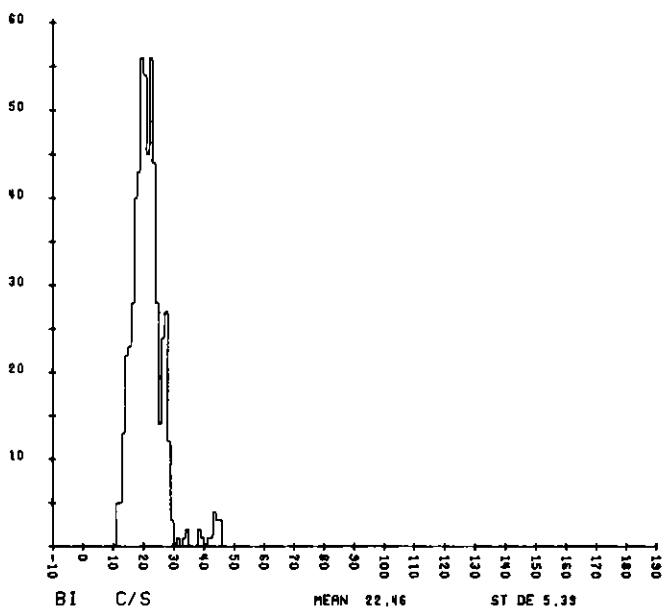
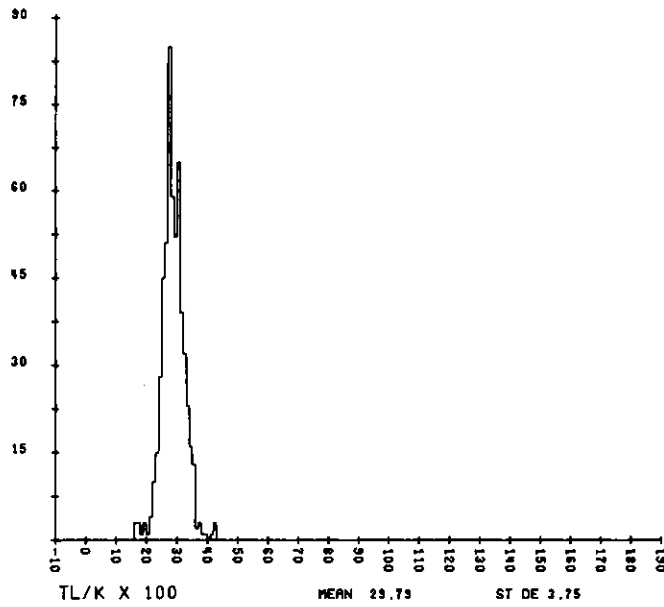
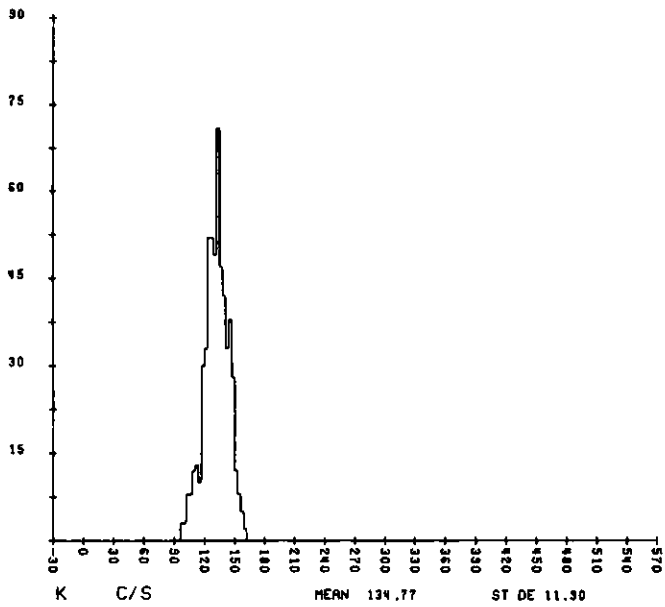


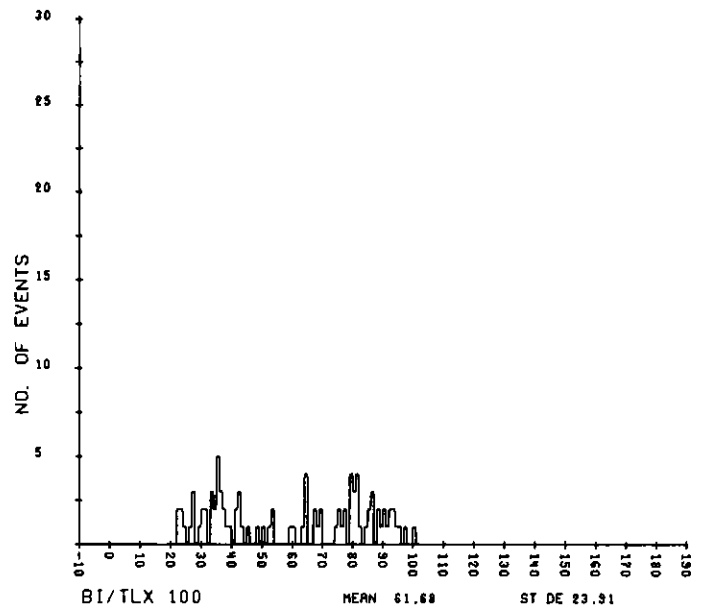
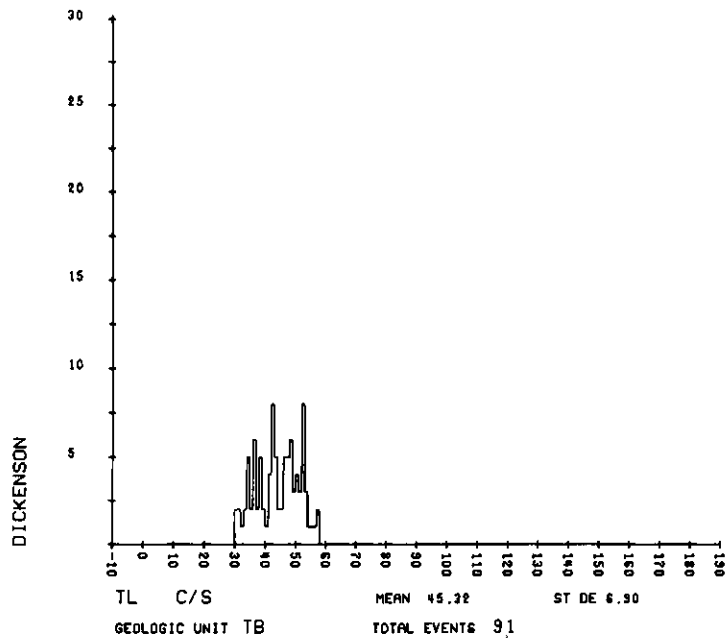
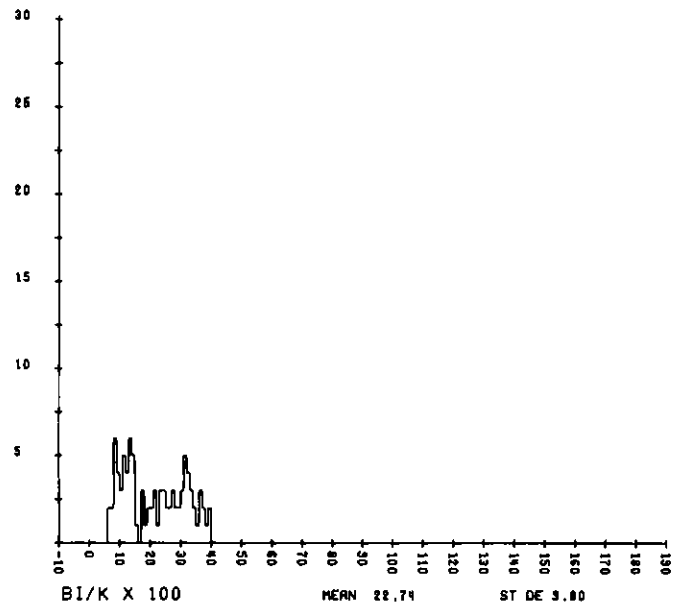
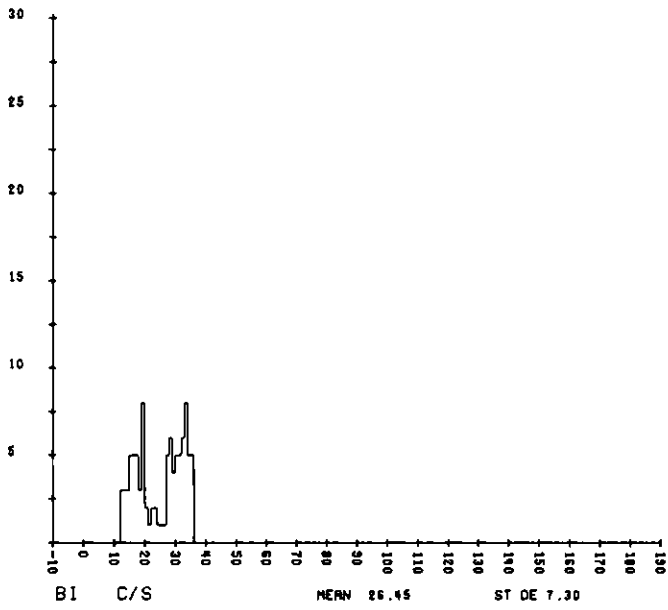
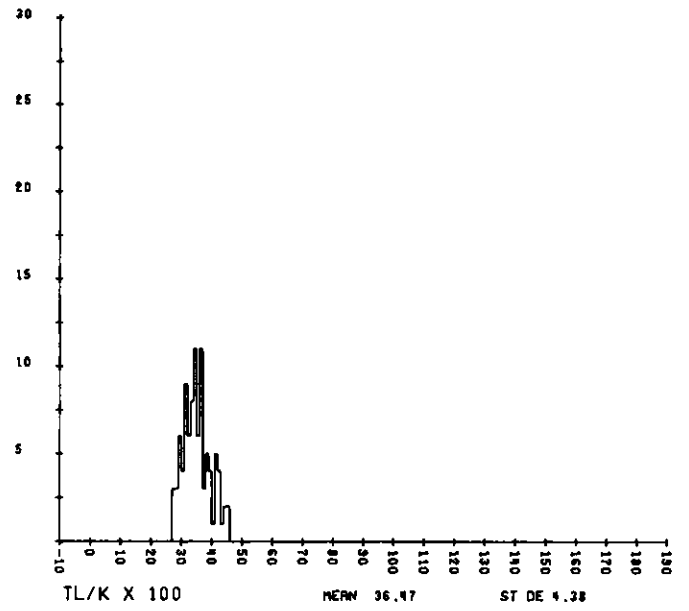
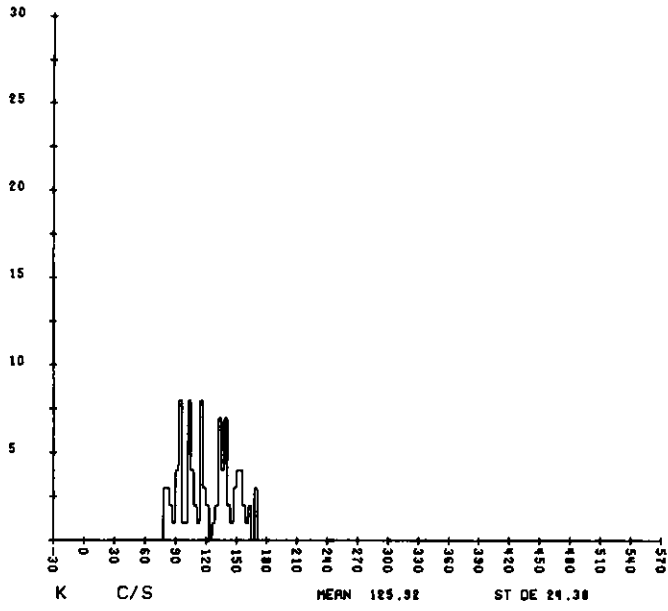
DICKENSON

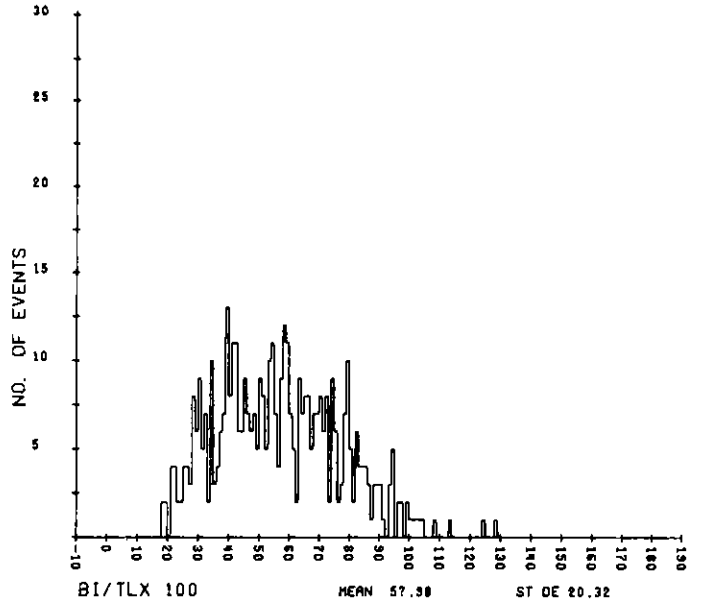
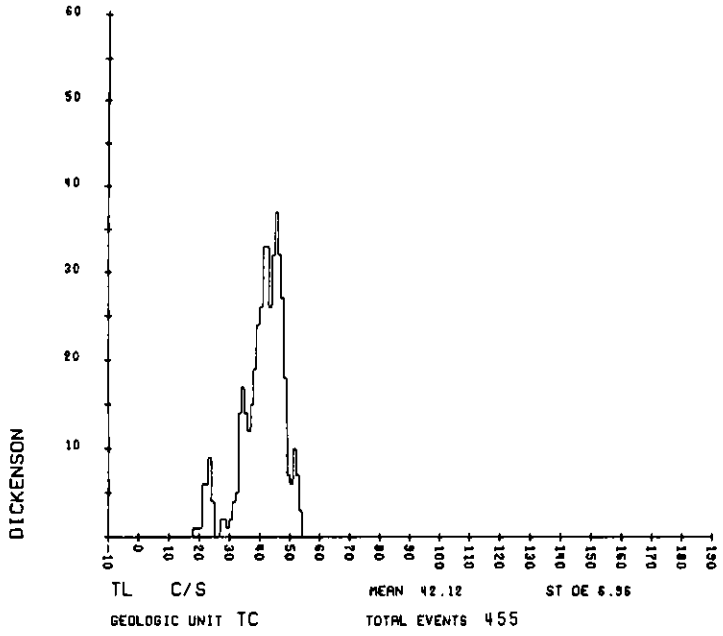
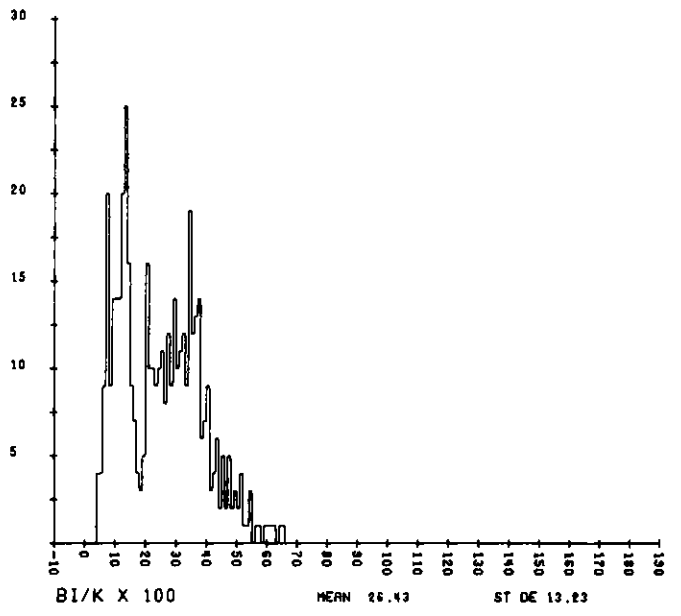
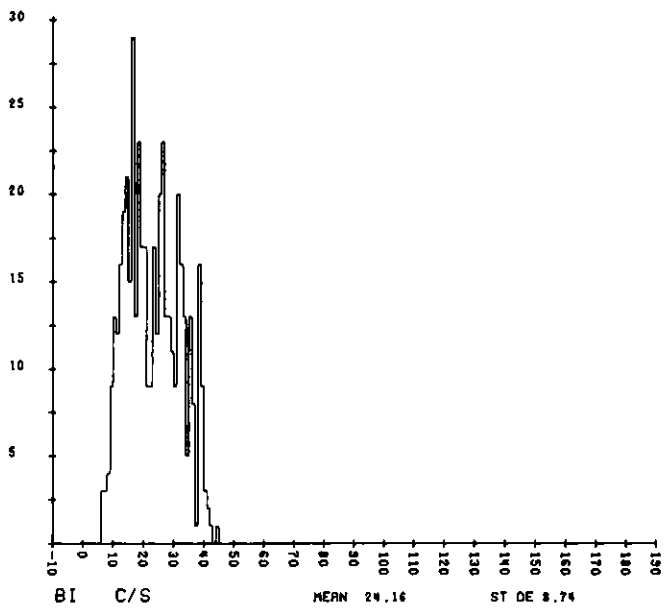
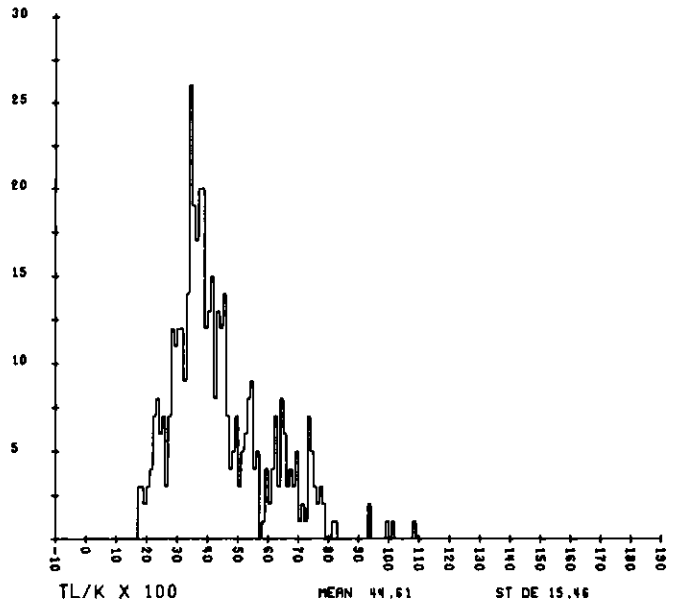
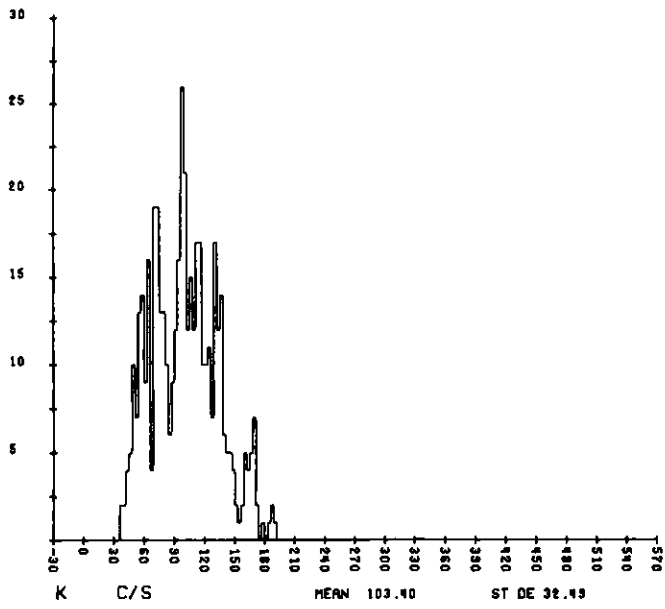
GEOLOGIC UNIT KP





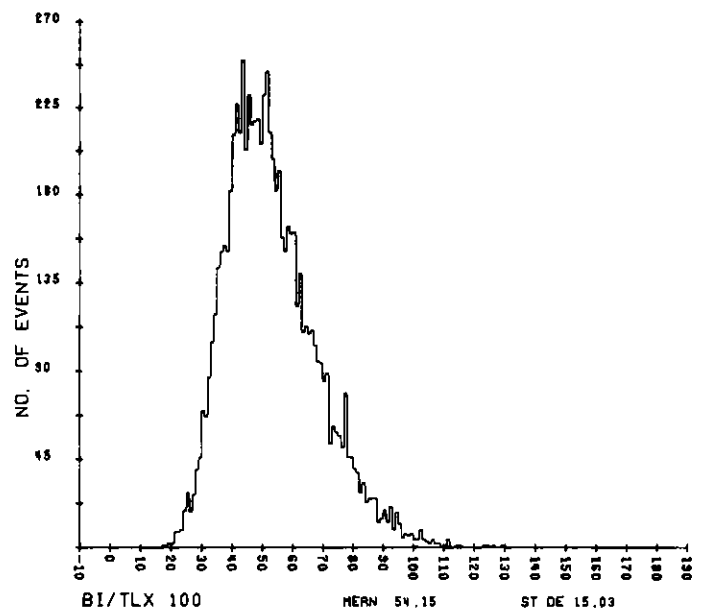
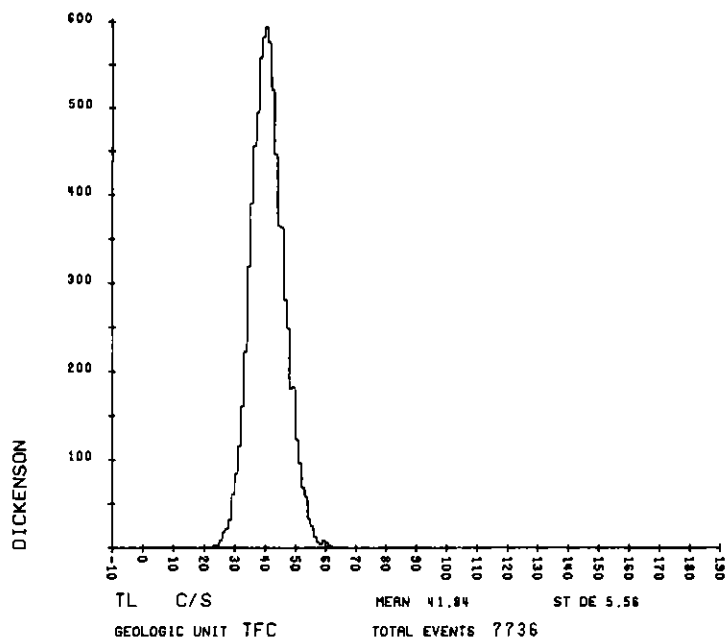
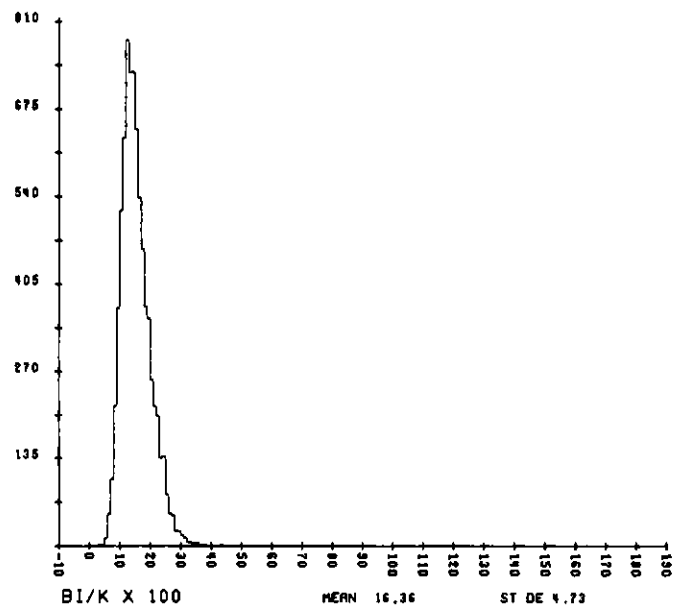
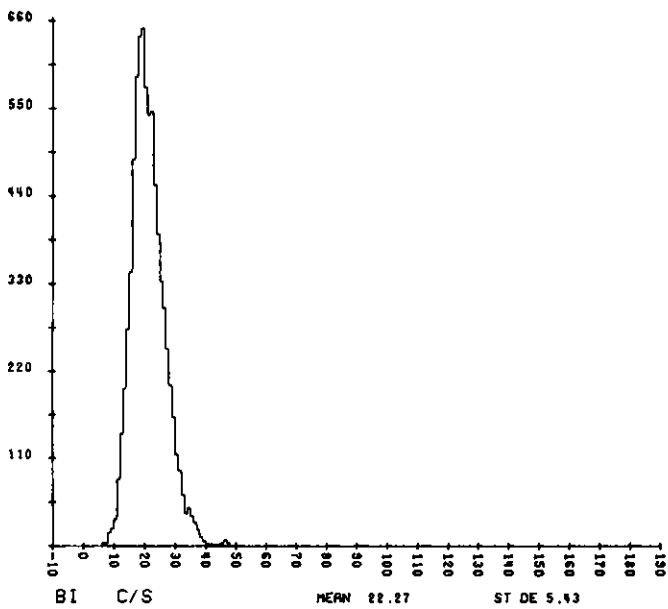
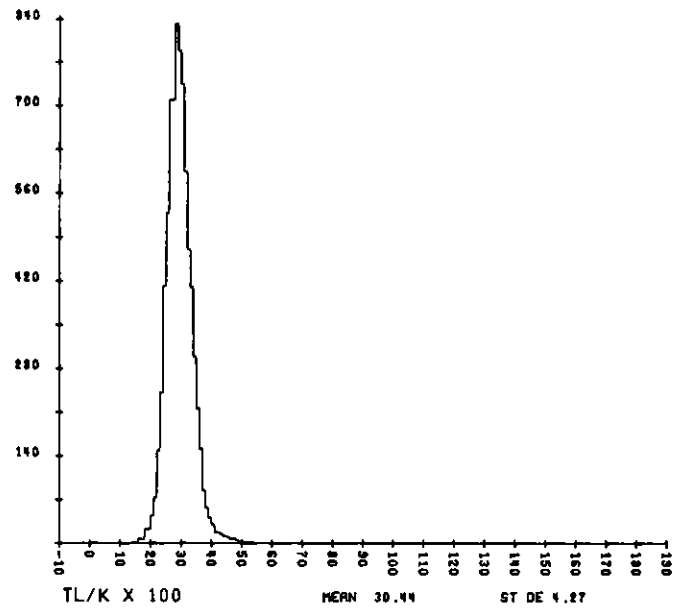
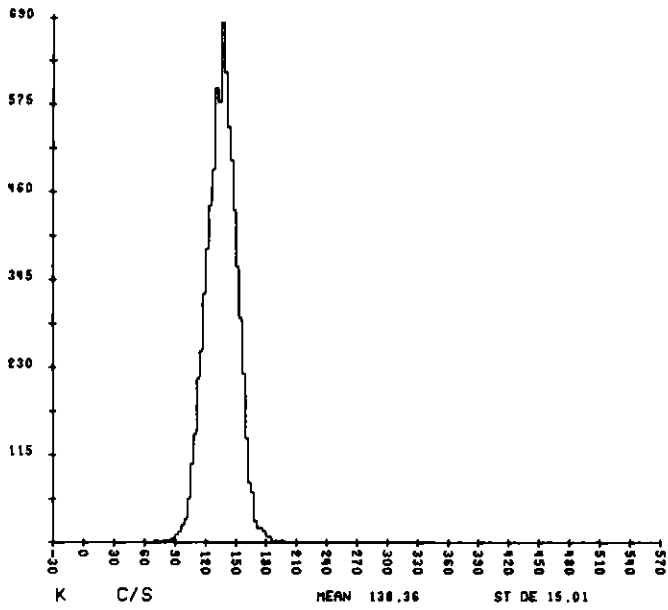


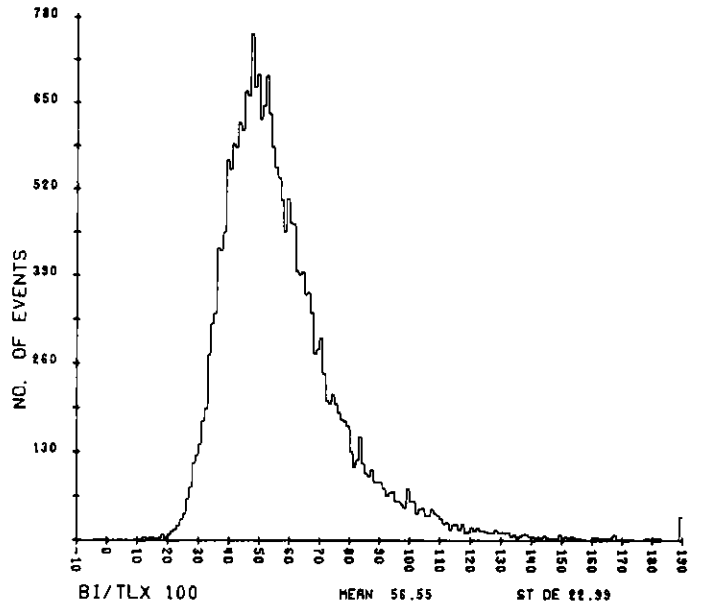
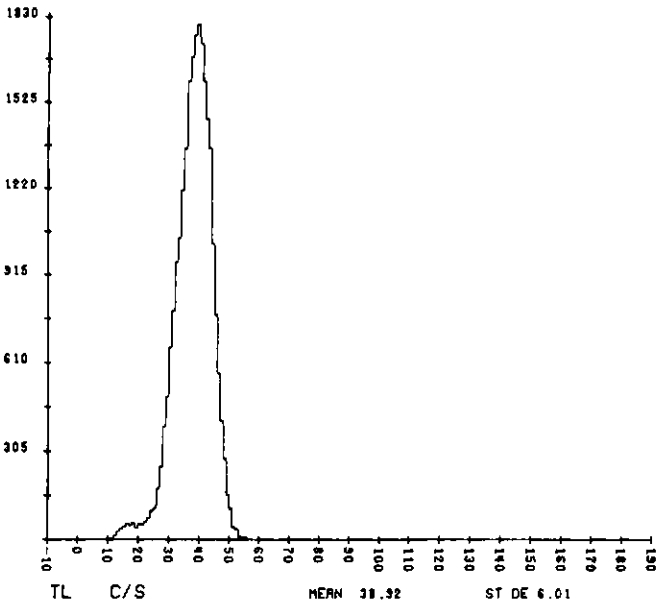
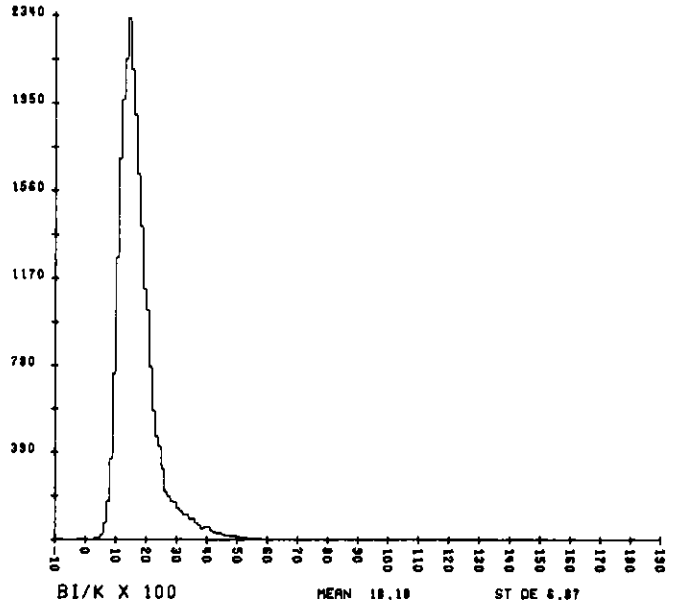
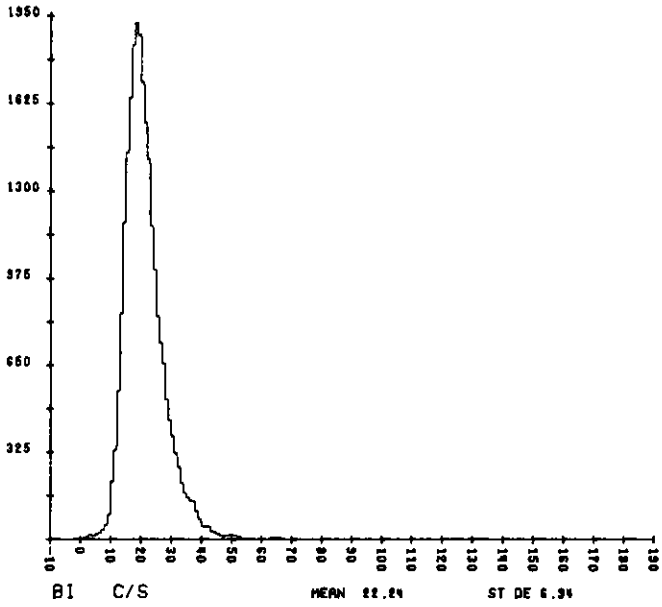
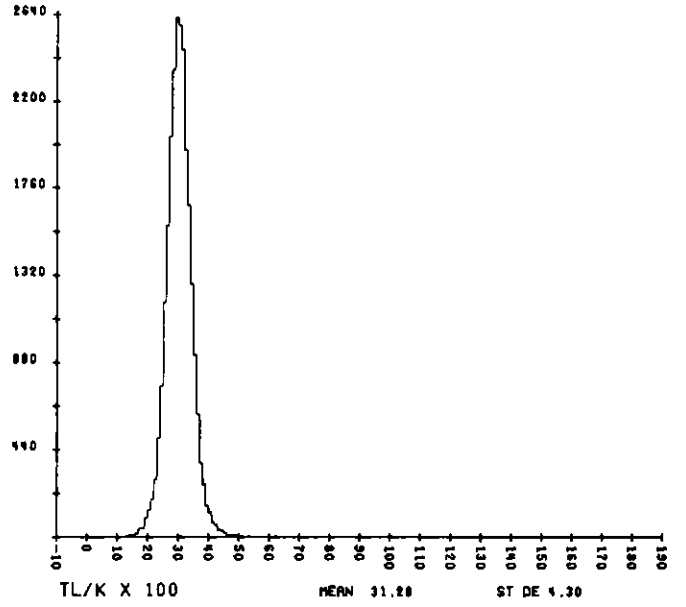
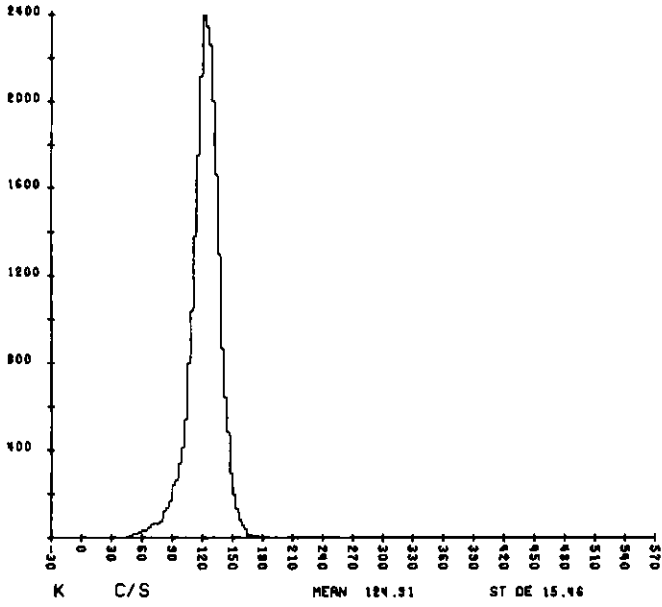




DICKENSON

GEOLOGIC UNIT TC

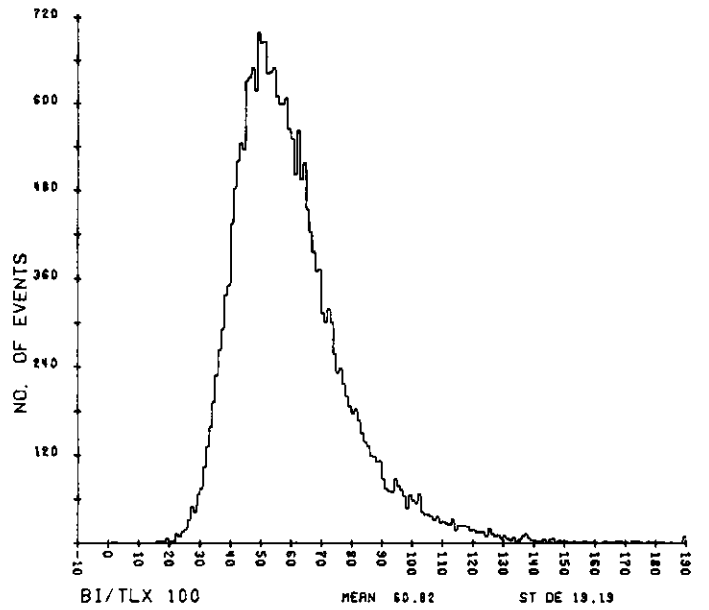
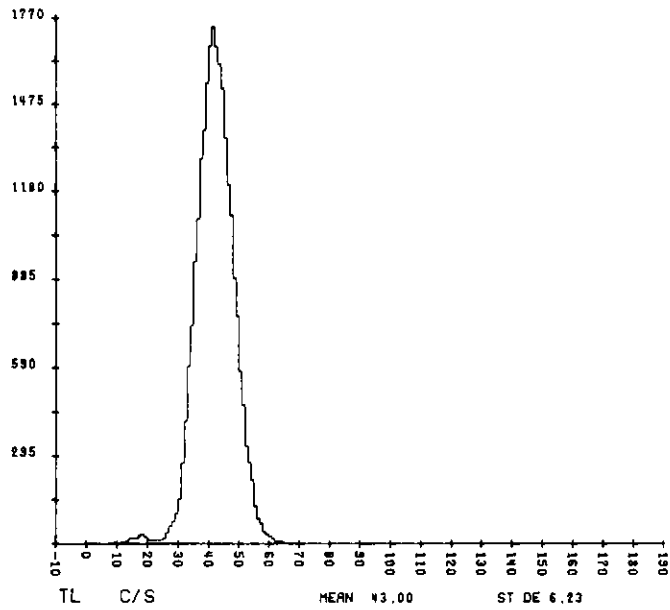
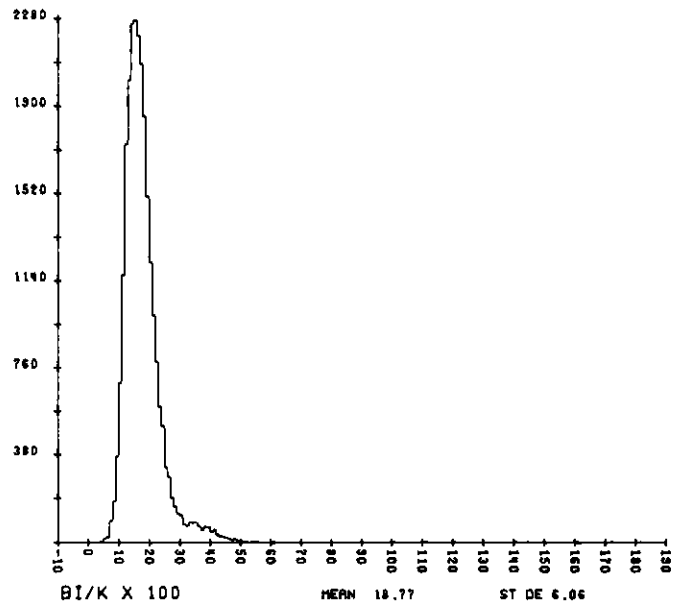
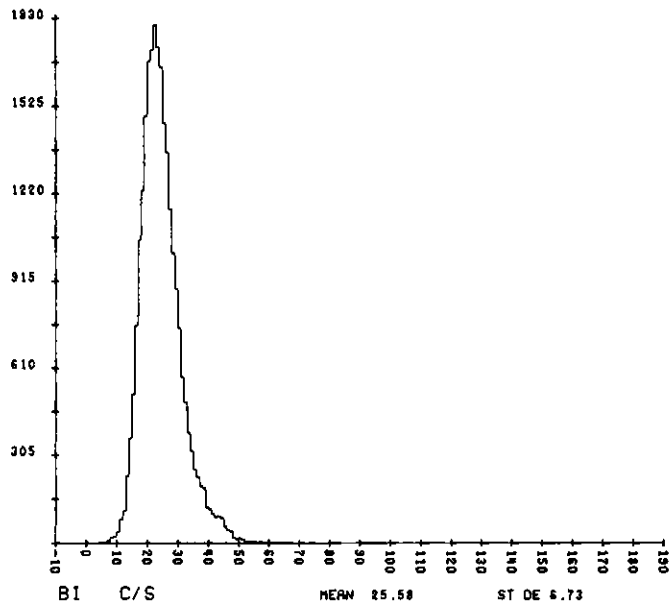
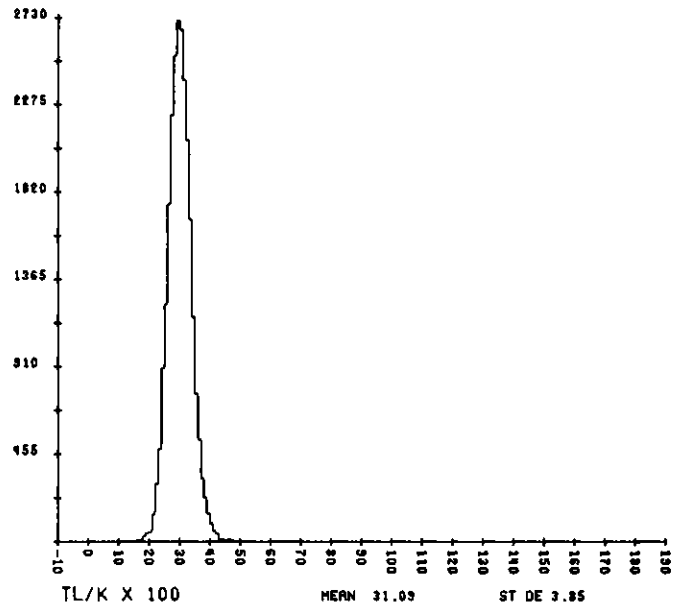
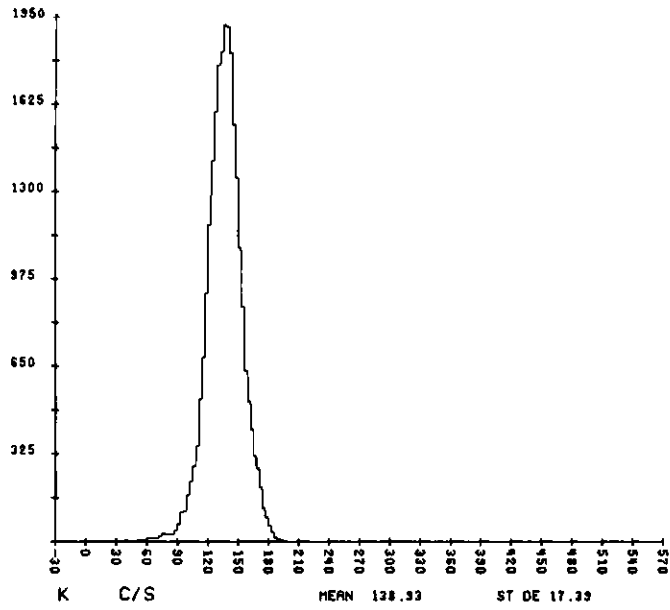




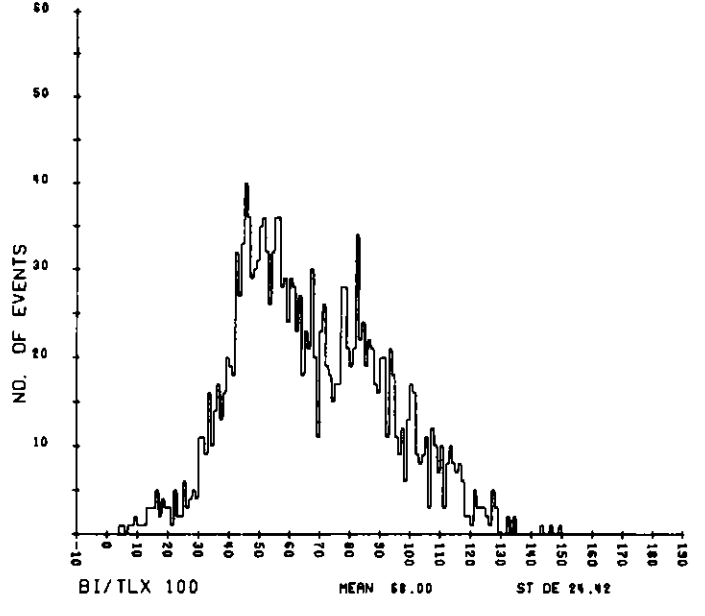
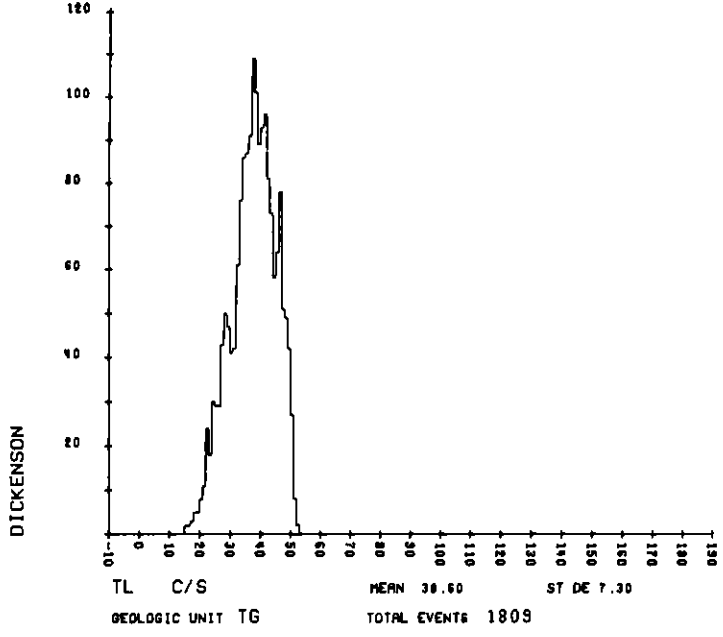
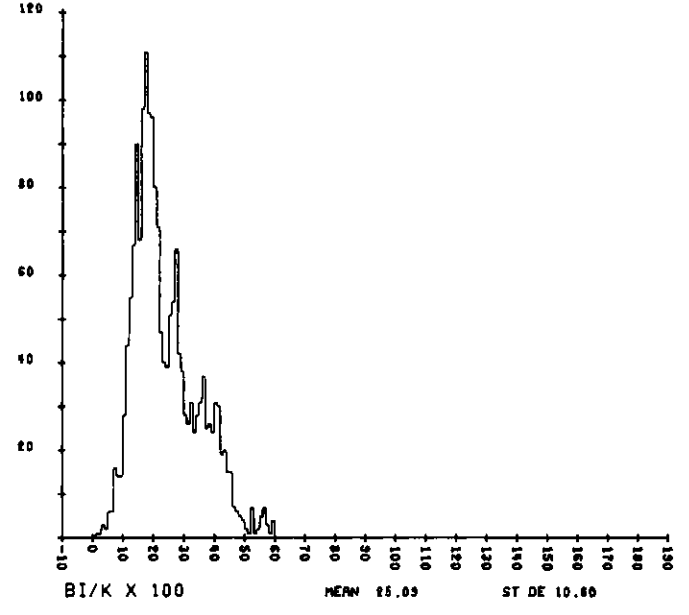
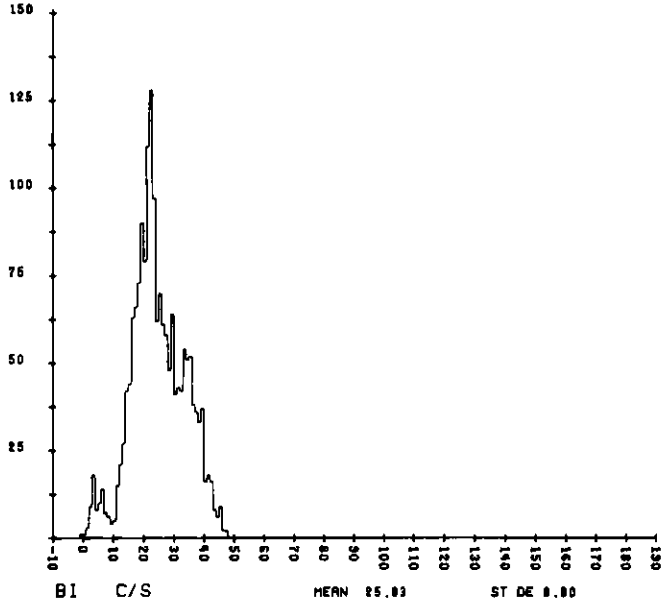
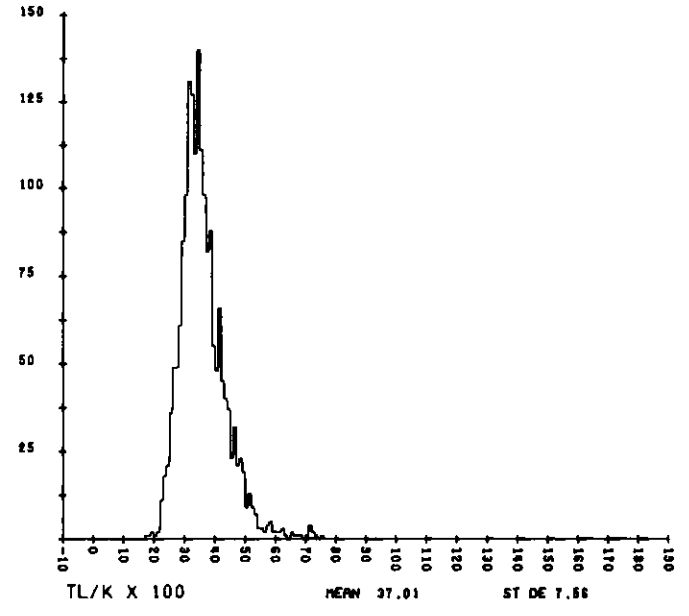
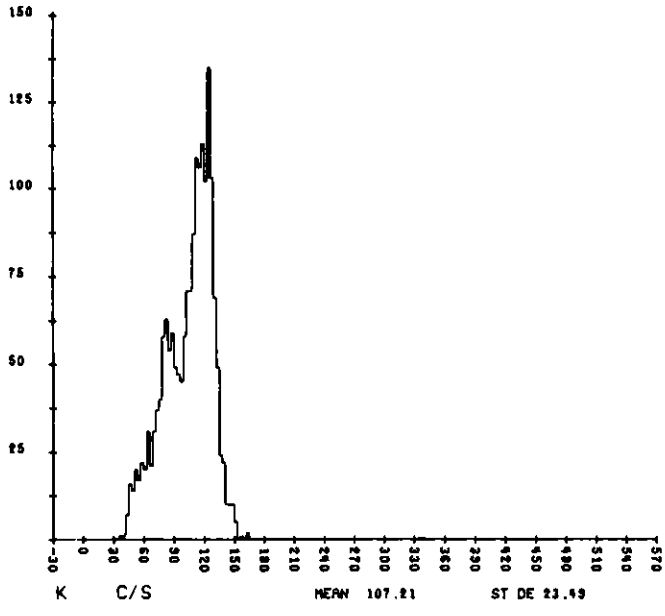
DICKENSON

GEOLOGIC UNIT TFS TOTAL EVENTS 24571

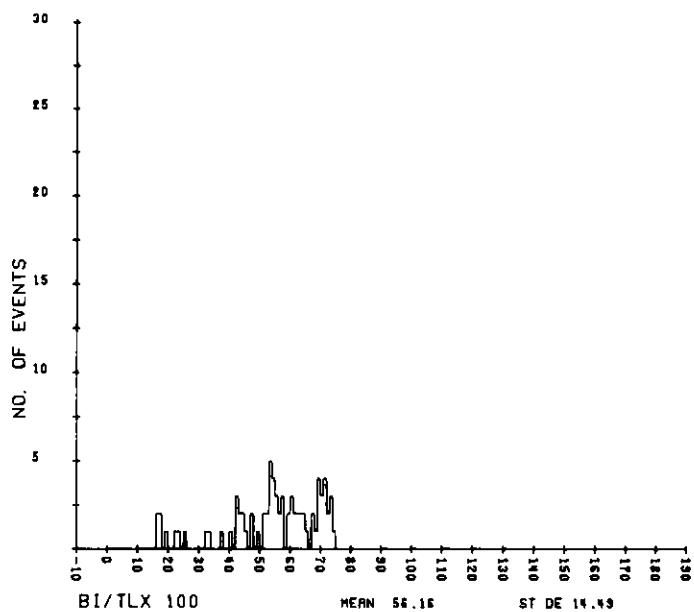
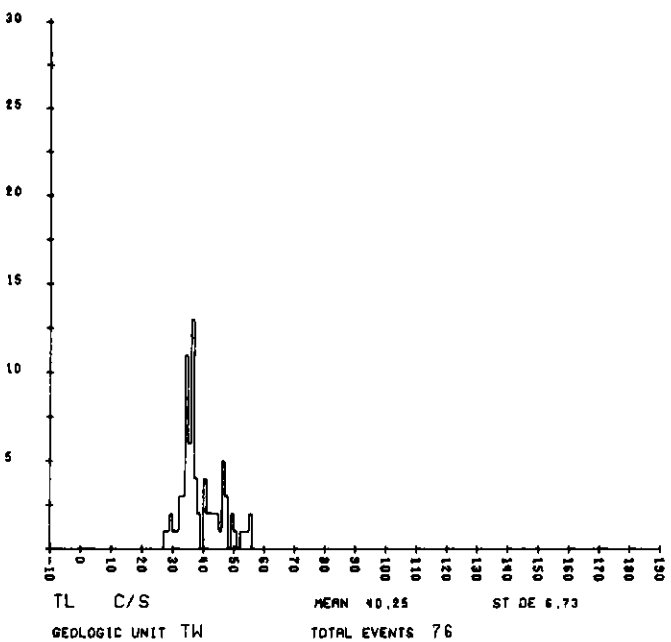
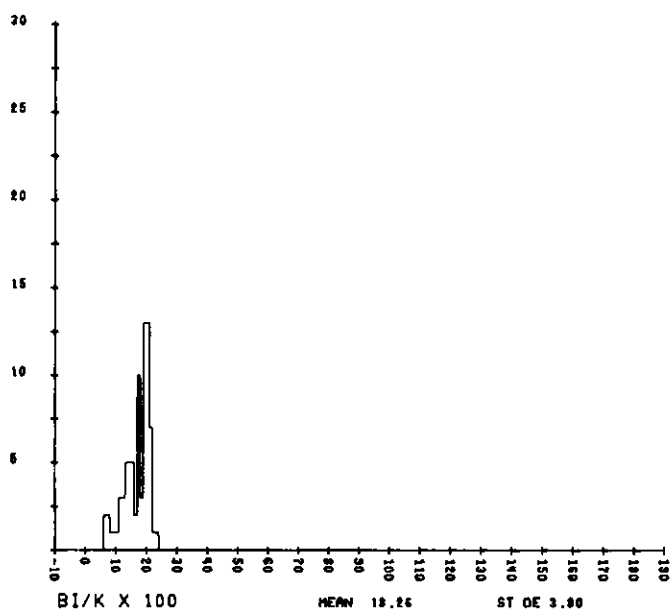
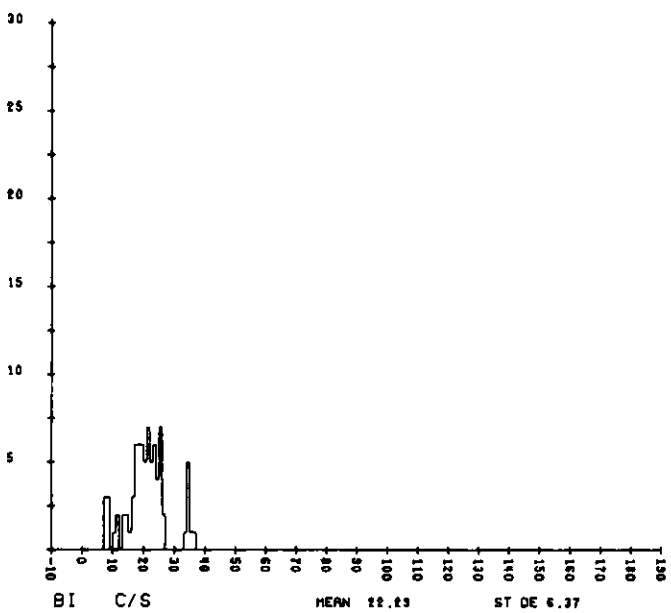
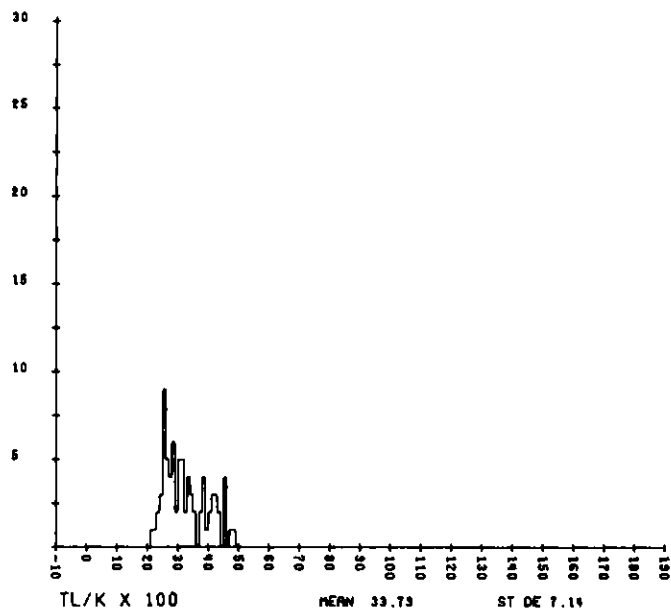
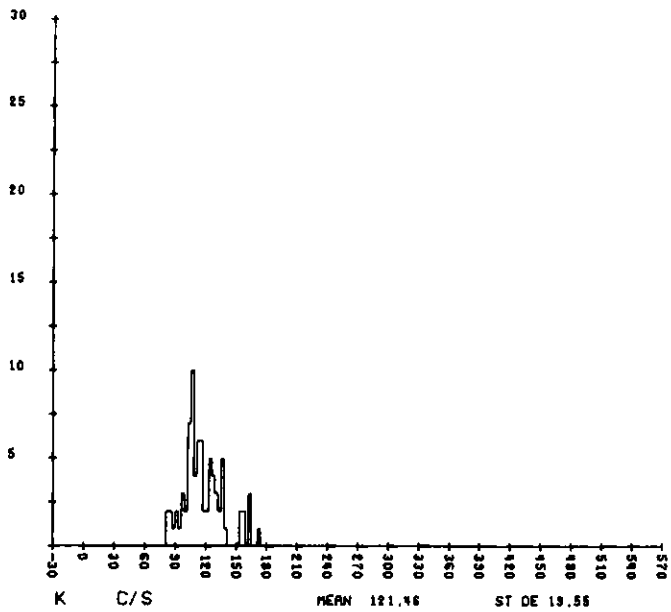
DICKENSON



GEOLOGIC UNIT TFT TOTAL EVENTS 24738



DICKENSON





APPENDIX II

DESCRIPTION OF MAGNETIC TAPES AND LISTINGS

A. DESCRIPTION OF DATA TAPES

A1. General

All data tapes are 9-track, 800 BPI (NRZI), odd parity, EBCDIC code. Each tape contains a gum label giving the survey project name, month and year of survey, tape type, subcontractor name, date tape created, tape reel count, tape recording characteristics, block size in Bytes and location of tape format information.

The general description for each of the tape types is as follows:

<u>Block Number</u>	<u>Description</u>
1	Format Description
2	Tape Identification
3	First Data Block
4	Second Data Block
.	.
.	.
.	Last Data Block
EOF	

A2. Raw Spectral Data Tapes

Block Size (Physical Record): 6600 characters  
 Logical Record, Data : 1100 characters

1. Format Description Block (Block 1)

The Format Description utilizes 4248 characters. The remaining 2352 characters of this block are blanks.

<u>Line Number</u>	<u>Character Number</u>	
1	01 0978	(DATA TAPE TYPE AND FORMAT SPECIFICATION DATE CODES)
2		
3		RAW SPECTRAL DATA TAPE
4		
5		FORMAT FOR TAPE IDENTIFICATION BLOCK (SECOND BLOCK ON TAPE)
6		
7	ITEM	FORMAT DESCRIPTION
8	1	A40 QUADRANGLE NAME AS PROJECT IDENTIFICATION
9	2	A20 NAME OF SUBCONTRACTOR
10	3	I4 APPROXIMATE DATE OF SURVEY (MONTH, YEAR)

Line Number	12345678901234567890123456789012345678901234567890123456789012	Character Number	
11	4	I1	AERIAL SYSTEM IDENTIFICATION CODE
12	5	A20	AIRCRAFT IDENTIFICATION BY TYPE AND FAA NUMBER
13	6	I3	BFEC CALIBRATION REPORT NUMBER
14	7	F6.3	4PI SYSTEM DATA COLLECTION INTERVAL TO THREE DECIMAL PLACES IN SECONDS
15			
16	8	F6.3	2PI SYSTEM DATA COLLECTION INTERVAL TO THREE DECIMAL PLACES IN SECONDS
17			
18	9	I3	NUMBER OF CHANNELS (0-3 MEV) FOR 4PI SYSTEM
19	10	I3	NUMBER OF CHANNELS (0-3 MEV) FOR 2PI SYSTEM
20	11	I3	NUMBER OF FLIGHT LINES ON THIS TAPE
21	12	I4	FIRST FLIGHT LINE NUMBER ON THIS TAPE
22	13	I6	FIRST RECORD NUMBER OF FIRST FLIGHT LINE
23	14	I3	JULIAN DATE (DAY OF YEAR) FIRST FLIGHT LINE WAS COLLECTED
24			
25	15-17	I4,I6,I3	REPEAT OF ITEMS 12-14 FOR SECOND FLIGHT LINE ON THIS TAPE
26			
27	*	*	*
28	*	*	*
29	*	*	*
30	306-308	I4,I6,I3	REPEAT OF ITEMS 12-14 FOR 99TH FLIGHT LINE ON THIS TAPE
31			
32			
33			FORMAT FOR RAW SPECTRAL DATA RECORD (THIRD THRU LAST BLOCK ON TAPE)
34			
35	ITEM	FORMAT	DESCRIPTION
36	1	I1	AERIAL SYSTEM IDENTIFICATION CODE
37	2	I4	FLIGHT LINE NUMBER
38	3	I6	RECORD IDENTIFICATION NUMBER
39	4	I6	GMT TIME OF DAY (HHMMSS)
40	5	F8.4	LATITUDE TO FOUR DECIMAL PLACES IN DEGREES
41	6	F8.4	LONGITUDE TO FOUR DECIMAL PLACES IN DEGREES
42	7	F6.1	TERRAIN CLEARANCE TO ONE DECIMAL PLACE IN METERS
43	8	F7.1	TOTAL MAGNETIC FIELD INTENSITY TO ONE DECIMAL PLACE IN GAMMAS
44			
45	9	A8	SURFACE GEOLOGIC MAP UNIT CODE
46	10	I4	QUALITY FLAG CODES
47	11	F4.1	OUTSIDE AIR TEMPERATURE TO ONE DECIMAL PLACE IN DEGREES CELSIUS
48			
49	12	F5.1	OUTSIDE AIR PRESSURE TO ONE DECIMAL PLACE IN MMHG
50	13	F5.3	LIVE TIME COUNTING PERIOD TO THREE DECIMAL PLACES IN SECONDS
51			
52	14	I4	SUMMED RAW OUTPUT FROM COSMIC CHANNELS (3-6 MEV) IN COUNTS
53			
54	15	I4	RAW OUTPUT FROM CHANNEL 1 IN COUNTS
55	16	I4	RAW OUTPUT FROM CHANNEL 2 IN COUNTS
56	*	*	*
57	*	*	*
58	*	*	*
59	270	I4	RAW OUTPUT FROM CHANNEL 256 IN COUNTS
-	-	-	2352 BLANK CHARACTERS

2. Tape Identification Block (Block 2)

The information and format for this block are indicated in lines 8 through 30 of the Format Description Block A2.1, and 1396 characters are produced. The remaining 5204 characters in this block are blanks.

If fewer than 99 flight lines exist, the unused flight line information, 13 characters per flight line, is filled with 9's through the 99th flight line.

3. Raw Spectral Data Blocks

The information and format for the logical records in these blocks are indicated in lines 36 through 59 of the Format Description Block A2.1. One logical record contains 1100 characters. There are six such logical records per 6600 character physical record or block.

The  $2\pi$  data logical record is recorded after the corresponding  $4\pi$  data collection intervals at a frequency dependent on the  $2\pi$  system data collection interval. For example, if the  $4\pi$  data collection interval is 1 second and the  $2\pi$  data collection interval is 10 seconds, then 10 records of  $4\pi$  data are recorded followed by 1 record of the  $2\pi$  data which was collected during the preceding 10 seconds. The format for the  $2\pi$  data is identical to that of the  $4\pi$  data, except for lines 40 through 49 of the Format Description Block given above. These variables are expressed in the  $2\pi$  record as all nines in the format specified for I and F fields, and all zeros for A fields.

A3. Single Record Reduced Data Tapes

Block Size (Physical Record): 6900 characters  
Logical Record, Data : 138 characters

1. Format Description Block (Block 1)

The Format Description utilizes 6768 characters. The remaining 132 characters of this block are blanks.

<u>Line</u> <u>Number</u>	<u>Character Number</u>
1	02 0978 (DATA TAPE TYPE AND FORMAT SPECIFICATION DATE CODES)
2	
3	SINGLE RECORD REDUCED DATA TAPE
4	
5	FORMAT FOR TAPE IDENTIFICATION BLOCK (SECOND BLOCK)
6	

Line Character Number  
 Number 12345678901234567890123456789012345678901234567890123456789012

7	ITEM	FORMAT	DESCRIPTION
8	1	A40	QUADRANGLE NAME AS PROJECT IDENTIFICATION
9	2	A20	NAME OF SUBCONTRACTOR
10	3	I4	APPROXIMATE DATE OF SURVEY (MONTH, YEAR)
11	4	I1	NUMBER OF AERIAL SYSTEMS USED TO COLLECT DATA FOR THIS QUADRANGLE
12			
13	5	I1	AERIAL SYSTEM IDENTIFICATION CODE FOR FIRST SYSTEM
14	6	A20	AIRCRAFT IDENTIFICATION BY TYPE AND FAA NUMBER FOR FIRST SYSTEM
15			
16	7	F6.1	NOMINAL ALTITUDE SYSTEM SENSITIVITY RELATIVE TO TERRESTRIAL POTASSIUM (K-40) TO ONE DECIMAL PLACE IN CPS PER PERCENT K FOR FIRST SYSTEM
17			
18			
19	8	F6.1	NOMINAL ALTITUDE SYSTEM SENSITIVITY RELATIVE TO TERRESTRIAL URANIUM (BI-214) TO ONE DECIMAL PLACE IN CPS PER PPM EQUIVALENT U
20			
21			
22	9	F6.1	NOMINAL ALTITUDE SYSTEM SENSITIVITY RELATIVE TO TERRESTRIAL THORIUM (TL-208) TO ONE DECIMAL PLACE IN CPS PER PPM EQUIVALENT TH
23			
24			
25	10	I6	BLANK FIELD (999999)
26	11	F6.3	4PI-SYSTEM DATA COLLECTION INTERVAL TO THREE DECIMAL PLACES IN SECONDS FOR FIRST SYSTEM
27			
28	12	F6.3	2PI-SYSTEM DATA COLLECTION INTERVAL TO THREE DECIMAL PLACES IN SECONDS FOR FIRST SYSTEM
29			
30	13	I3	NUMBER OF CHANNELS (0-3 MEV) IN 4PI SYSTEM FOR FIRST AERIAL SYSTEM
31			
32	14	I3	NUMBER OF CHANNELS (0-3 MEV) IN 2PI SYSTEM FOR FIRST AERIAL SYSTEM
33			
34	15-24	(SAME)	REPEAT OF ITEMS 5-14 FOR SECOND AERIAL SYSTEM
35	*	*	*
36	*	*	*
37	*	*	*
38	85-94	(SAME)	REPEAT OF ITEMS 5-14 FOR NINTH AERIAL SYSTEM
39	95	I3	NUMBER OF FLIGHT LINES ON THIS TAPE
40	96	I4	FIRST FLIGHT LINE NUMBER ON THIS TAPE
41	97	I6	FIRST RECORD NUMBER OF FIRST FLIGHT LINE
42	98	I3	JULIAN DATE (DAY OF YEAR) FIRST FLIGHT-LINE DATA WAS COLLECTED
43			
44	99-101	I4,I6,I3	REPEAT OF ITEMS 96-98 FOR SECOND FLIGHT LINE ON THIS TAPE
45			
46	*	*	*
47	*	*	*
48	*	*	*
49	390-392	I4,I6,I3	REPEAT OF ITEMS 96-98 FOR 99TH FLIGHT LINE ON THIS TAPE
50			
51			
52	FORMAT FOR SINGLE RECORD REDUCED DATA RECORD (THIRD THRU LAST BLOCK)		
53			
54	ITEM	FORMAT	DESCRIPTION
55	1	I1	AERIAL SYSTEM IDENTIFICATION CODE
56	2	I4	FLIGHT LINE NUMBER
57	3	I6	RECORD IDENTIFICATION NUMBER
58	4	I6	GMT TIME OF DAY (HHMMSS)
59	5	F8.4	LATITUDE TO FOUR DECIMAL PLACES IN DEGREES

Line Number	Character Number		
60	6	F8.4	LONGITUDE TO FOUR DECIMAL PLACES IN DEGREES
61	7	F6.1	TERRAIN CLEARANCE TO ONE DECIMAL PLACE IN METERS
62	8	F7.1	RESIDUAL (IGRF REMOVED) MAGNETIC FIELD INTENSITY TO ONE DECIMAL PLACE IN GAMMAS
64	9	A8	SURFACE GEOLOGIC MAP UNIT CODE
65	10	I4	QUALITY FLAG CODES
66	11	F6.1	APPARENT CONCENTRATION OF TERRESTRIAL POTASSIUM (K-40) TO ONE DECIMAL PLACE IN PERCENT K
68	12	F4.1	UNCERTAINTY IN TERRESTRIAL POTASSIUM TO ONE DECIMAL PLACE IN PERCENT K
70	13	F6.1	APPARENT CONCENTRATION OF TERRESTRIAL URANIUM (BI-214) TO ONE DECIMAL PLACE IN PPM EQUIVALENT U
72	14	F4.1	UNCERTAINTY IN TERRESTRIAL URANIUM TO ONE DECIMAL PLACE IN PPM EQUIVALENT U
74	15	F6.1	APPARENT CONCENTRATION OF TERRESTRIAL THORIUM (TL-208) TO ONE DECIMAL PLACE IN PPM EQUIVALENT TH
76	16	F4.1	UNCERTAINTY IN TERRESTRIAL THORIUM TO ONE DECIMAL PLACE IN PPM EQUIVALENT TH
78	17	F6.1	URANIUM-TO-THORIUM RATIO TO ONE DECIMAL PLACE IN PPM EQUIVALENT U PER PPM EQUIVALENT TH
80	18	F6.1	URANIUM-TO-POTASSIUM RATIO TO ONE DECIMAL PLACE IN PPM EQUIVALENT U PER PERCENT K
82	19	F6.1	THORIUM-TO-POTASSIUM RATIO TO ONE DECIMAL PLACE IN PPM EQUIVALENT TH PER PERCENT K
84	20	F8.1	GROSS GAMMA (0.4-3.0 MEV) COUNT RATE TO ONE DECIMAL PLACE IN COUNTS PER SECOND
86	21	F6.1	UNCERTAINTY IN GROSS GAMMA COUNT RATE TO ONE DECIMAL PLACE IN COUNTS PER SECOND
88	22	F5.1	ATMOSPHERIC BI-214 4PI CORRECTION TO ONE DECIMAL PLACE IN PPM EQUIVALENT U
90	23	F4.1	UNCERTAINTY IN ATMOSPHERIC BI-214 4PI CORRECTION TO ONE DECIMAL PLACE IN PPM EQUIVALENT U
92	24	F4.1	OUTSIDE AIR TEMPERATURE TO ONE DECIMAL PLACE IN DEGREES CELSIUS
94	25	F5.1	OUTSIDE AIR PRESSURE TO ONE DECIMAL PLACE IN MMHG

2. Tape Identification Block (Block 2)

The information and format for this block are indicated in lines 8 through 49 of the Format Description Block A3.1, and 1922 characters are produced. The remaining 4978 characters of this block are blanks.

If less than nine aerial systems are used, the space allocated for additional systems is filled with 9's in the format specified for each item using I and F fields, and with zeros for A fields.

Similarly, if fewer than 99 flight lines exist, the unused flight line information, 13 characters per flight line, is filled with 9's through the 99th flight line.

### 3. Single Record Reduced Data Blocks

The information and format for the logical records in these blocks are indicated in lines 55 through 94 of the Format Description Block A3.1. One logical record contains 138 characters. There are 50 such logical records per 6900 character physical record or block.

The data appearing in locations specified by lines 68, 72, 76, 86 and 90 of the Format Description Block A3.1 are 9's in the format specified in each case.

### A4. Statistical Analysis Data Tapes

Block Size (Physical Record): 8000 characters  
Logical Record, Data : 160 characters

#### 1. Format Description Block (Block 1)

The Format Description utilizes 7560 characters. The remaining 440 characters are blanks.

<u>Line Number</u>	<u>Character Number</u>		
	12345678901234567890123456789012345678901234567890123456789012		
1	03	0978	(DATA TAPE TYPE AND FORMAT SPECIFICATION DATE CODES)
2			
3			STATISTICAL ANALYSIS DATA TAPE
4			
5			FORMAT FOR TAPE IDENTIFICATION BLOCK (SECOND BLOCK)
6			
7	ITEM	FORMAT	DESCRIPTION
8	1	A40	QUADRANGLE NAME AS PROJECT IDENTIFICATION
9	2	A20	NAME OF SUBCONTRACTOR
10	3	I4	APPROXIMATE DATE OF SURVEY (MONTH, YEAR)
11	4	I1	NUMBER OF AERIAL SYSTEMS USED TO COLLECT DATA FOR
12			THIS QUADRANGLE
13	5	I1	AERIAL SYSTEM IDENTIFICATION CODE FOR FIRST SYSTEM
14	6	A20	AIRCRAFT IDENTIFICATION BY TYPE AND FAA NUMBER FOR
15			FIRST SYSTEM
16	7	F6.1	NOMINAL ALTITUDE SYSTEM SENSITIVITY RELATIVE TO
17			TERRESTRIAL POTASSIUM (K-40) TO ONE DECIMAL PLACE
18			IN CPS PER PERCENT K
19	8	F6.1	NOMINAL ALTITUDE SYSTEM SENSITIVITY RELATIVE TO
20			TERRESTRIAL URANIUM (BI-214) TO ONE DECIMAL PLACE
21			IN CPS PER PPM EQUIVALENT U
22	9	F6.1	NOMINAL ALTITUDE SYSTEM SENSITIVITY RELATIVE TO
23			TERRESTRIAL THORIUM (TL-208) TO ONE DECIMAL PLACE
24			IN CPS PER PPM EQUIVALENT TH
25	10	I6	BLANK FIELD (999999)
26	11	F6.3	4PI-SYSTEM DATA COLLECTION INTERVAL TO THREE DECIMAL
27			PLACES IN SECONDS FOR FIRST SYSTEM
28	12	F6.3	2PI-SYSTEM DATA COLLECTION INTERVAL TO THREE DECIMAL
29			PLACES IN SECONDS FOR FIRST SYSTEM

Line Number	Character Number		
	12345678901234567890123456789012345678901234567890123456789012		
30	13	I3	NUMBER OF CHANNELS (0-3 MEV) IN 4PI SYSTEM FOR FIRST AERIAL SYSTEM
31			
32	14	I3	NUMBER OF CHANNELS (0-3 MEV) IN 2PI SYSTEM FOR FIRST AERIAL SYSTEM
33			
34	15-24	(SAME)	REPEAT OF ITEMS 5-14 FOR SECOND AERIAL SYSTEM
35	*	*	*
36	*	*	*
37	*	*	*
38	85-94	(SAME)	REPEAT OF ITEMS 5-14 FOR NINTH AERIAL SYSTEM
39	95	I3	NUMBER OF FLIGHT LINES ON THIS TAPE
40	96	I4	FIRST FLIGHT LINE NUMBER ON THIS TAPE
41	97	I6	FIRST RECORD NUMBER OF FIRST FLIGHT LINE
42	98	I3	JULIAN DATE (DAY OF YEAR) FIRST FLIGHT LINE DATA WAS COLLECTED
43			
44	99-101	I4,I6,I3	REPEAT OF ITEMS 96-98 FOR SECOND FLIGHT LINE ON THIS TAPE
45			
46	*	*	*
47	*	*	*
48	*	*	*
49	390-392	I4,I6,I3	REPEAT OF ITEMS 96-98 FOR 99TH FLIGHT LINE ON THIS TAPE
50			
51			
52	FORMAT FOR STATISTICAL ANALYSIS DATA RECORD (THIRD THRU LAST BLOCK)		
53			
54	ITEM	FORMAT	DESCRIPTION
55	1	I1	AERIAL SYSTEM IDENTIFICATION CODE
56	2	I4	FLIGHT LINE NUMBER
57	3	I6	RECORD IDENTIFICATION NUMBER
58	4	I6	GMT TIME OF DAY (HHMMSS)
59	5	F8.4	LATITUDE TO FOUR DECIMAL PLACES IN DEGREES
60	6	F8.4	LONGITUDE TO FOUR DECIMAL PLACES IN DEGREES
61	7	F6.1	TERRAIN CLEARANCE TO ONE DECIMAL PLACE IN METERS
62	8	F7.1	RESIDUAL (IGRF REMOVED) MAGNETIC FIELD INTENSITY TO ONE DECIMAL PLACE IN GAMMAS
63			
64	9	A8	SURFACE GEOLOGIC MAP UNIT CODE
65	10	I5	QUALITY FLAG CODES
66	11	F6.1	AVERAGED CONCENTRATION OF TERRESTRIAL POTASSIUM (K-40) TO ONE DECIMAL PLACE IN PERCENT K
67			
68	12	F4.1	UNCERTAINTY IN TERRESTRIAL POTASSIUM TO ONE DECIMAL PLACE IN PERCENT K
69			
70	13	F5.1	POTASSIUM STANDARD DEVIATION FROM THE MEAN TO ONE DECIMAL PLACE AND ALGEBRAICALLY SIGNED
71			
72	14	F6.1	AVERAGED CONCENTRATION OF TERRESTRIAL URANIUM (BI-214) TO ONE DECIMAL PLACE IN PPM EQUIVALENT U
73			
74	15	F4.1	UNCERTAINTY IN TERRESTRIAL URANIUM TO ONE DECIMAL PLACE IN PPM EQUIVALENT U
75			
76	16	F5.1	URANIUM STANDARD DEVIATION FROM THE MEAN TO ONE DECIMAL PLACE AND ALGEBRAICALLY SIGNED
77			
78	17	F6.1	AVERAGED CONCENTRATION OF TERRESTRIAL THORIUM (TL-208) TO ONE DECIMAL PLACE IN PPM EQUIVALENT TH
79			
80	18	F4.1	UNCERTAINTY IN TERRESTRIAL THORIUM TO ONE DECIMAL PLACE IN PPM EQUIVALENT TH
81			



Line Number	Character Number	
82	19	F5.1 THORIUM STANDARD DEVIATION FROM THE MEAN TO ONE DECIMAL PLACE AND ALGEBRAICALLY SIGNED
83		
84	20	F8.1 GROSS GAMMA (0.4-3.0 MEV) COUNT RATE TO ONE DECIMAL PLACE IN COUNTS PER SECOND
85		
86	21	F6.1 UNCERTAINTY IN GROSS GAMMA COUNT RATE TO ONE DECIMAL PLACE IN COUNTS PER SECOND
87		
88	22	F5.1 ATMOSPHERIC BI-214 4PI CORRECTION TO ONE DECIMAL PLACE IN PPM EQUIVALENT U
89		
90	23	F4.1 UNCERTAINTY IN ATMOSPHERIC BI-214 4PI CORRECTION TO ONE DECIMAL PLACE IN PPM EQUIVALENT U
91		
92	24	F6.1 AVERAGED URANIUM-TO-THORIUM RATIO TO ONE DECIMAL PLACE IN PPM EQUIVALENT U PER PPM EQUIVALENT TH
93		
94	25	F5.1 URANIUM-TO-THORIUM RATIO STANDARD DEVIATION FROM THE MEAN TO ONE DECIMAL PLACE AND ALGEBRAICALLY SIGNED
95		
96	26	F6.1 AVERAGED URANIUM-TO-POTASSIUM RATIO TO ONE DECIMAL PLACE IN PPM EQUIVALENT U PER PERCENT K
97		
98	27	F5.1 URANIUM-TO-POTASSIUM RATIO STANDARD DEVIATION FROM THE MEAN TO ONE DECIMAL PLACE AND ALGEBRAICALLY SIGNED
99		
100		
101	28	F6.1 AVERAGED THORIUM-TO-POTASSIUM RATIO TO ONE DECIMAL PLACE IN PPM EQUIVALENT TH PER PERCENT K
102		
103	29	F5.1 THORIUM-TO-POTASSIUM RATIO STANDARD DEVIATION FROM THE MEAN TO ONE DECIMAL PLACE AND ALGEBRAICALLY SIGNED
104		
105		

## 2. Tape Identification Block (Block 2)

The information and format for this block are indicated in lines 8 through 49 of the Format Description Block A4.1, and 1922 characters are produced. The remaining 6078 characters of this block are blanks.

If less than nine aerial systems are used, the space allocated for additional systems is filled with 9's in the format specified for each item using I and F fields, and with zeros for A fields.

Similarly, if fewer than 99 flight lines exist, the unused flight line information, 13 characters per flight line, is filled with 9's through the 99th flight line.

## 3. Statistical Analysis Data Blocks

The information and format for the logical records in these blocks are indicated in lines 55 through 103 of the Format Description Block A4.1. One logical record contains 160 characters. There are 50 such logical records per 8000 character physical record or block.

The data appearing in locations specified by lines 68, 74, 80, 86 and 90 of the Format Description Block A4.1 are 9's in the format specified in each case.

## A5. Magnetic Data Tapes

Block Size (Physical Record): 8000 characters  
Logical Record (Data) : 80 characters

### 1. Format Description Block (Block 1)

The Format Description utilizes 3384 characters. The remaining 4616 characters are blanks.

<u>Line Number</u>	<u>Character Number</u>		
	1234567890123456789012345678901234567890123456789012345678901234567890123456789012		
1	04	0978	(DATA TAPE TYPE AND FORMAT SPECIFICATION DATE CODES)
2			
3	MAGNETIC DATA TAPE		
4			
5	FORMAT FOR TAPE IDENTIFICATION BLOCK (SECOND BLOCK)		
6			
7	ITEM	FORMAT	DESCRIPTION
8	1	A40	QUADRANGLE NAME AS PROJECT IDENTIFICATION
9	2	A20	NAME OF SUBCONTRACTOR
10	3	I4	APPROXIMATE DATE OF SURVEY (MONTH, YEAR)
11	4	I3	NUMBER OF FLIGHT LINES ON THIS TAPE
12	5	I4	FIRST FLIGHT LINE ON THIS TAPE
13	6	I6	FIRST RECORD NUMBER OF FIRST FLIGHT LINE
14	7	I3	JULIAN DATE (DAY OF YEAR) FIRST FLIGHT LINE DATA WAS
15			COLLECTED
16	8	F8.4	LATITUDE OF GROUND BASE STATION TO FOUR DECIMAL
17			PLACES IN DEGREES FOR FIRST FLIGHT LINE
18	9	F8.4	LONGITUDE OF GROUND BASE STATION TO FOUR DECIMAL
19			PLACES IN DEGREES FOR FIRST FLIGHT LINE
20	10-14	(SAME)	REPEAT OF ITEMS 5-9 FOR SECOND FLIGHT LINE ON THIS
21			TAPE
22	*	*	*
23	*	*	*
24	*	*	*
25	495-499	(SAME)	REPEAT OF ITEMS 5-9 FOR 99TH FLIGHT LINE ON THIS
26			TAPE
27			
28	FORMAT FOR MAGNETIC DATA RECORD (THIRD THRU LAST BLOCK)		
29			
30	ITEM	FORMAT	DESCRIPTION
31	1	I1	AERIAL SYSTEM IDENTIFICATION CODE
32	2	I4	FLIGHT LINE NUMBER
33	3	I6	RECORD IDENTIFICATION NUMBER
34	4	I6	GMT TIME OF DAY (HHMMSS)
35	5	F8.4	LATITUDE TO FOUR DECIMAL PLACES IN DEGREES
36	6	F8.4	LONGITUDE TO FOUR DECIMAL PLACES IN DEGREES
37	7	F6.1	TERRAIN CLEARANCE TO ONE DECIMAL PLACE IN METERS
38	8	F5.1	OUTSIDE AIR PRESSURE TO ONE DECIMAL PLACE IN MMHG
39	9	A8	SURFACE GEOLOGIC MAP UNIT CODE
40	10	F7.1	TOTAL MAGNETIC FIELD INTENSITY TO ONE DECIMAL PLACE
41			IN GAMMAS
42	11	F7.1	RESIDUAL (IGRF REMOVED) MAGNETIC FIELD INTENSITY

Line Number	Character Number			
	12345678901234567890123456789012345678901234567890123456789012345678901234567890123456789012			

44	12	F7.1	DIURNAL MAGNETIC INTENSITY VARIATION TO ONE DECIMAL PLACE IN GAMMAS
45			
46	13	F7.1	MAGNETIC DEPTH-TO-BASEMENT TO ONE DECIMAL PLACE IN METERS (IF REQUIRED)
47			

2. Tape Identification Block (Block 2)

The information and format for this block are indicated in lines 8 through 25 of the Format Description Block A5.1, and 2938 characters are produced. The remaining 5062 characters of this block are blanks.

If fewer than 99 flight lines exist, the unused flight line information, 29 characters per flight line, is filled with 9's through the 99th flight line in the format indicated.

3. Magnetic Data Blocks

The information and format for the logical records in these blocks are indicated in lines 31 through 46 of the Format Description Block A5.1. One logical record contains 80 characters. There are 100 such logical records per 8000 character physical record or block.

If the magnetic depth-to-basement is not required, this item is expressed as 99999.9.

A6. Statistical Analysis Summary Tapes

Block Size (Physical Record): 7000 characters  
 Logical Record (Data) : 140 characters

1. Format Description Block (Block 1)

The Format Description utilizes 4320 characters. The remaining 2680 characters are blanks.

Line Number	Character Number			
	12345678901234567890123456789012345678901234567890123456789012345678901234567890123456789012			

1	05	0978	(DATA TAPE TYPE AND FORMAT SPECIFICATION DATE CODE)
2			
3			STATISTICAL ANALYSIS SUMMARY TAPE (OR FILE)
4			
5			FORMAT FOR TAPE IDENTIFICATION BLOCK (SECOND BLOCK)
6			
7	ITEM	FORMAT	DESCRIPTION
8	1	A40	QUADRANGLE NAME AS PROJECT IDENTIFICATION
9	2	A20	NAME OF SUBCONTRACTOR
10	3	I4	APPROXIMATE DATE OF SURVEY (MONTH, YEAR)
11	4	I6	NUMBER OF GEOLOGIC MAP UNITS USED FOR THIS

Line Character Number  
 Number 12345678901234567890123456789012345678901234567890123456789012

Line Number	ITEM	FORMAT	DESCRIPTION
12			QUADRANGLE
13			
14			FORMAT FOR STATISTICAL ANALYSIS SUMMARY DATA RECORD (THIRD THRU LAST BLOCK)
15			
16			
17	1	A8	SURFACE GEOLOGIC MAP UNIT IDENTIFYING CODE
18	2	I6	TOTAL RECORDS FOR GEOLOGIC MAP UNIT
19	3	I6	NUMBER OF POTASSIUM RECORDS COMPUTED FOR GEOLOGIC UNIT
20	4	F6.1	POTASSIUM CONCENTRATION MEAN TO ONE DECIMAL PLACE IN PERCENT K
21	5	F6.1	POTASSIUM CONCENTRATION STANDARD DEVIATION TO ONE DECIMAL PLACE IN PERCENT K
22	6	A3	POTASSIUM CONCENTRATION DISTRIBUTION CODE
23	7	I6	NUMBER OF URANIUM RECORDS COMPUTED FOR GEOLOGIC UNIT
24	8	F6.1	URANIUM CONCENTRATION MEAN TO ONE DECIMAL PLACE IN PPM EQUIVALENT U
25	9	F6.1	URANIUM CONCENTRATION STANDARD DEVIATION TO ONE DECIMAL PLACE IN PPM EQUIVALENT U
26	10	A3	URANIUM CONCENTRATION DISTRIBUTION CODE
27	11	I6	NUMBER OF THORIUM RECORDS COMPUTED FOR GEOLOGIC UNIT
28	12	F6.1	THORIUM CONCENTRATION MEAN TO ONE DECIMAL PLACE IN PPM EQUIVALENT TH
29	13	F6.1	THORIUM CONCENTRATION STANDARD DEVIATION TO ONE DECIMAL PLACE IN PPM EQUIVALENT TH
30	14	A3	THORIUM CONCENTRATION DISTRIBUTION CODE
31	15	I6	NUMBER OF URANIUM-TO-THORIUM RATIO RECORDS COMPUTED FOR GEOLOGIC UNIT
32	16	F6.1	URANIUM-TO-THORIUM RATIO MEAN TO ONE DECIMAL PLACE IN PPM EQUIVALENT U PER PPM EQUIVALENT TH
33	17	F6.1	URANIUM-TO-THORIUM RATIO STANDARD DEVIATION TO ONE DECIMAL PLACE IN PPM EQUIVALENT U PER PPM EQUIVALENT TH
34	18	A3	URANIUM-TO-THORIUM RATIO DISTRIBUTION CODE
35	19	I6	NUMBER OF URANIUM-TO-POTASSIUM RATIO RECORDS COMPUTED FOR GEOLOGIC UNIT
36	20	F6.1	URANIUM-TO-POTASSIUM RATIO MEAN TO ONE DECIMAL PLACE IN PPM EQUIVALENT U PER PERCENT K
37	21	F6.1	URANIUM-TO-POTASSIUM RATIO STANDARD DEVIATION TO ONE DECIMAL PLACE IN PPM EQUIVALENT U PER PERCENT K
38	22	A3	URANIUM-TO-POTASSIUM RATIO DISTRIBUTION CODE
39	23	I6	NUMBER OF THORIUM-TO-POTASSIUM RATIO RECORDS COMPUTED FOR GEOLOGIC UNIT
40	24	F6.1	THORIUM-TO-POTASSIUM RATIO MEAN TO ONE DECIMAL PLACE IN PPM EQUIVALENT TH PER PERCENT K
41	25	F6.1	THORIUM-TO-POTASSIUM RATIO STANDARD DEVIATION TO ONE DECIMAL PLACE IN PPM EQUIVALENT TH PER PERCENT K
42	26	A3	THORIUM-TO-POTASSIUM RATIO DISTRIBUTION CODE

2. Tape Identification Block (Block 2)

The information and format for this block are indicated in lines 8 through 11 of the Format Description Block A6.1, and 70 characters are produced. The remaining 6930 characters of this block are blanks.

3. Statistical Analysis Summary Data Blocks

The information and format for the logical records in these blocks are indicated in lines 18 through 60 of the Format Description Block A6.1. One logical record contains 140 characters. There are 50 such logical records per 7000 character physical record or block.

**B. DESCRIPTION OF LISTINGS**

**B1. Single record reduced data listings: include the following information on Microfiche:**

<u>ITEM</u>	<u>DESCRIPTION</u>
REC	Sequential record number
Lat	Location Y in latitude
Long	Location X in longitude
RMag	Residual magnetic field, gammas
Alt	Surface altitude
GEO UNIT	Geologic Type
AKUT	A=Altitude; K=Potassium; U=Uranium T=Thorium - Results of statistical adequacy test
COS	Cosmic c/s
BiAir	Airborne <sup>214</sup> Bi, 4π data
GC	Gross count, .4 MeV - 2.8 MeV
T <sub>l</sub>	<sup>208</sup> T <sub>l</sub> c/s
Bi	<sup>214</sup> Bi c/s
K	<sup>40</sup> K c/s
BI:T <sub>l</sub>	Ratio
BI:k	Ratio
T <sub>l</sub> :K	Ratio
TEMP	Outside Air Temperature (°C)
BP	Atmospheric Pressure (In. Hg)

**B2. Averaged record data listings: include the following information on Microfiche:**

<u>ITEM</u>	<u>DESCRIPTION</u>
REC	Sequential Record number
GEO UNIT	Geologic type
AKUT	A=Altitude; K=Potassium; U=Uranium; T=Thorium - Results of statistical adequacy test
Long	Longitude of X location of geologic type
Lat	latitude of Y location of geologic type
RMag	Residual magnetic field, gammas
COS	Cosmic, 4π
BiAir	Atmospheric Bi, 4π
GC	Gross count, c/s

ITEMDESCRIPTION

$T_{\ell}$	$T_{\ell}$ value, c/s
Rank	$T_{\ell}$ standard deviation rank
$B_i$	$B_i$ value, c/s
Rank	$B_i$ standard deviation rank
$K$	$K$ value, c/s
Rank	$K$ standard deviation rank
$B_i/T_{\ell}$	Ratio value
Rank	$B_i/T_{\ell}$ standard deviation rank
$B_i/K$	Ratio value
Rank	$B_i/K$ standard deviation rank
$T_{\ell}/K$	Ratio value
Rank	$T_{\ell}/K$ standard deviation rank

GEODATA INT. INC.		SINGLE REC LISTING DICKENSON MLI			MAP LINE 1															
REC	LAT	LONG	RHAG	ALT	GEOUNT	A	K	U	T	COS	BIAIR	GC	TL	BI	K	BI:TL	BI:K	TL:K	TEMP	BP
4276	46.0219	104.0252	-194.1	413	ZNA	0	0	1	0	45	6.0	1652	25	36	163	1.440	0.221	0.153	29.8	21.28
4277	46.0219	104.0244	-232.6	450	ZNA	0	0	1	1	47	6.0	215	0	1	23	1.000	0.043	0.043	29.8	21.28
4278	46.0219	104.0235	-233.6	359	ZNA	0	0	1	0	46	6.0	1534	31	19	134	0.613	0.142	0.231	29.8	21.28
4279	46.0219	104.0227	-232.7	362	ZNA	0	0	1	0	46	6.0	1616	40	19	135	0.475	0.141	0.296	29.8	21.28
4280	46.0219	104.0209	-232.9	359	ZNA	0	0	1	0	45	6.0	1516	44	10	127	0.227	0.079	0.346	29.8	21.28
4281	46.0219	104.0201	-233.3	352	ZNA	0	0	0	0	47	6.0	1581	33	33	146	1.000	0.226	0.226	29.8	21.28
4282	46.0219	104.0193	-233.2	348	ZNA	0	0	1	0	46	6.0	1595	44	14	127	0.318	0.110	0.346	29.8	21.28
4283	46.0219	104.0184	-232.9	340	ZNA	0	0	1	0	47	6.0	1705	50	19	150	0.380	0.127	0.333	29.8	21.28
4284	46.0219	104.0176	-236.0	345	ZNA	0	0	0	0	45	6.0	1573	39	22	139	0.564	0.158	0.281	29.8	21.28
4285	46.0219	104.0168	-235.8	348	ZNA	0	0	0	0	47	6.0	1627	38	29	144	0.763	0.201	0.264	29.8	21.28
4286	46.0219	104.0159	-235.1	351	ZNA	0	0	1	0	46	6.0	1581	39	22	138	0.564	0.159	0.283	29.8	21.28
4287	46.0219	104.0151	-235.2	356	ZNA	0	0	1	0	46	6.0	1629	53	15	128	0.283	0.117	0.414	29.8	21.28
4288	46.0219	104.0143	-231.3	356	ZNA	0	0	1	0	46	6.0	1477	31	20	122	0.645	0.164	0.254	29.8	21.28
4289	46.0219	104.0134	-230.1	359	ZNA	0	0	1	0	46	6.0	1543	37	15	139	0.405	0.108	0.266	29.8	21.28
4290	46.0219	104.0126	-231.4	370	ZNA	0	0	1	0	46	6.0	1525	37	19	120	0.514	0.158	0.308	29.8	21.28
4291	46.0219	104.0117	-231.1	385	ZNA	0	0	0	0	47	6.0	1570	41	27	103	0.659	0.262	0.398	29.9	21.29
4292	46.0219	104.0109	-230.8	421	ZNA	0	0	0	0	46	6.0	1613	47	27	119	0.574	0.227	0.395	29.9	21.29
4293	46.0219	104.0101	-230.5	439	ZNA	0	0	0	0	46	6.0	1589	36	33	110	0.917	0.300	0.327	29.9	21.29
4294	46.0219	104.0092	-229.7	435	ZNA	0	0	1	0	46	6.0	1576	34	18	153	0.529	0.118	0.222	29.9	21.29
4295	46.0219	104.0084	-230.0	435	ZNA	0	0	0	0	46	6.0	1486	35	29	119	0.829	0.244	0.294	29.9	21.29
4296	46.0219	104.0076	-229.4	435	ZNA	0	0	1	0	46	6.0	1511	39	20	158	0.513	0.127	0.247	29.9	21.29
4297	46.0219	104.0067	-229.9	443	ZNA	0	0	0	0	46	6.0	1464	25	24	114	0.960	0.211	0.219	29.9	21.29
4298	46.0219	104.0059	-229.0	444	ZNA	0	0	1	0	46	6.0	1528	34	22	140	0.647	0.157	0.243	29.9	21.29
4299	46.0219	104.0051	-227.9	440	ZNA	0	0	1	0	47	6.0	1581	32	16	127	0.500	0.126	0.252	29.9	21.29
4300	46.0219	104.0042	-228.8	432	ZNA	0	0	1	0	46	6.0	1480	33	18	110	0.545	0.164	0.300	29.9	21.29
4301	46.0219	104.0034	-227.2	430	ZNA	0	0	0	0	46	6.0	1492	37	29	119	0.784	0.244	0.311	29.9	21.29
4302	46.0219	104.0026	-227.4	422	ZNA	0	0	0	0	45	6.0	1487	42	24	120	0.571	0.200	0.350	29.9	21.29
4303	46.0219	104.0017	-226.6	408	ZNA	0	0	1	0	46	10.9	1433	22	22	134	1.000	0.164	0.164	29.9	21.29
4304	46.0219	104.0009	-225.8	400	ZNA	0	0	0	0	45	10.9	1438	29	25	119	0.862	0.210	0.244	29.9	21.29
4305	46.0219	104.0001	-225.5	391	ZNA	0	0	1	0	46	10.9	1417	25	20	132	0.800	0.152	0.189	29.9	21.29
4306	46.0219	103.9992	-224.9	383	ZNA	0	0	1	0	46	10.9	1480	40	12	128	0.300	0.094	0.313	29.9	21.29
4307	46.0219	103.9984	-225.1	376	ZNA	0	0	0	0	47	10.9	1487	28	33	132	1.179	0.250	0.212	29.9	21.29
4308	46.0219	103.9975	-224.5	373	ZNA	0	0	1	0	45	10.9	1373	36	19	108	0.528	0.176	0.333	29.9	21.29
4309	46.0219	103.9967	-224.4	365	KFH	0	0	1	0	46	10.9	1430	28	9	143	0.321	0.063	0.196	29.9	21.29
4310	46.0219	103.9959	-224.3	359	KFH	0	0	1	0	46	10.9	1458	33	5	136	0.152	0.037	0.243	29.9	21.29
4311	46.0219	103.9950	-224.9	356	KFH	0	0	1	0	46	10.9	1491	28	9	145	0.321	0.062	0.193	29.9	21.29
4312	46.0219	103.9942	-225.1	353	KFH	0	0	0	0	46	11.6	1465	30	24	122	0.800	0.197	0.246	29.9	21.29
4313	46.0219	103.9934	-224.0	349	KFH	0	0	0	0	47	11.6	1469	17	31	130	1.824	0.238	0.131	29.9	21.29
4314	46.0219	103.9925	-222.1	345	KFH	0	0	0	0	46	11.6	1505	29	22	130	0.759	0.169	0.223	29.9	21.29
4315	46.0219	103.9917	-221.7	350	KFH	0	0	1	0	46	11.6	1392	34	13	142	0.382	0.092	0.239	29.9	21.29
4316	46.0219	103.9909	-221.3	369	KFH	0	0	1	0	46	11.6	1474	48	17	121	0.354	0.140	0.397	29.9	21.29
4317	46.0219	103.9900	-221.1	378	KFH	0	0	1	0	46	11.6	1306	27	17	115	0.630	0.148	0.235	29.9	21.29
4318	46.0219	103.9892	-221.1	389	KFH	0	0	0	0	46	11.6	1326	30	24	96	0.800	0.250	0.313	29.9	21.29
4319	46.0219	103.9884	-220.2	396	KFH	0	0	0	0	45	11.6	1331	19	22	132	1.158	0.167	0.144	29.9	21.29
4320	46.0219	103.9875	-219.7	402	KFH	0	0	1	0	45	11.6	1263	27	16	138	0.593	0.116	0.196	29.9	21.29
4321	46.0219	103.9867	-219.3	401	KFH	0	0	0	0	46	12.0	1296	32	29	119	0.906	0.244	0.269	29.9	21.29
4322	46.0219	103.9859	-218.7	396	KFH	0	0	1	0	46	12.0	1345	31	13	122	0.419	0.107	0.254	29.9	21.29
4323	46.0219	103.9850	-218.7	387	KFH	0	0	1	0	46	12.0	1415	30	14	130	0.467	0.108	0.231	29.9	21.29
4324	46.0219	103.9842	-218.7	369	KFH	0	0	1	0	46	12.0	1382	25	9	133	0.360	0.068	0.188	29.9	21.29
4325	46.0219	103.9833	-217.7	351	KFH	0	0	1	0	46	12.0	1388	33	0	148	0.030	0.007	0.223	29.9	21.29
4326	46.0218	103.9825	-217.2	336	KP	0	0	1	0	47	12.0	1359	40	3	113	0.075	0.027	0.354	29.9	21.29
4327	46.0218	103.9817	-216.9	328	KP	0	0	1	0	46	12.0	1387	31	20	109	0.645	0.183	0.284	29.9	21.29
4328	46.0218	103.9808	-217.8	324	KP	0	0	1	0	45	12.0	1368	32	17	145	0.531	0.117	0.221	29.9	21.29
4329	46.0218	103.9800	-217.0	338	KP	0	0	1	0	46	12.0	1375	25	17	118	0.680	0.144	0.212	29.9	21.29



GEO DATA INT. INC. AVERAGE REC LISTING DICKENSON MAPLI MAP LINE 1  
 DICKENSON MAPLINES(1-15)  
 MAPLINE 1

RCN	GEO UNIT	A	K	U	T	LONG	LAT	RMAG	COS	BIAIR	GC
TL RANK	BI RANK	K RANK	BI/TL RANK	BI/K RANK	TL/K RANK						
4276	ZNA	0	0	1	0	104.0252	46.0219	-194.1	45	6.0	1652
	25-1	36		163+1	1.440		0.208	0.145-1			
4277	ZNA	0	0	1	1	104.0244	46.0219	-232.6	47	6.0	215
	0	1		23-3	1.000		0.030	0.000			
4278	ZNA	0	0	1	0	104.0235	46.0219	-233.6	46	6.0	1534
4279	ZNA	0	0	0	0	104.0227	46.0219	-232.7	46	6.0	1616
	31-1	19		134+0	0.613		0.132	0.215-1			
4280	ZNA	0	0	0	0	104.0209	46.0219	-232.9	45	6.0	1516
	32-0	17-1		121-0	0.540-0		0.133-0	0.246-0			
4281	ZNA	0	0	0	0	104.0201	46.0219	-233.3	47	6.0	1561
	40+0	20-0		136+0	0.497-0		0.137-0	0.275-0			
4282	ZNA	0	0	0	0	104.0193	46.0219	-233.2	46	6.0	1595
	41+0	20-0		137+0	0.484-0		0.137-0	0.283-0			
4283	ZNA	0	0	0	0	104.0184	46.0219	-232.9	47	6.0	1705
	42+0	21-0		140+0	0.504-0		0.141-0	0.280-0			
4284	ZNA	0	0	0	0	104.0176	46.0219	-236.0	45	6.0	1573
	42+0	22-0		140+0	0.524-0		0.147-0	0.280-0			
4285	ZNA	0	0	0	0	104.0168	46.0219	-235.8	47	6.0	1627
	41+0	21-0		138+0	0.525-0		0.148-0	0.281-0			
4286	ZNA	0	0	0	0	104.0159	46.0219	-235.1	46	6.0	1561
	41+0	21-0		136+0	0.515-0		0.145-0	0.280-0			
4287	ZNA	0	0	0	0	104.0151	46.0219	-235.2	46	6.0	1629
	40+0	19-0		132+0	0.486-0		0.138-0	0.285-0			
4288	ZNA	0	0	0	0	104.0143	46.0219	-231.3	46	6.0	1477
	39-0	19-0		128+0	0.493-0		0.139-0	0.283-0			
4289	ZNA	0	0	0	0	104.0134	46.0219	-230.1	46	6.0	1543
	39-0	19-0		125-0	0.495-0		0.143-0	0.290-0			
4290	ZNA	0	0	0	0	104.0126	46.0219	-231.4	46	6.0	1525
	39-0	21-0		120-0	0.549-0		0.165-0	0.301-0			
4291	ZNA	0	0	0	0	104.0117	46.0219	-231.1	47	6.0	1570
	39-0	23-0		118-0	0.606+0		0.184-0	0.304-0			
4292	ZNA	0	0	0	0	104.0109	46.0219	-230.8	46	6.0	1613
	39+0	25-0		119-0	0.641+0		0.195-0	0.304-0			
4293	ZNA	0	0	0	0	104.0101	46.0219	-230.5	46	6.0	1589
	38-0	26+0		123-0	0.680+0		0.196-0	0.288-0			
4294	ZNA	0	0	0	0	104.0092	46.0219	-229.7	46	6.0	1576
	36-0	25-0		129+0	0.687+0		0.181-0	0.263-0			
4295	ZNA	0	0	0	0	104.0084	46.0219	-230.0	46	6.0	1486
	35-0	24-0		132+0	0.699+0		0.173-0	0.247-0			
4296	ZNA	0	0	0	0	104.0076	46.0219	-229.4	46	6.0	1511
	33-0	23-0		134+0	0.681+0		0.159-0	0.233-0			
4297	ZNA	0	0	0	0	104.0067	46.0219	-229.9	46	6.0	1464
	32-0	21-0		131+0	0.669+0		0.154-0	0.230-0			
4298	ZNA	0	0	0	0	104.0059	46.0219	-229.0	46	6.0	1528
	32-0	21-0		128+0	0.654+0		0.154-0	0.236-0			
4299	ZNA	0	0	0	0	104.0051	46.0219	-227.9	47	6.0	1581
	33-0	20-0		125-0	0.625+0		0.154-0	0.247-0			
4300	ZNA	0	0	0	0	104.0042	46.0219	-228.8	46	6.0	1480
	33-0	21-0		121-0	0.641+0		0.164-0	0.255-0			
4301	ZNA	0	0	0	0	104.0034	46.0219	-227.2	46	6.0	1492
	34-0	22-0		121-0	0.671+0		0.173-0	0.258-0			
4302	ZNA	0	0	0	0	104.0026	46.0219	-227.4	45	6.0	1467
	32-0	23-0		122-0	0.705+0		0.175-0	0.249-0			

GEODATA INT. INC. AVERAGE REC LISTING DICKENSON MAPLI MAP LINE 1  
 DICKENSON MAPLINES(1-15)  
 MAPLINE 1

RCN	GEO UNIT	A	K	U	T	LONG	LAT	RMAG	COS	BIAIR	GC
TL RANK	ZNA	BI RANK	K RANK	BI/TL RANK	BI/K RANK	TL/K RANK					
4276	25-1	36	163+1	1.440	0.208	0.145-1	45	6.0	1652		
4277	0	1	23-3	1.000	0.030	0.000	47	6.0	215		
4278	31-1	19	134+0	0.613	0.132	0.215-1	46	6.0	1534		
4279	32-0	17-1	121-0	0.540-0	0.133-0	0.246-0	46	6.0	1616		
4280	37-0	17-1	127+0	0.474-0	0.128-0	0.270-0	45	6.0	1516		
4281	40+0	20-0	136+0	0.497-0	0.137-0	0.275-0	47	6.0	1581		
4282	41+0	20-0	137+0	0.484-0	0.137-0	0.283-0	46	6.0	1595		
4283	42+0	21-0	140+0	0.504-0	0.141-0	0.280-0	47	6.0	1705		
4284	42+0	22-0	140+0	0.524-0	0.147-0	0.280-0	45	6.0	1573		
4285	41+0	21-0	138+0	0.525-0	0.148-0	0.281-0	47	6.0	1627		
4286	41+0	21-0	136+0	0.515-0	0.145-0	0.280-0	46	6.0	1581		
4287	40+0	19-0	132+0	0.486-0	0.138-0	0.285-0	46	6.0	1629		
4288	39-0	19-0	128+0	0.493-0	0.139-0	0.283-0	46	6.0	1477		
4289	39-0	19-0	125-0	0.495-0	0.143-0	0.290-0	46	6.0	1543		
4290	39-0	21-0	120-0	0.549-0	0.165-0	0.301-0	46	6.0	1525		
4291	39-0	23-0	118-0	0.606+0	0.184-0	0.304-0	47	6.0	1570		
4292	39+0	25-0	119-0	0.641+0	0.195-0	0.304-0	46	6.0	1613		
4293	38-0	26+0	123-0	0.680+0	0.196-0	0.288-0	46	6.0	1589		
4294	36-0	25-0	129+0	0.687+0	0.181-0	0.263-0	46	6.0	1576		
4295	35-0	24-0	132+0	0.699+0	0.173-0	0.247-0	46	6.0	1486		
4296	33-0	23-0	134+0	0.681+0	0.159-0	0.233-0	46	6.0	1511		
4297	32-0	21-0	131+0	0.669+0	0.154-0	0.230-0	46	6.0	1464		
4298	32-0	21-0	128+0	0.654+0	0.154-0	0.236-0	46	6.0	1528		
4299	33-0	20-0	125-0	0.625+0	0.154-0	0.247-0	47	6.0	1581		
4300	33-0	21-0	121-0	0.641+0	0.164-0	0.255-0	46	6.0	1480		
4301	34-0	22-0	121-0	0.671+0	0.173-0	0.258-0	46	6.0	1492		
4302	32-0	23-0	122-0	0.705+0	0.175-0	0.249-0	45	6.0	1467		

APPENDIX III  
PRODUCTION SUMMARY

APPENDIX III

PRODUCTION SUMMARY - SURVEY TIME PERIOD

<u>ML/TL</u>	<u>DATE FLOWN</u>	<u>SURVEY LINE MILES</u>	<u>AVERAGE SPEED/DAY</u>	<u>AVERAGE ALTITUDE/DAY</u>
ML4-7	9/25/78	380	135	413
ML8-15	9/26/78	760	135	415
ML16-21	9/27/78	570	136	426
ML1-3, 22-23,TL1- 6	10/1/78	889	143	423

TABLE AIII-1 Test Line Results

UNIT	Sept. 1979			Oct. 1979
	9/25	9/26	9/27*	10/1*
PRE COS	43.00	43.06	43.05	43.02
POS COS	43.07	43.03	-	43.08
T1	34.96	35.09	43.97	39.48
T1	35.02	35.11	-	38.96
Bi	16.97	17.03		26.28
Bi	17.10	16.45	-	27.01
K	131.92	132.32	132.41	128.58
K	130.84	130.98	-	129.11
GC	1481.70	1485.70	1518.05	1514.02
GC	1473.96	1441.99	-	1523.97
BiAir	11.21	12.73	11.68	18.34
BiAir	13.10	12.69	-	16.29
ALT	399.62	398.54	400.18	406.90
ALT	403.71	400.93	-	401.37

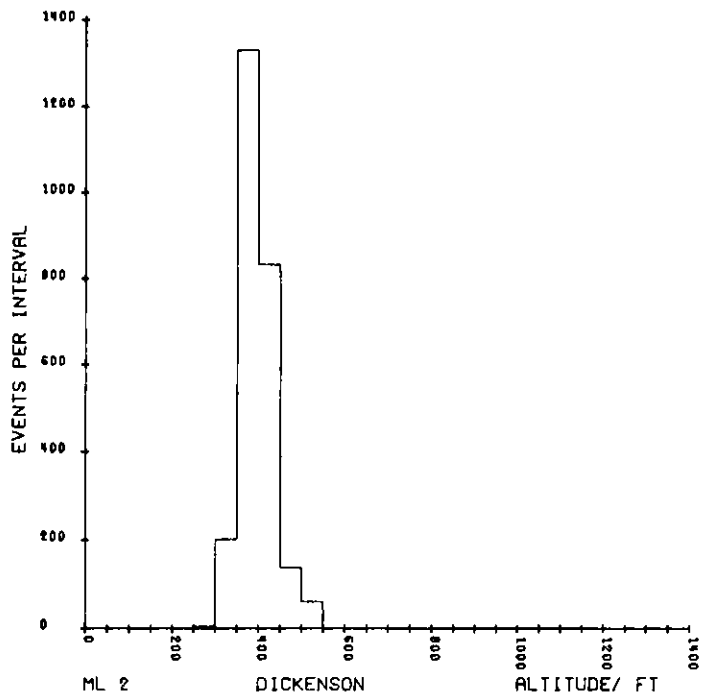
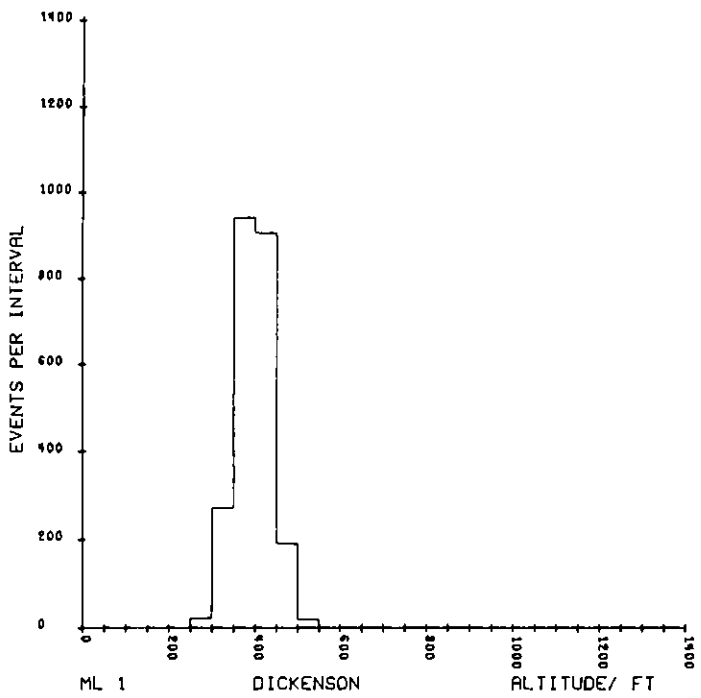
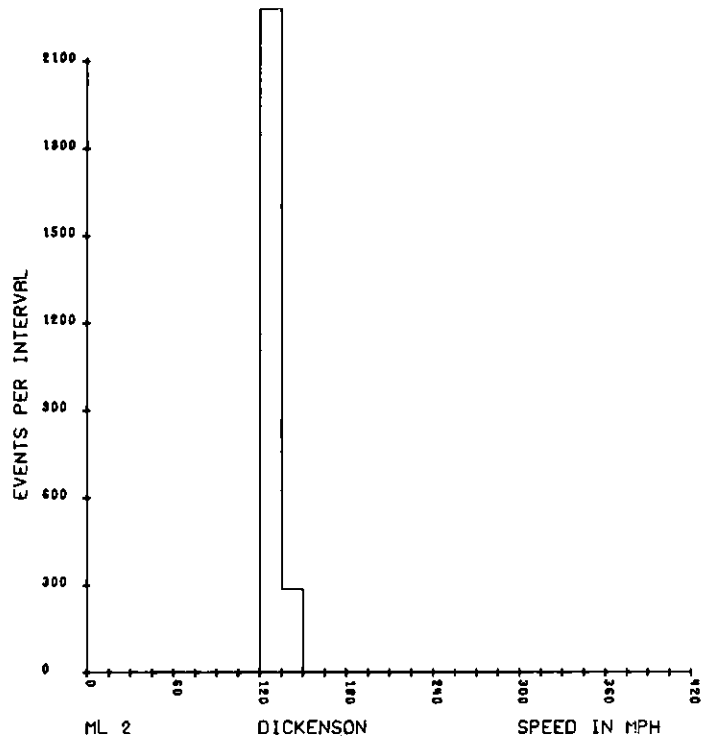
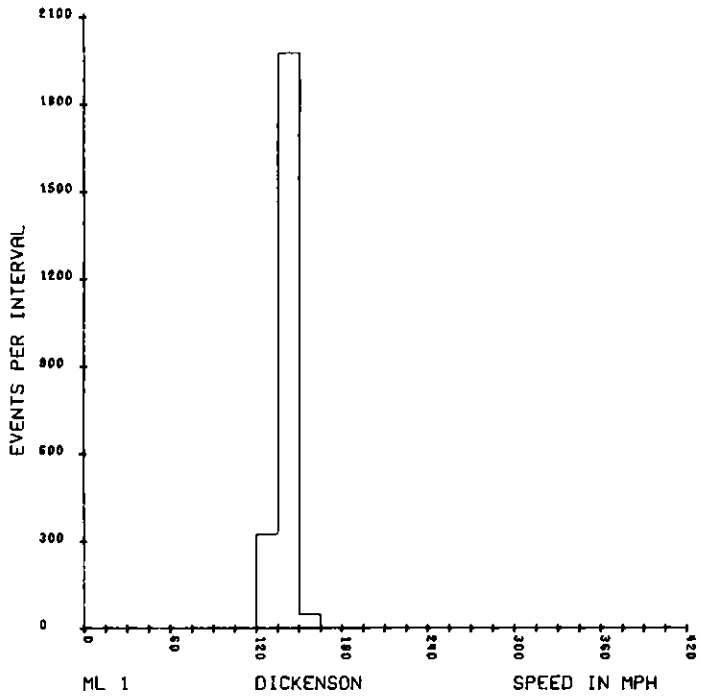
\*New Test Line

TABLE AIII-2 Average Speed and Altitude Determined from Data of Appendix II

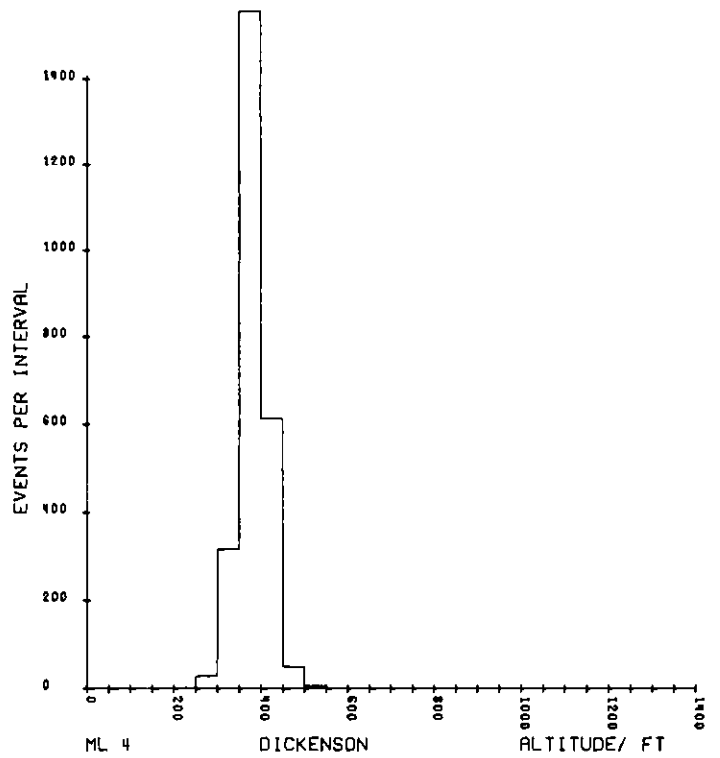
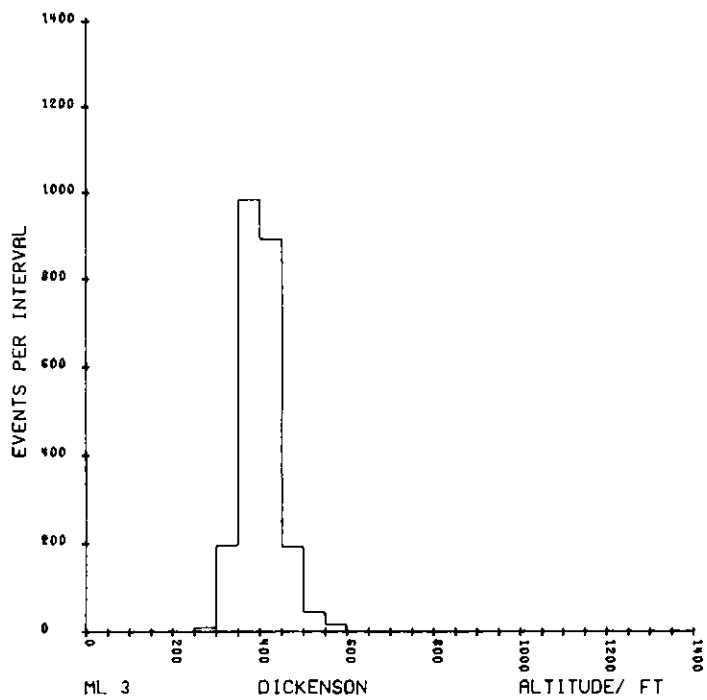
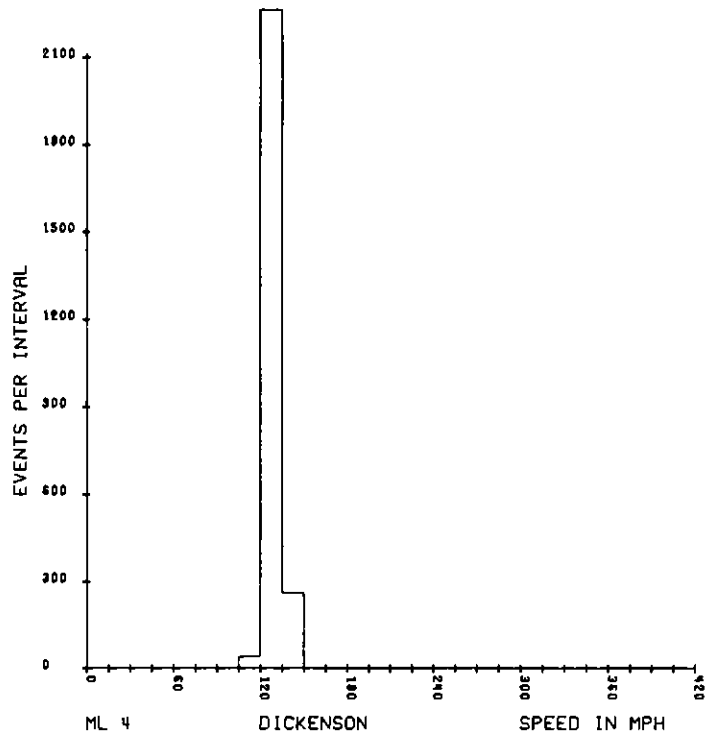
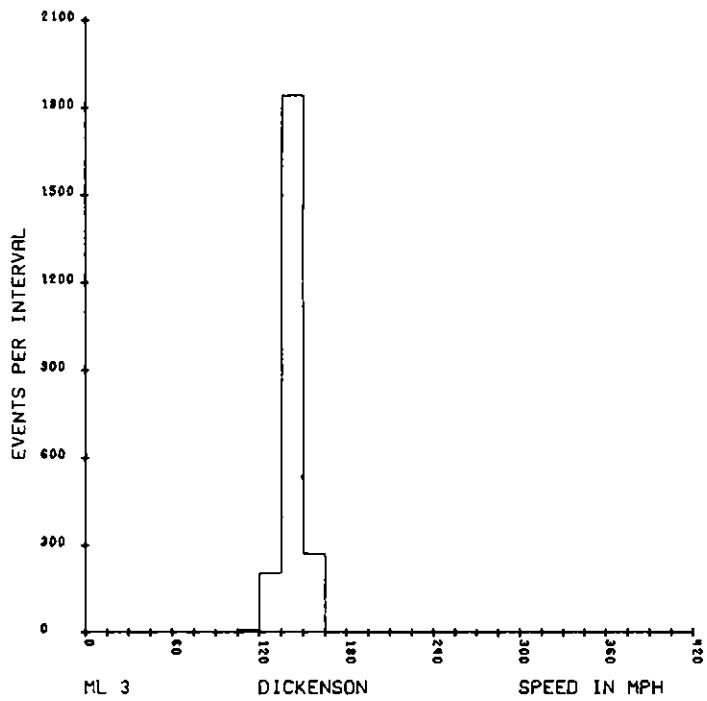
<u>LINE</u>	<u>AVERAGE SPEED, MPH</u>	<u>AVERAGE ALTITUDE, FT</u>	<u>LINE</u>	<u>AVERAGE SPEED, MPH</u>	<u>AVERAGE ALTITUDE, FT</u>
ML1	148	422			
2	137	421			
3	150	427			
4	136	407			
5	136	422			
6	134	410			
7	135	414			
8	134	405			
9	137	409			
10	137	414			
11	135	426			
12	135	411			
13	135	425			
14	135	408			
15	135	424			
16	135	414			
17W	132	419			
17E	135	415			
18	135	420			
19	134	419			
20	136	416			
21W	137	449			
21E	136	443			
22	132	425			
23	146	443			
TL1	142	420			
2	142	411			
3	143	433			
4	146	416			
5	142	449			
6	148	410			

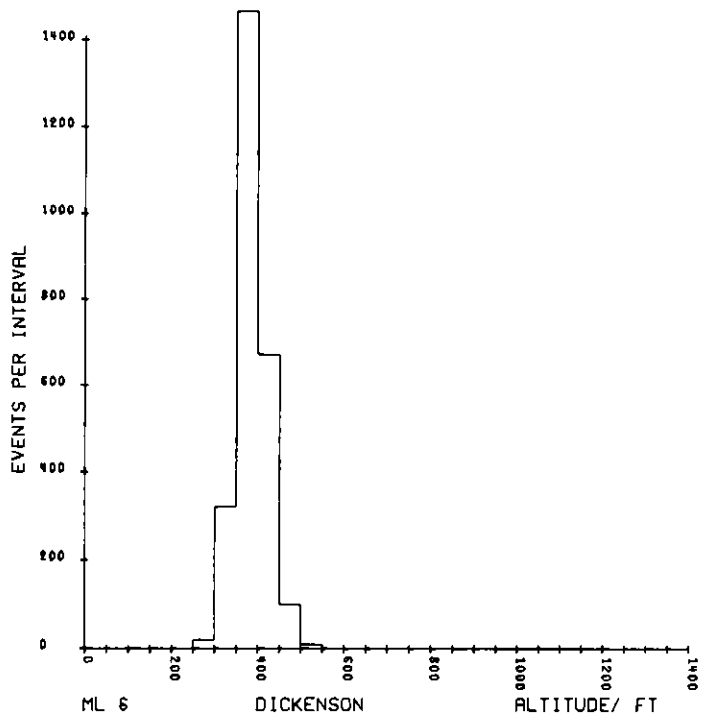
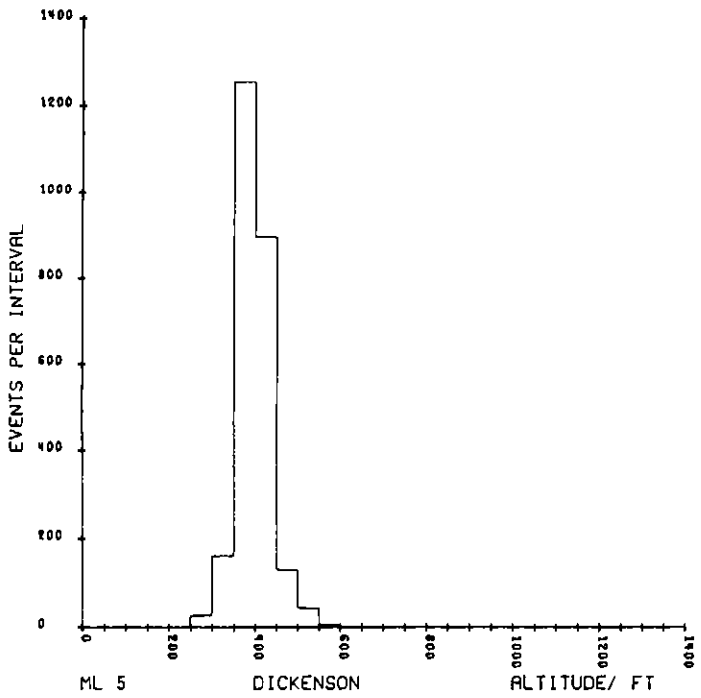
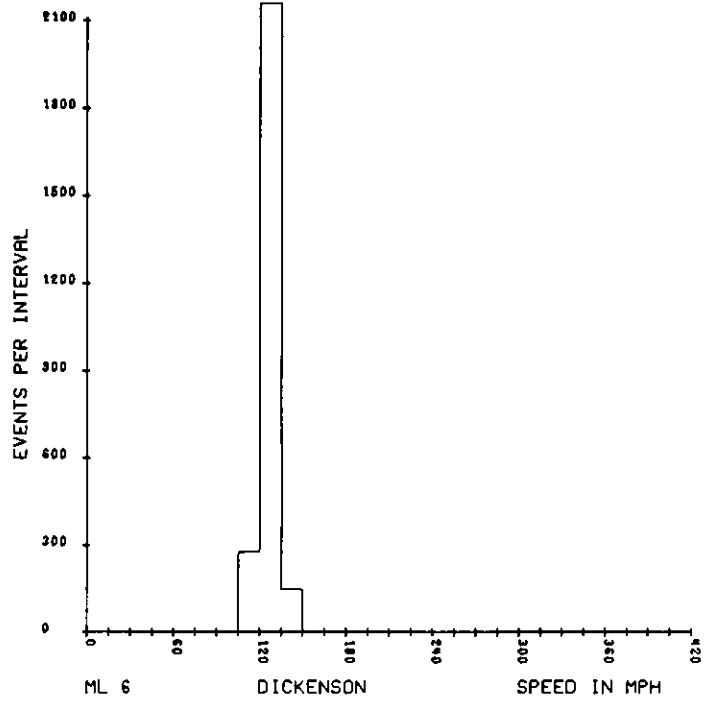
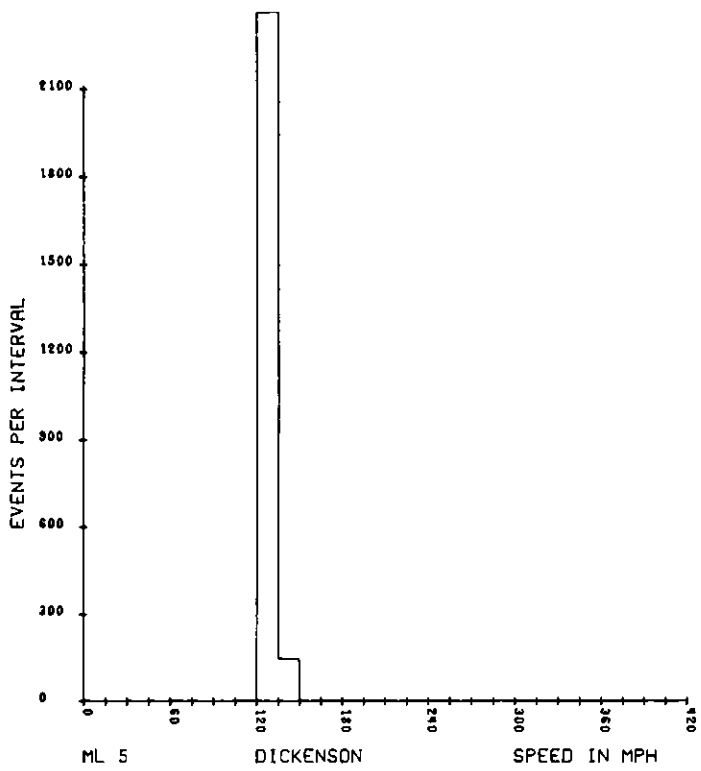
TABLE AIII-3 Diurnal Corrections to Map Line Data

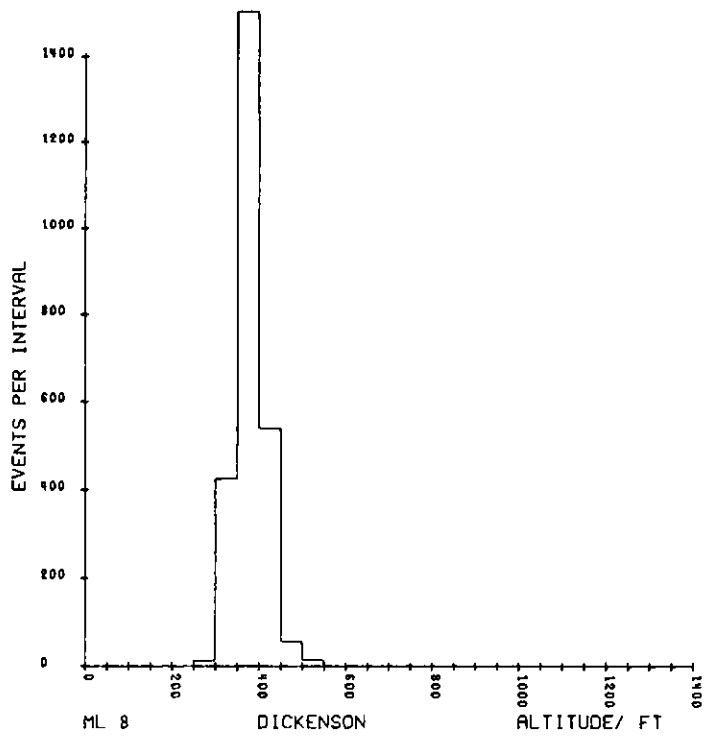
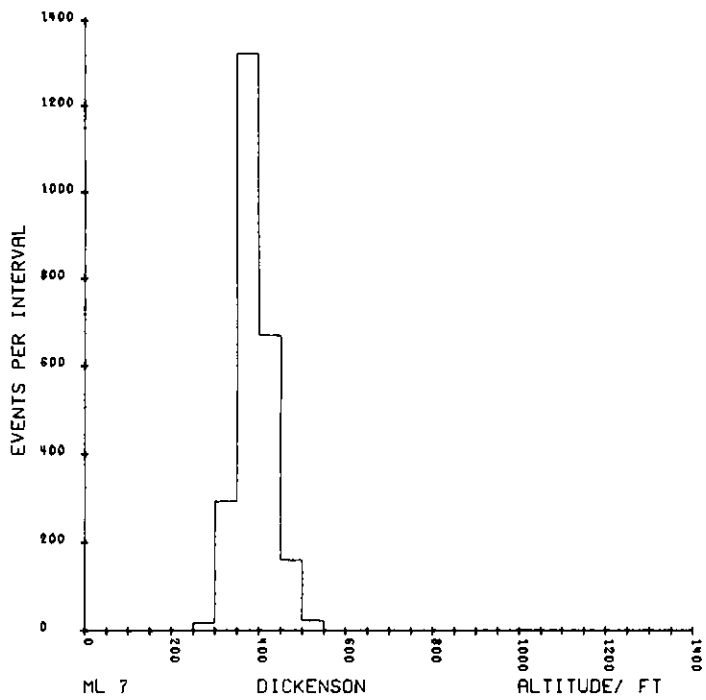
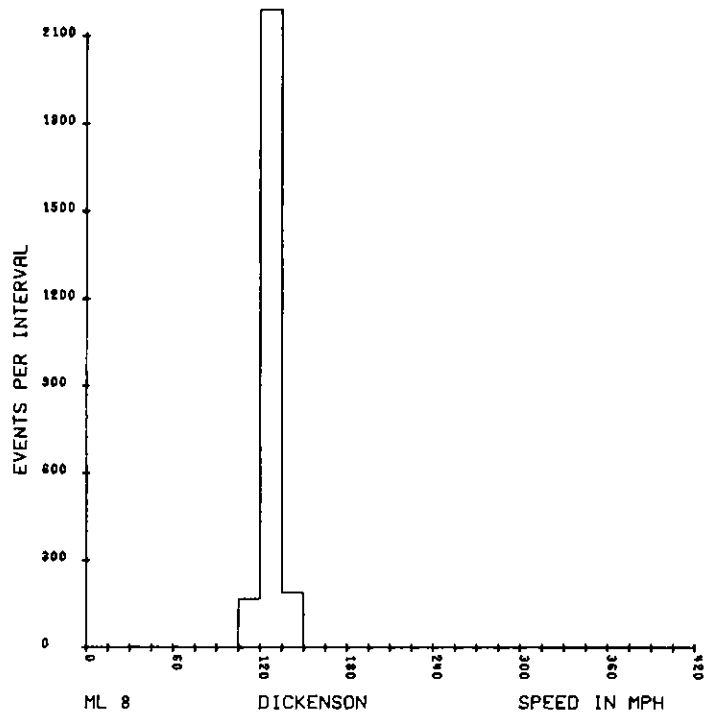
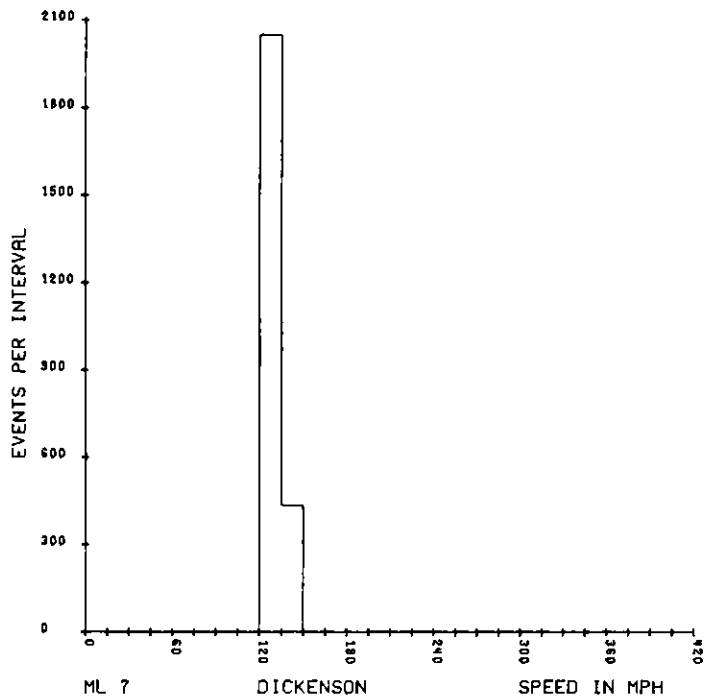
<u>LINE</u>	<u>DIURNAL CORRECTIONS IN GAMMAS</u>	<u>LINE</u>	<u>DIURNAL CORRECTIONS IN GAMMAS</u>
ML 1	-8		
2	-10		
3	-12		
4	0		
5	-6		
6	-10		
7	-11		
8	8		
9	11		
10	13		
11	5		
12	0		
13	-10		
14	-10		
15	-11		
16	9		
17W	10		
17E	12		
18	13		
19	3		
20	-2		
21W	-6		
21E	-9		
22	0		
23	7		
TL 1	5		
2	8		
3	10		
4	12		
5	13		
6	-5		

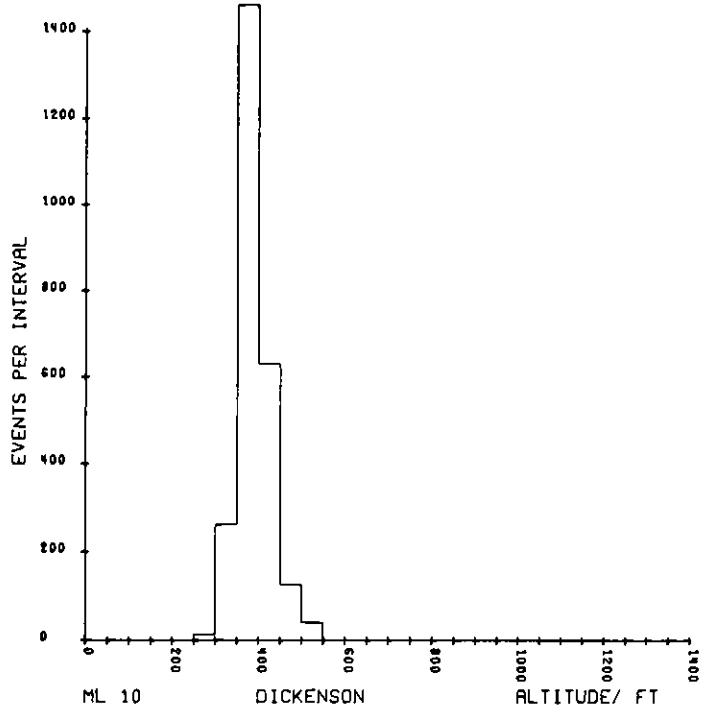
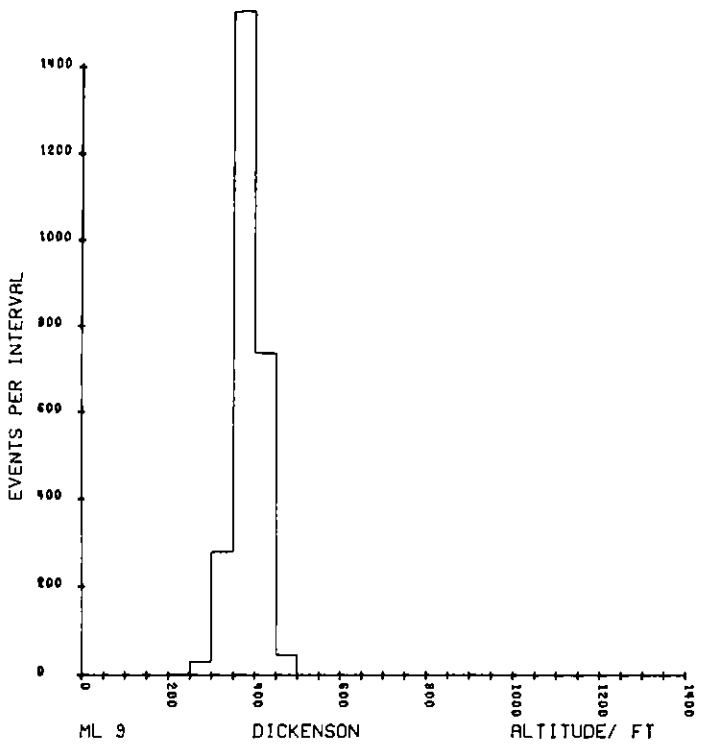
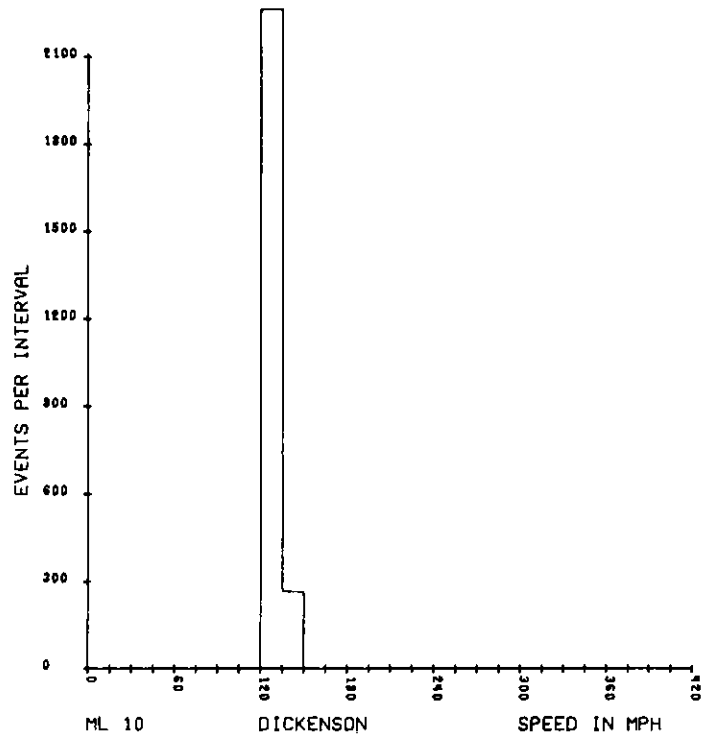
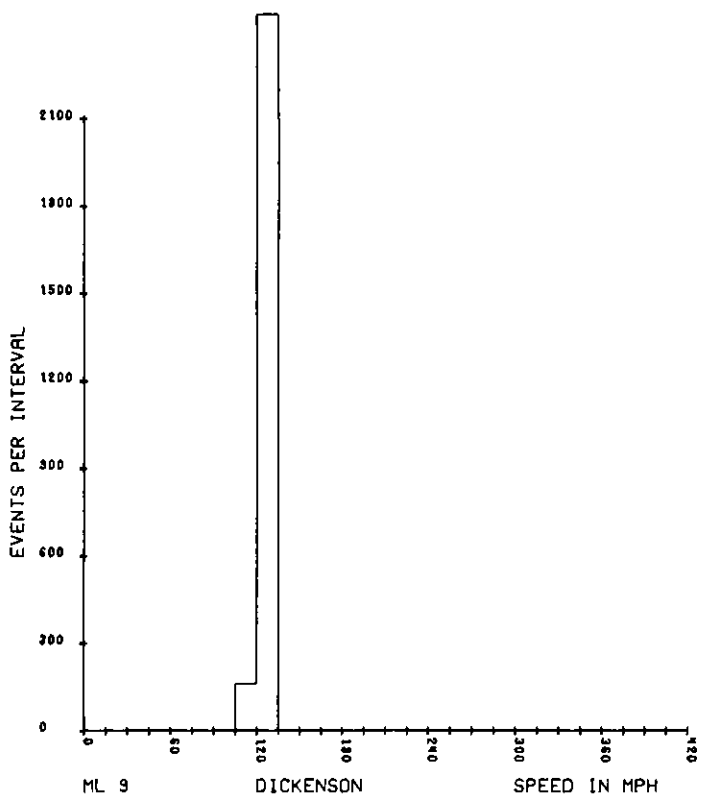


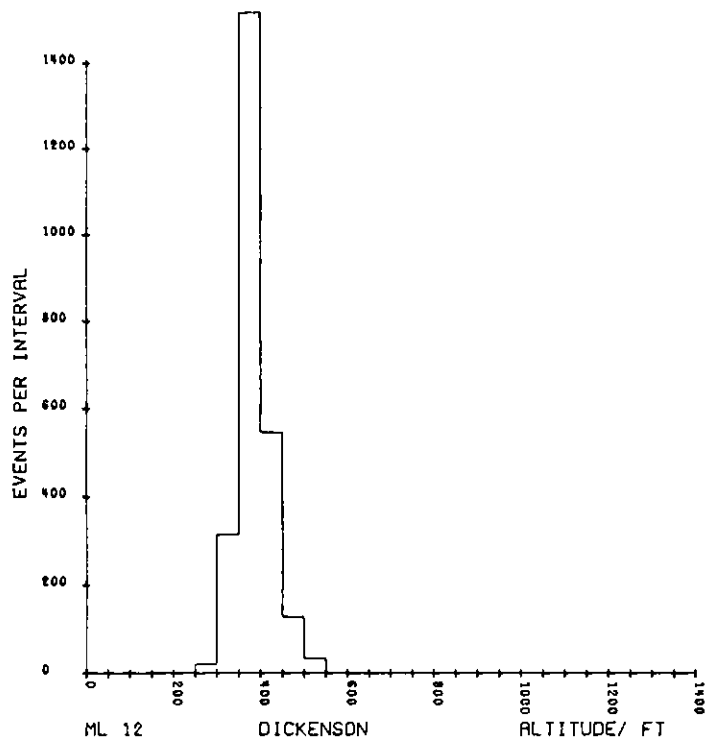
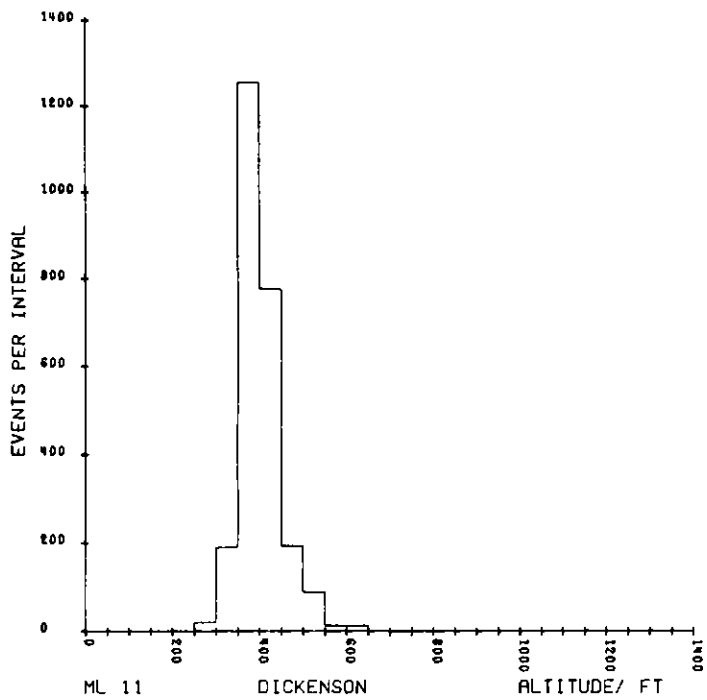
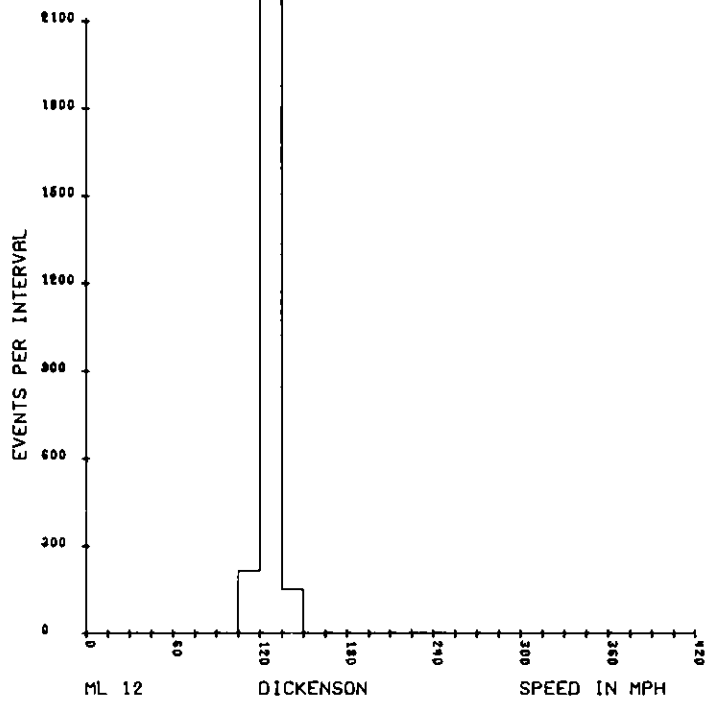
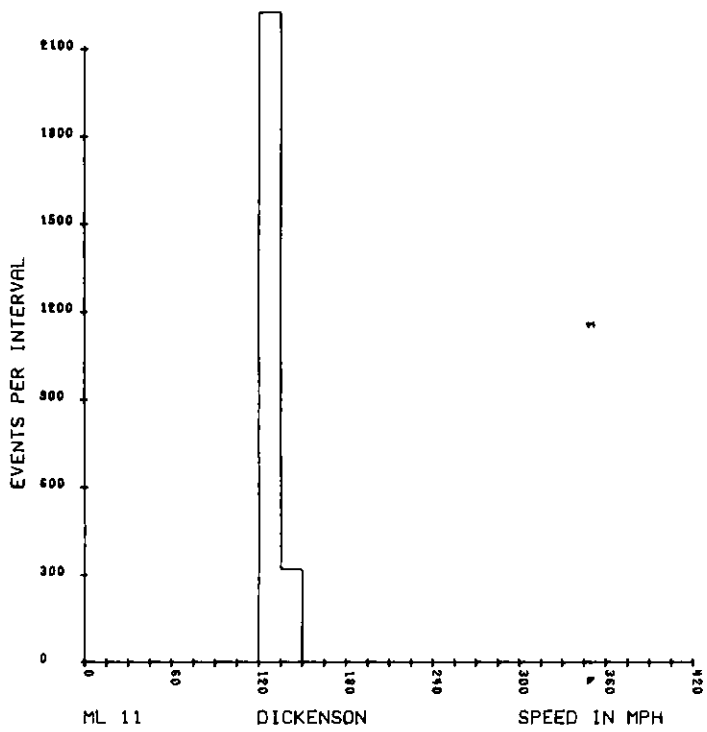


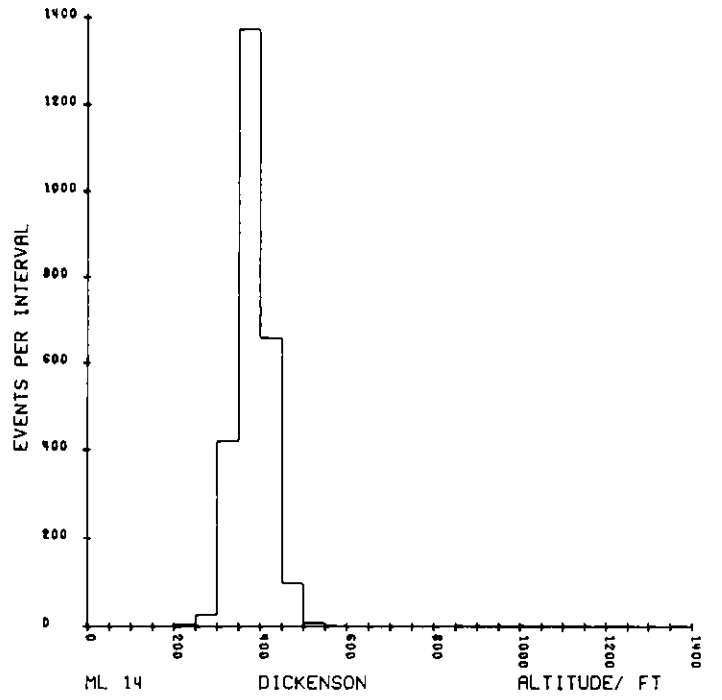
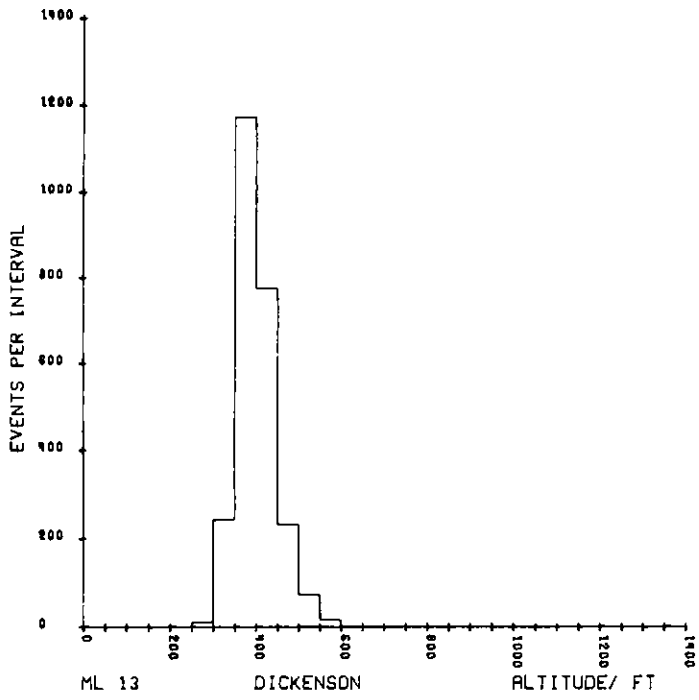
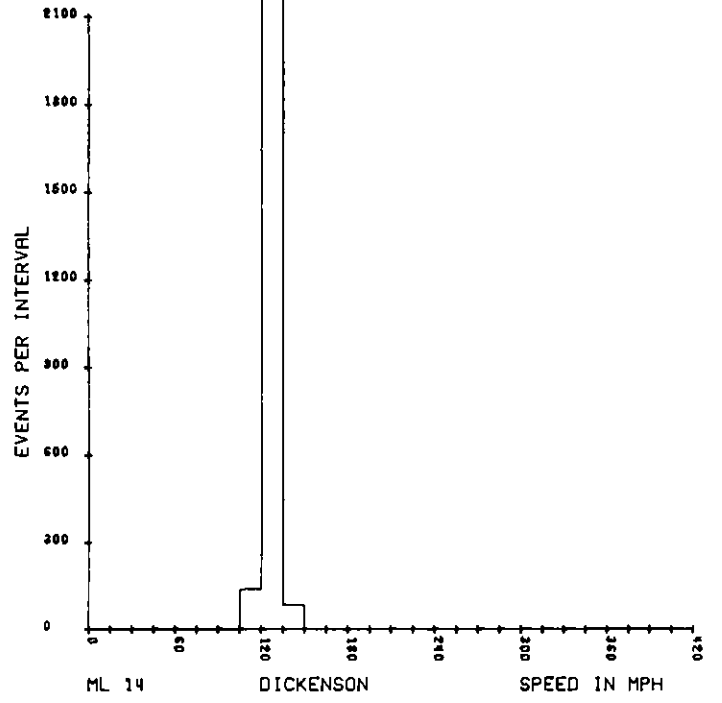
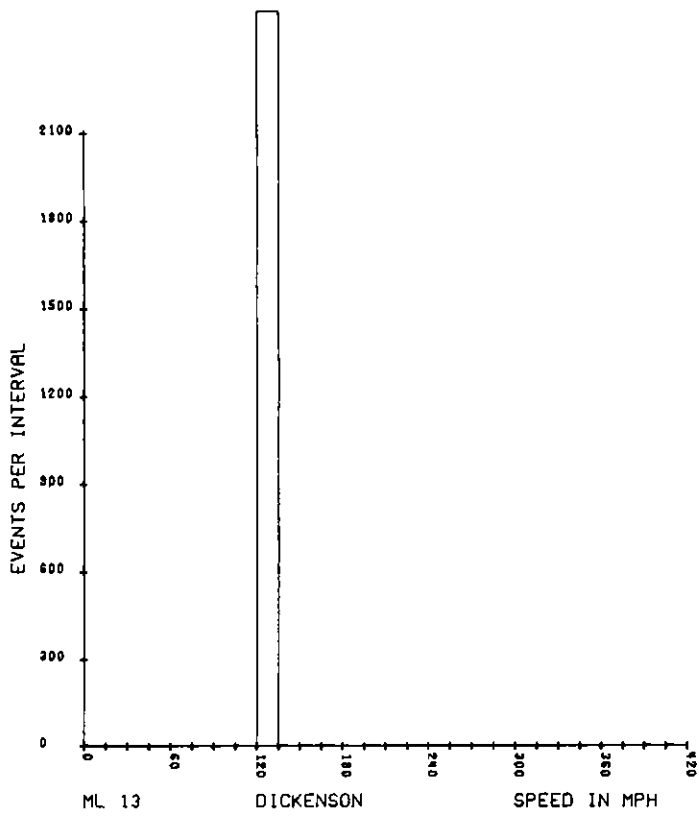


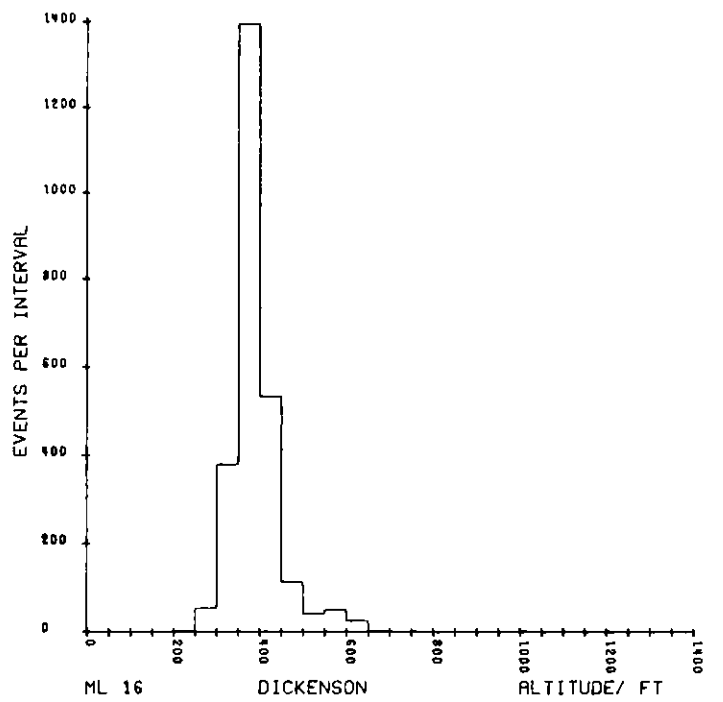
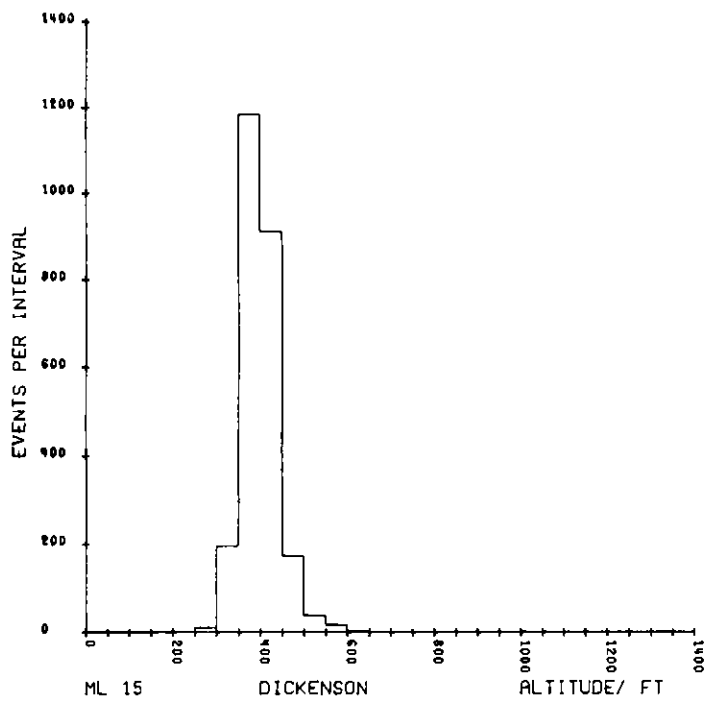
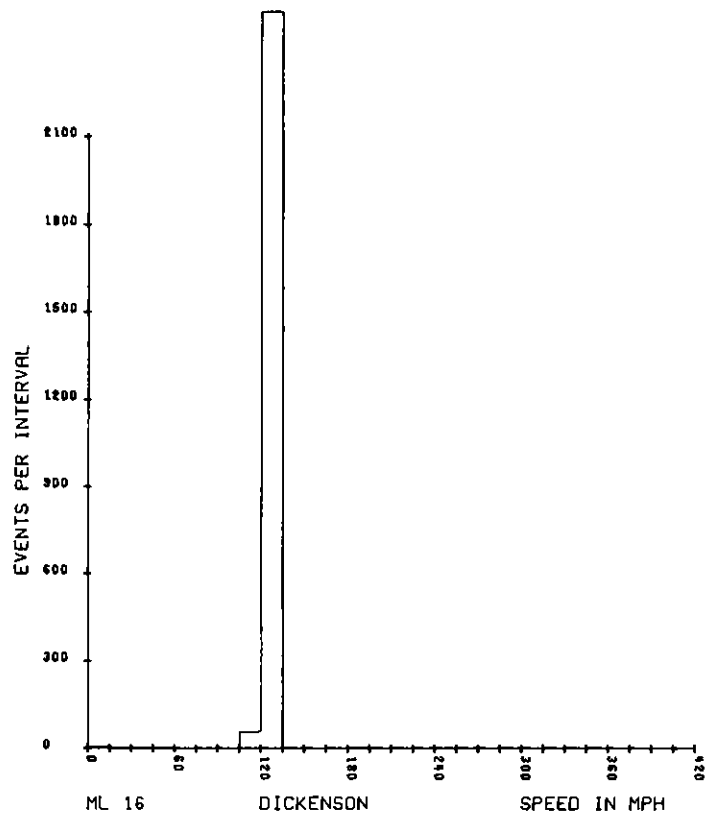
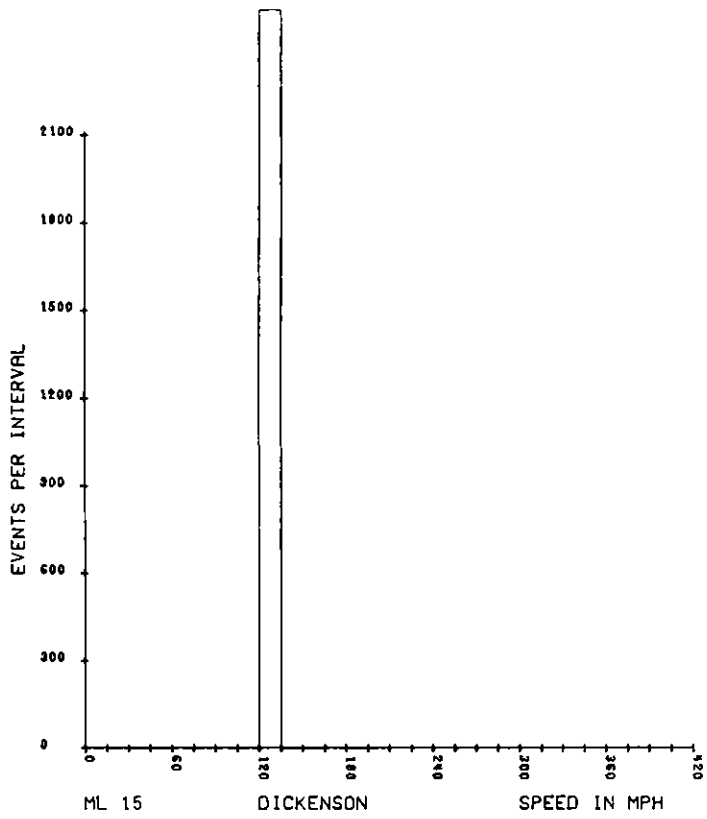


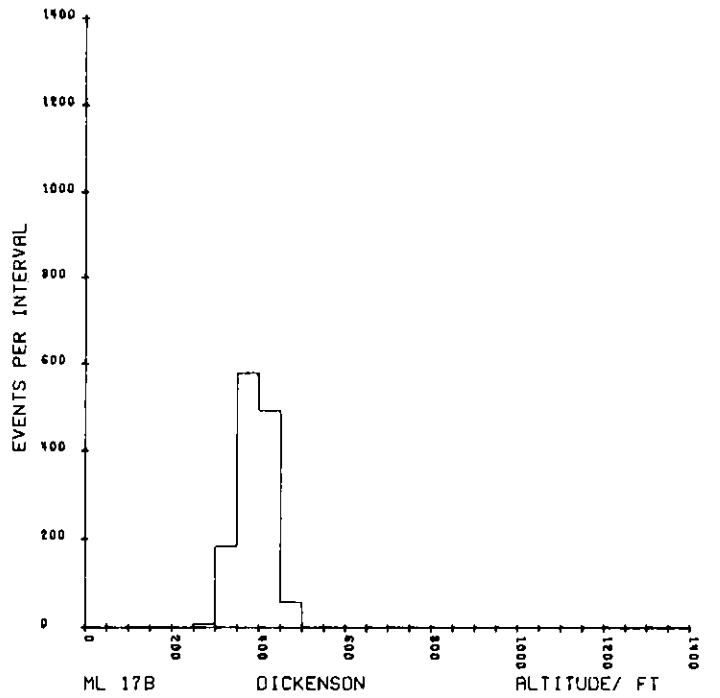
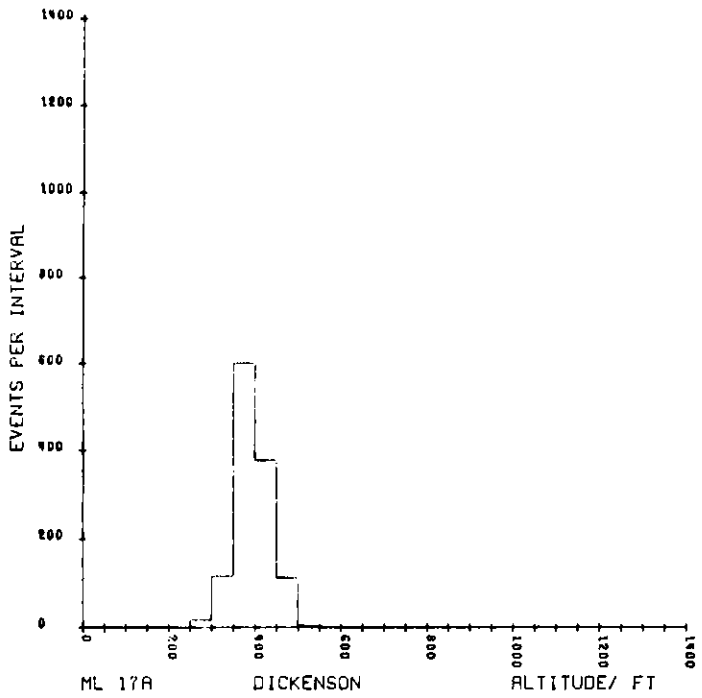
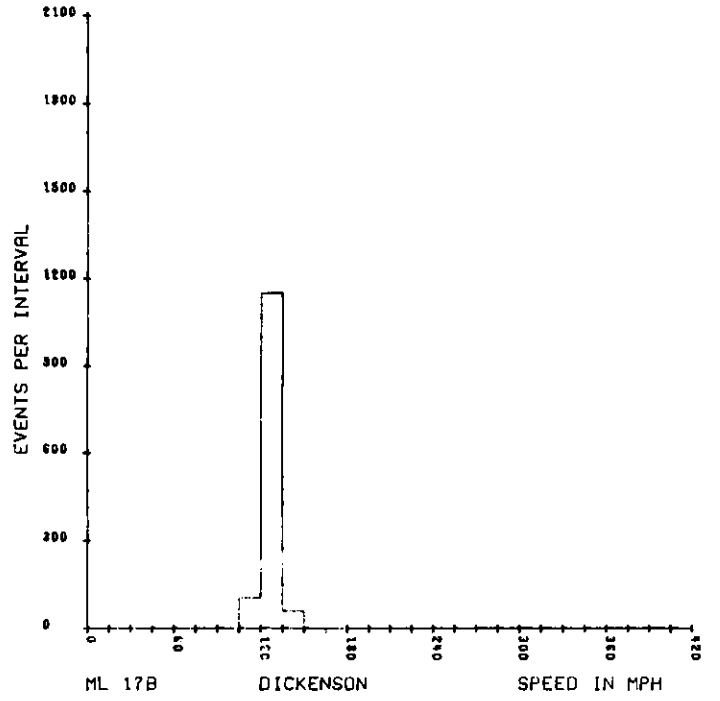
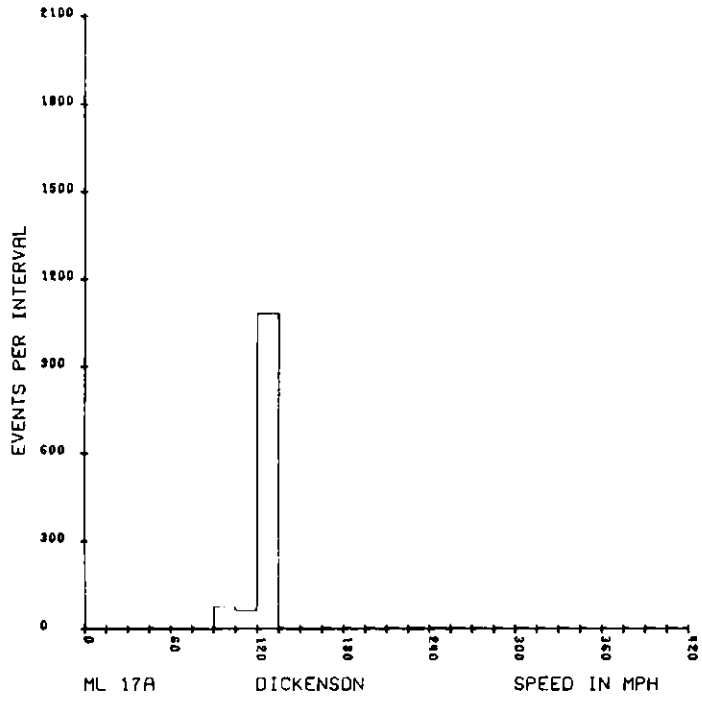




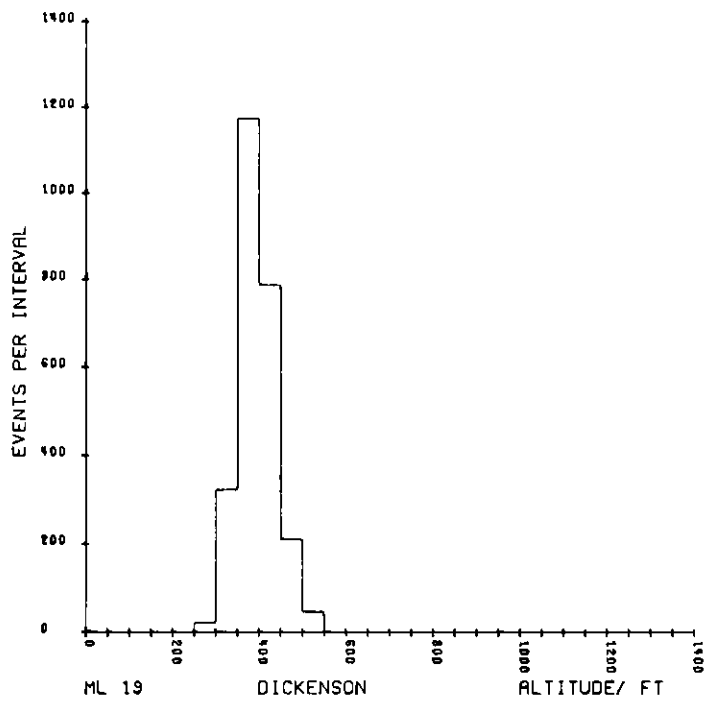
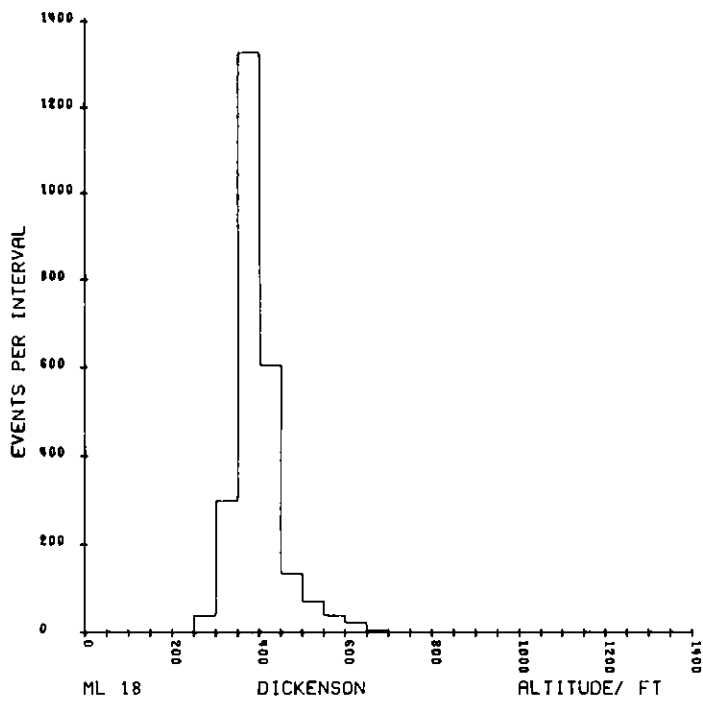
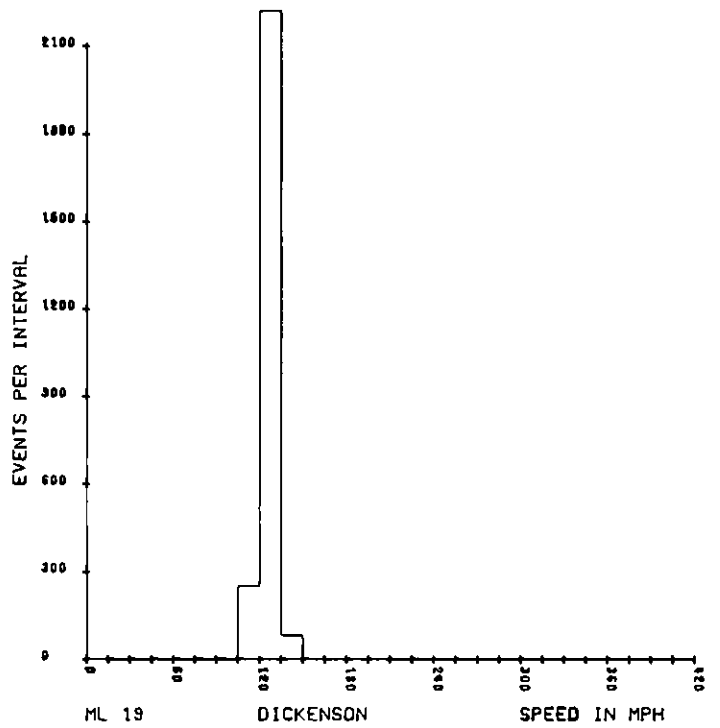
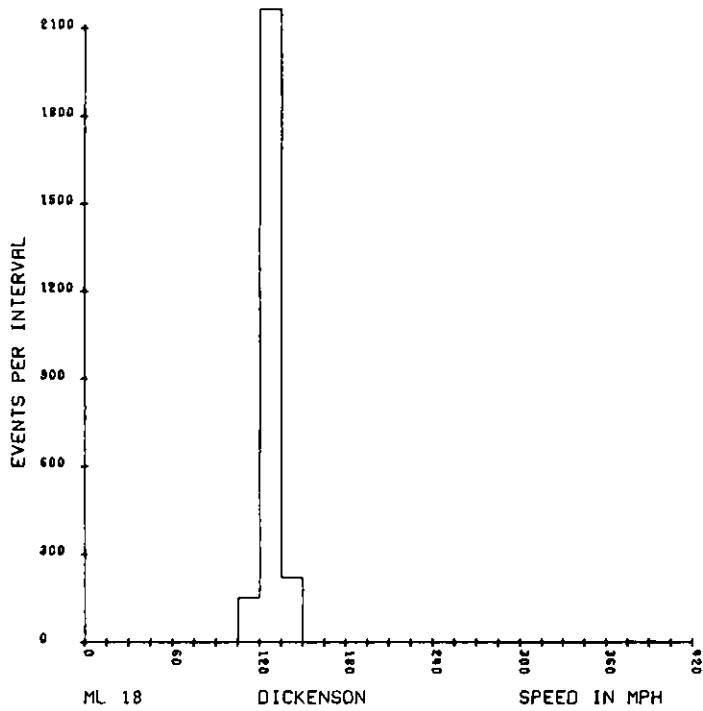


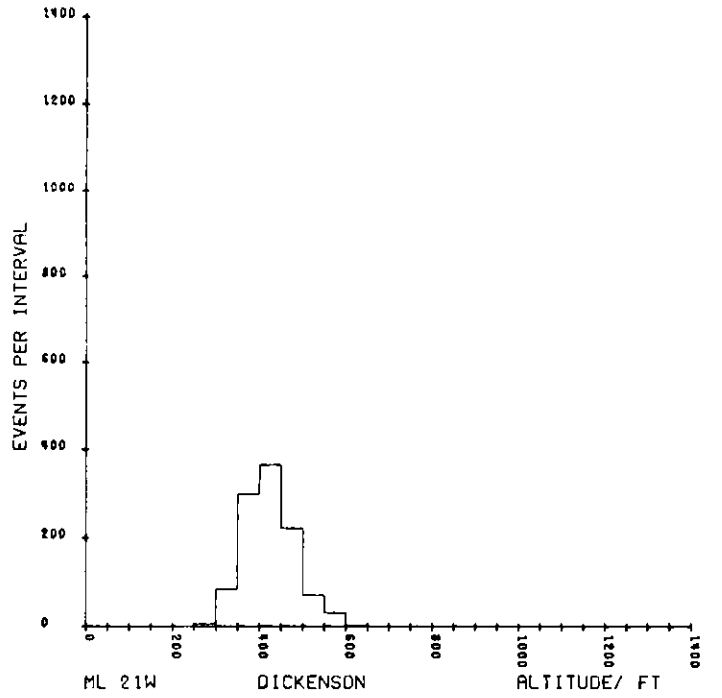
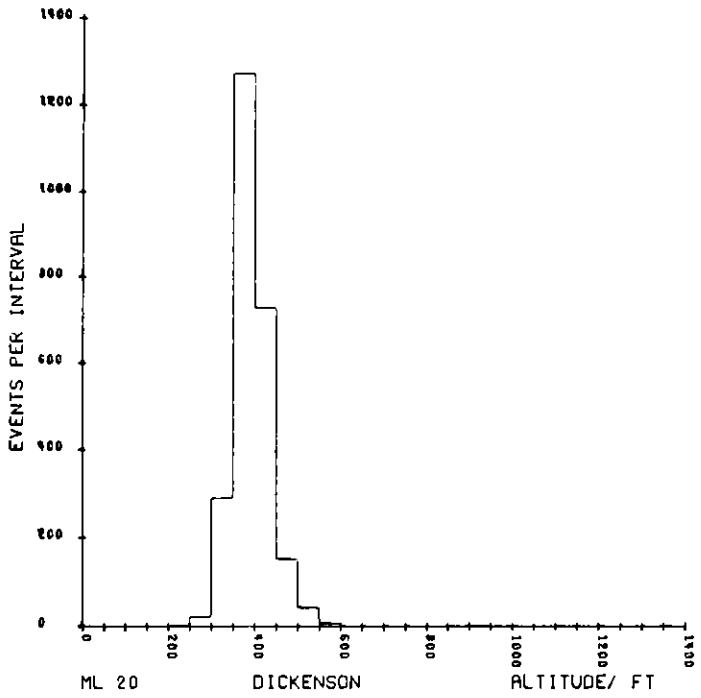
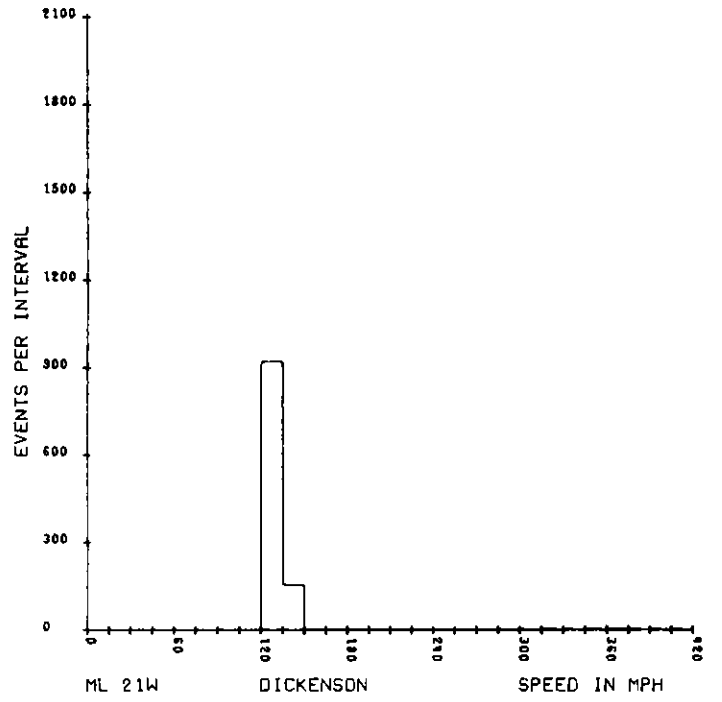
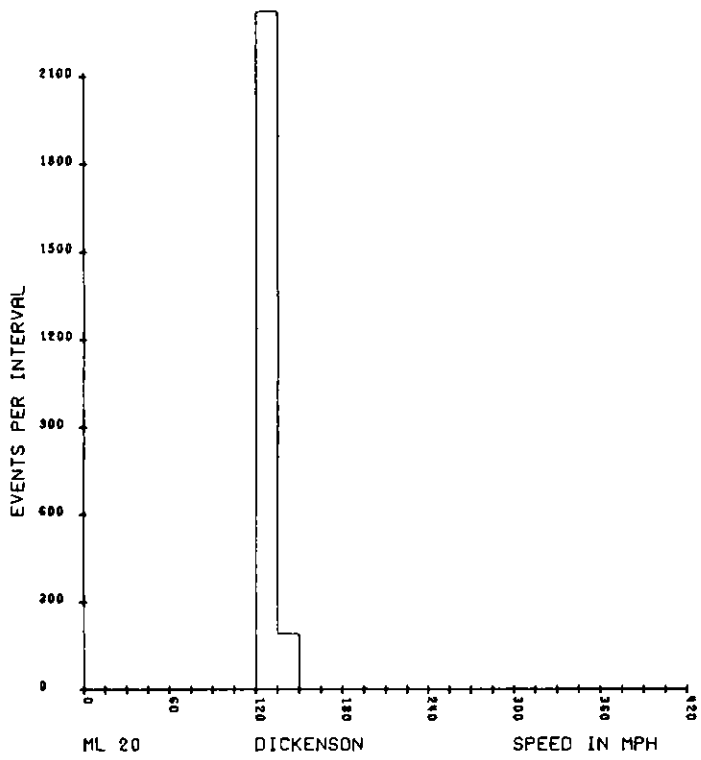


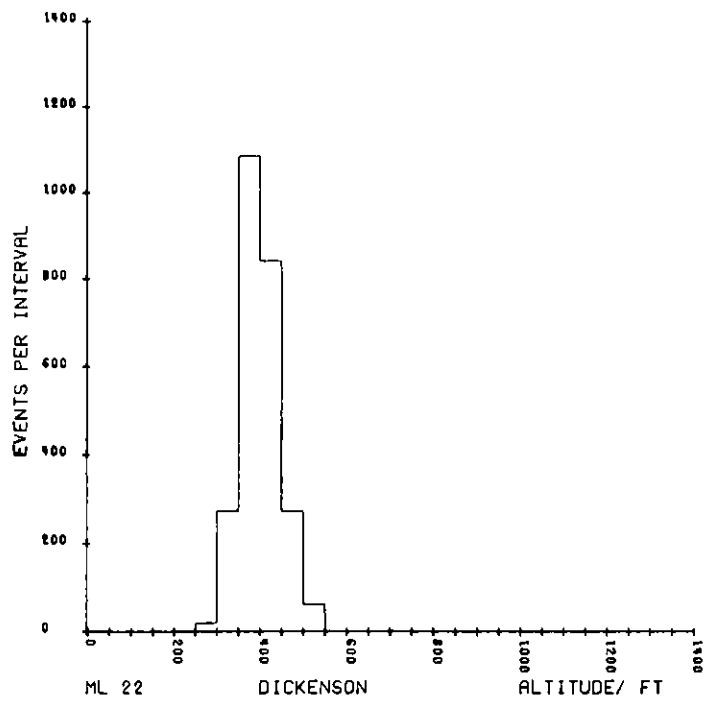
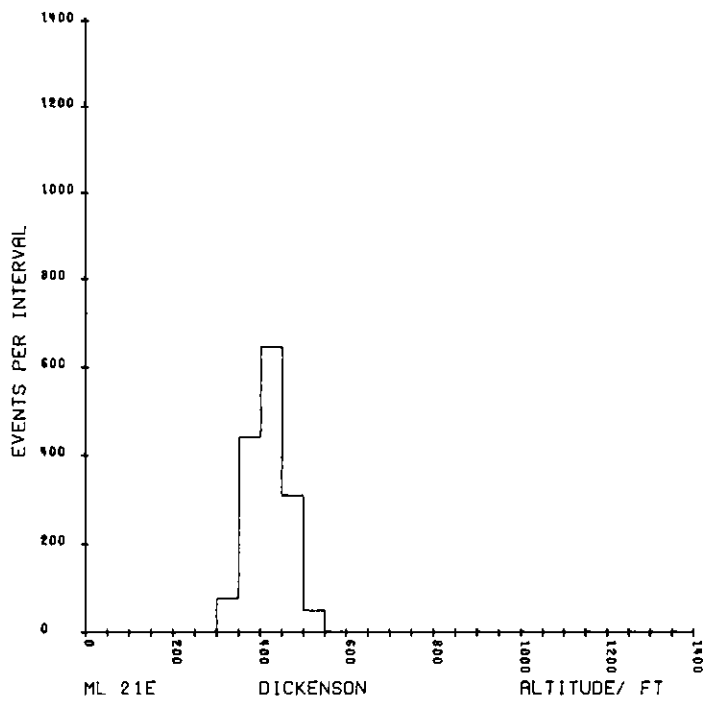
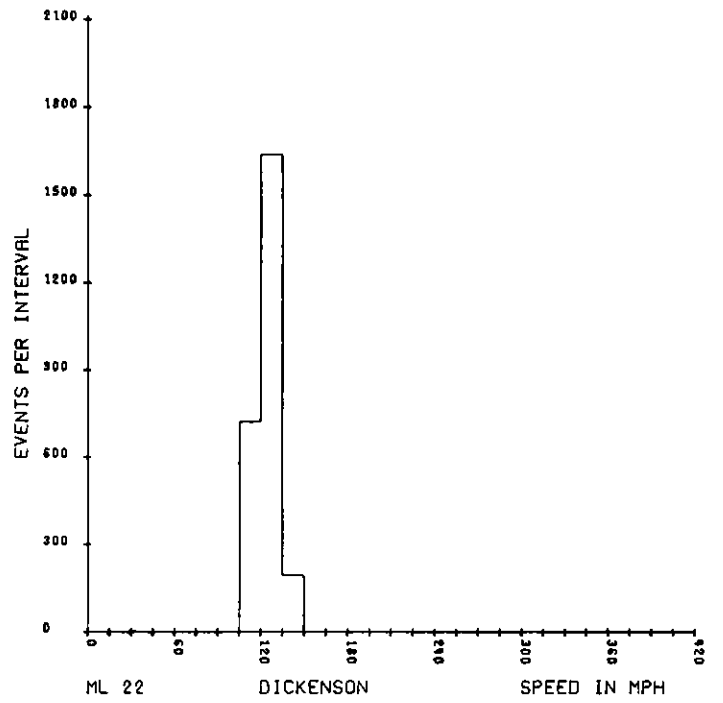
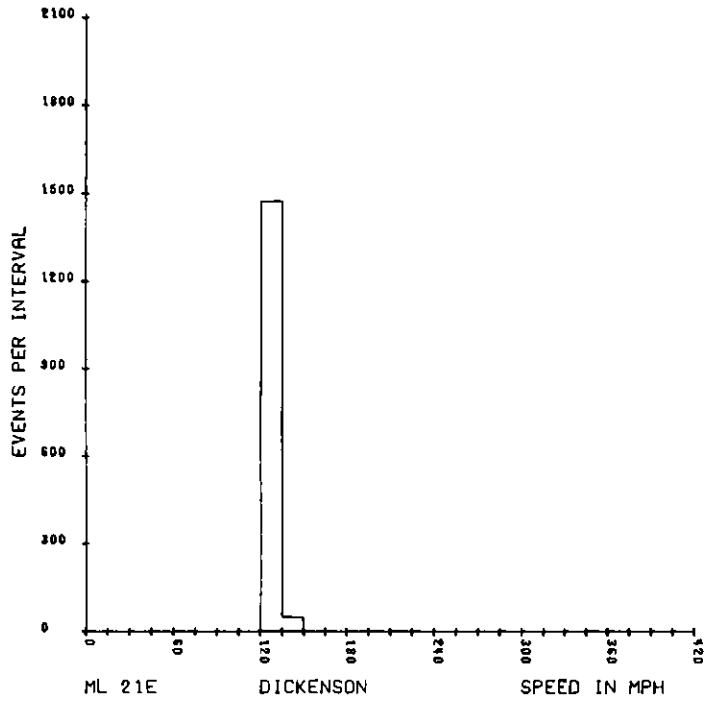


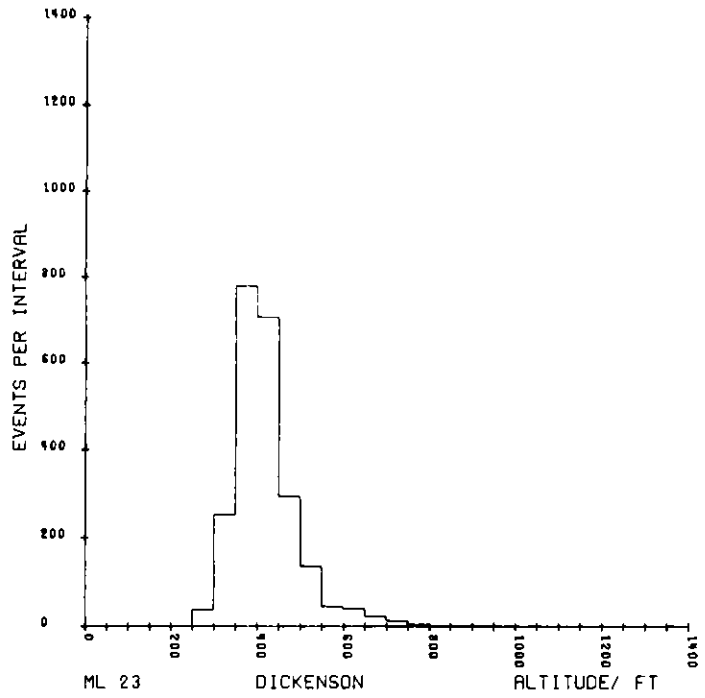
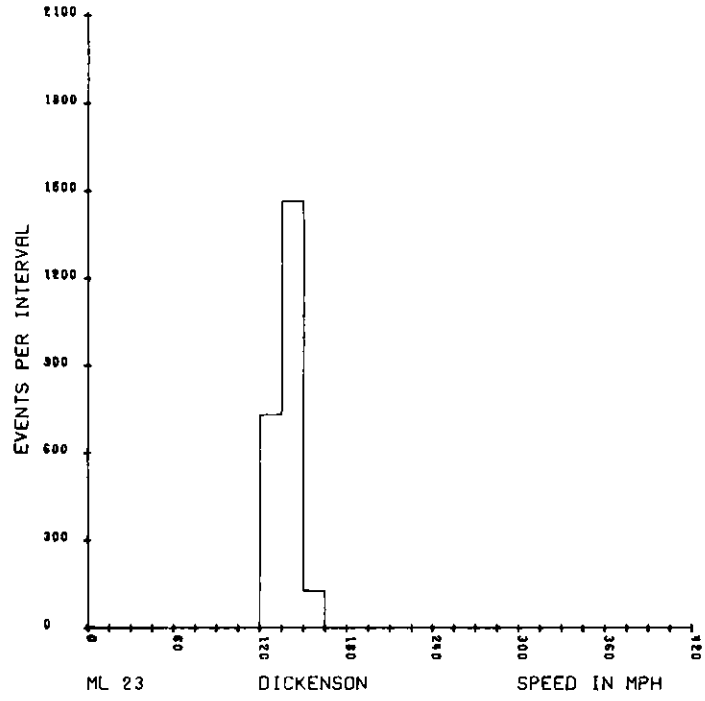


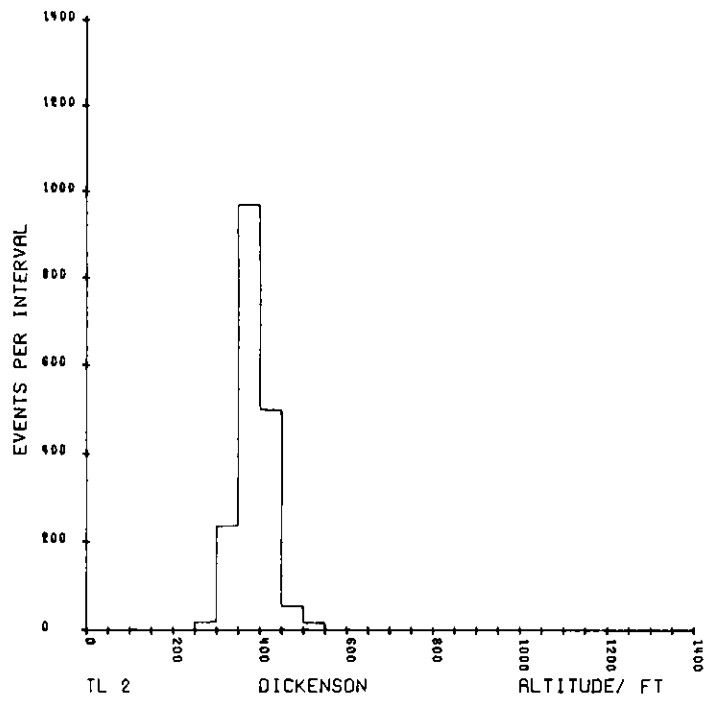
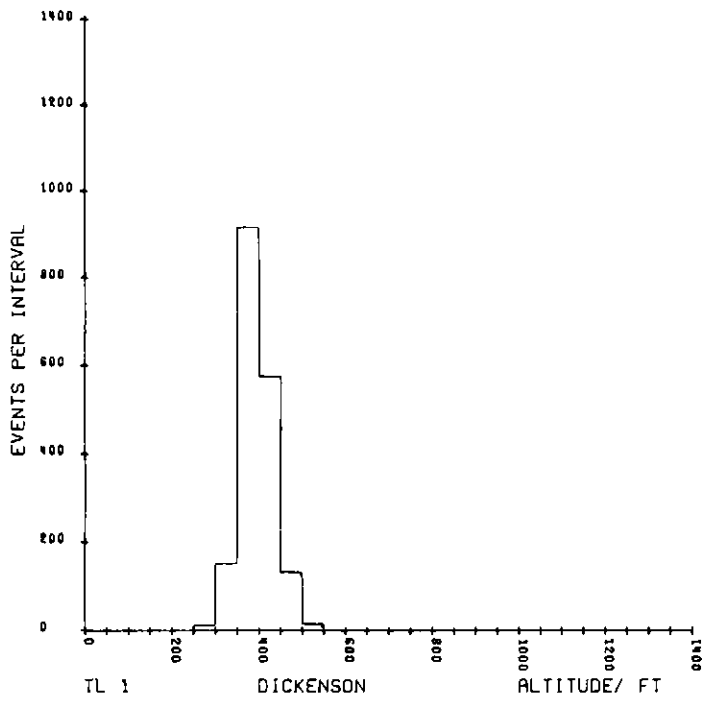
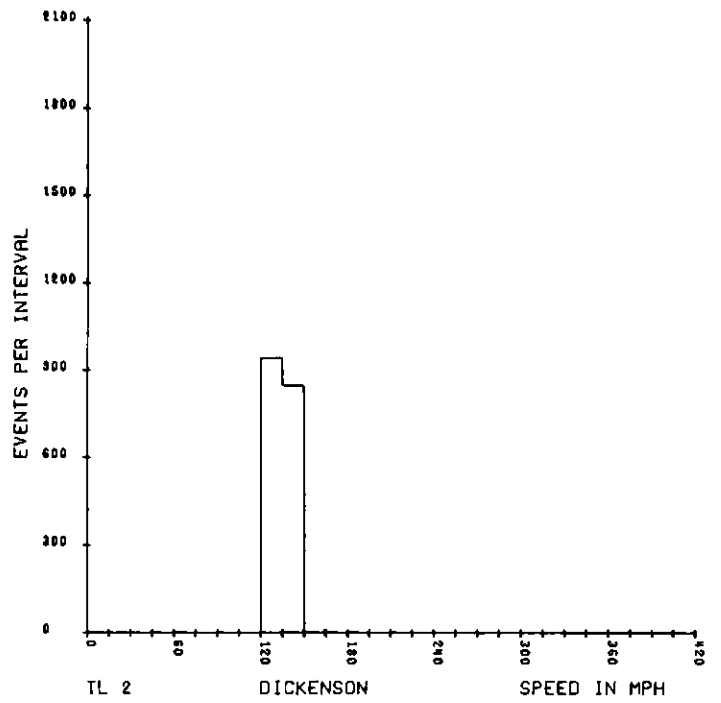
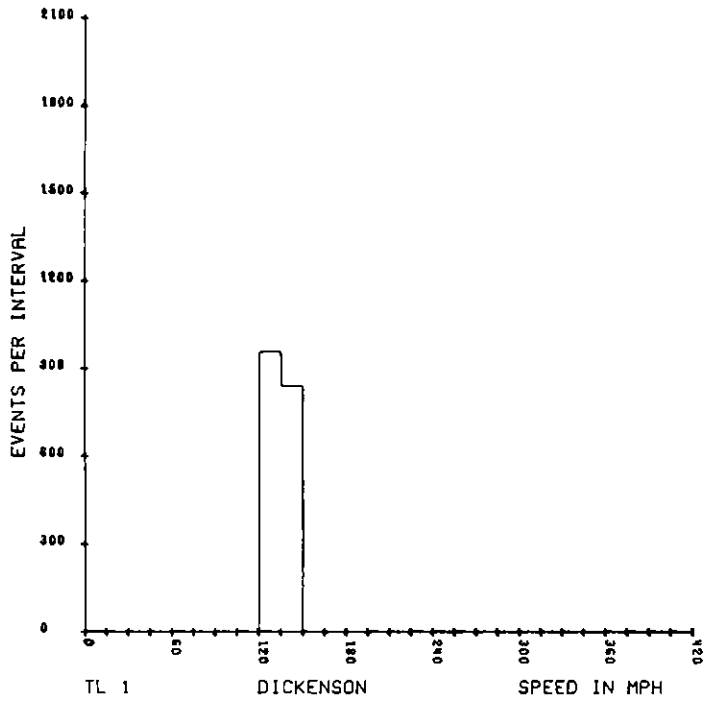


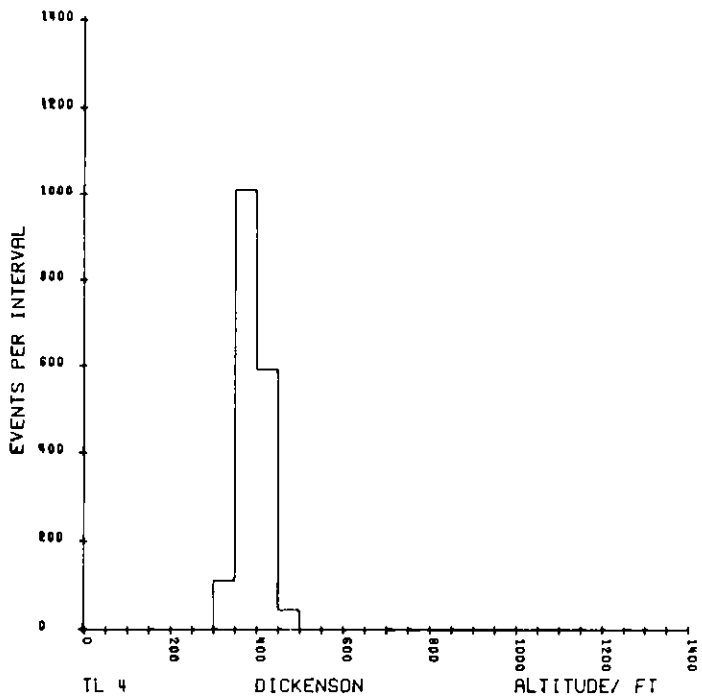
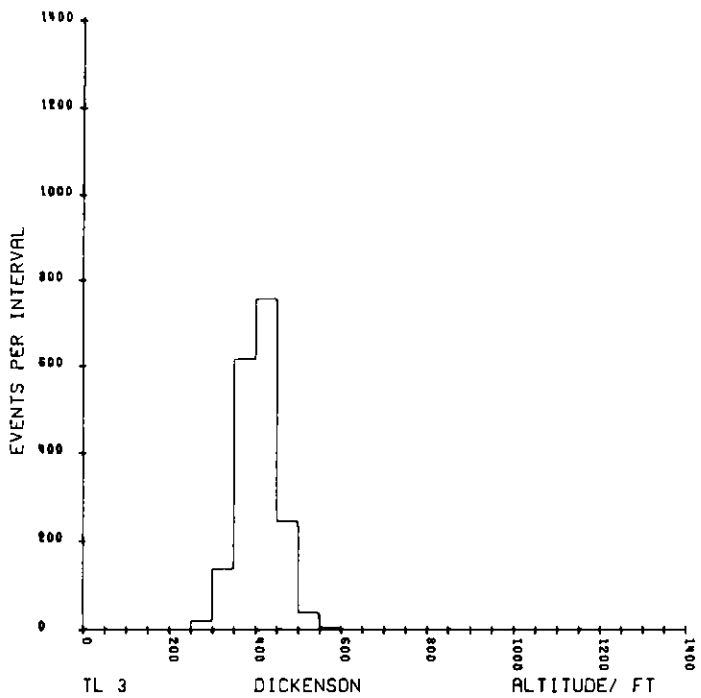
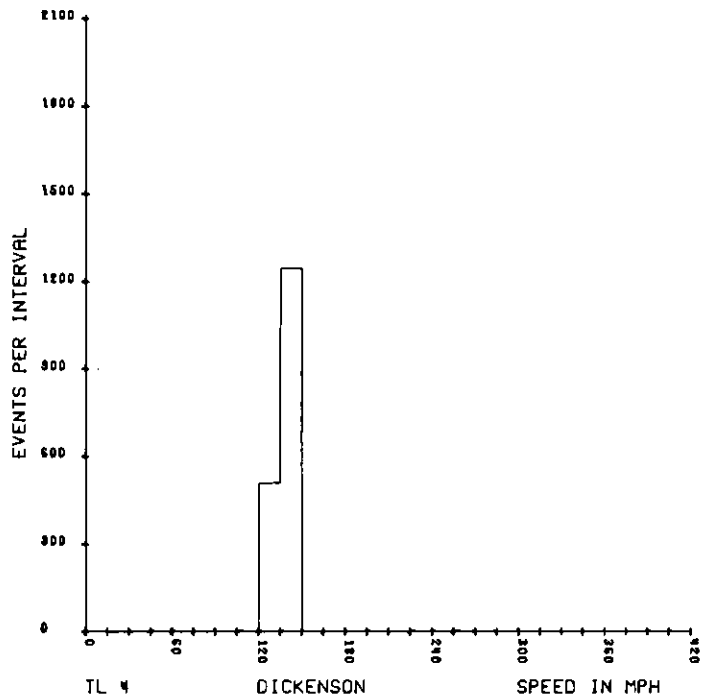
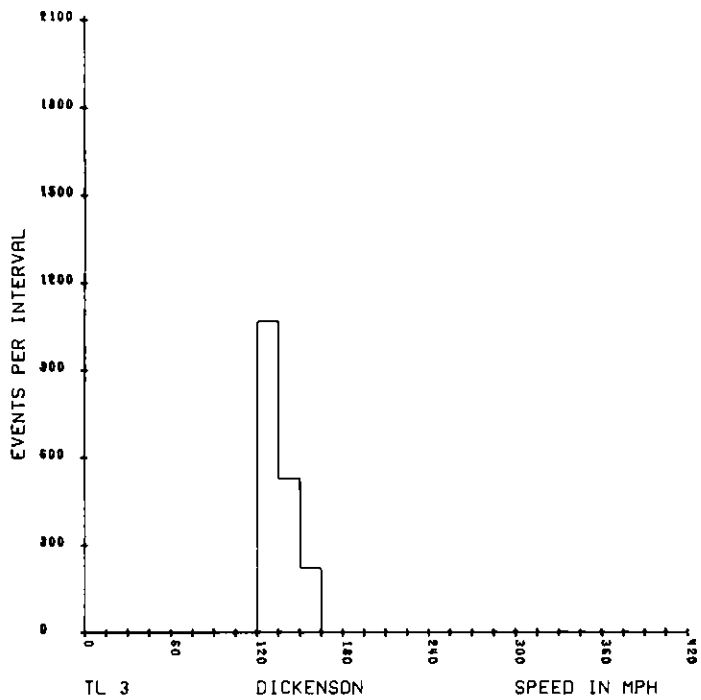


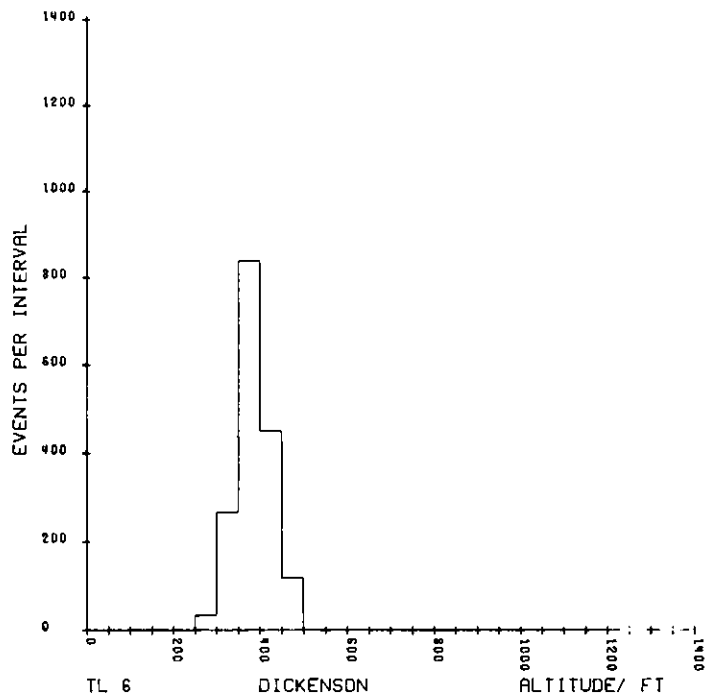
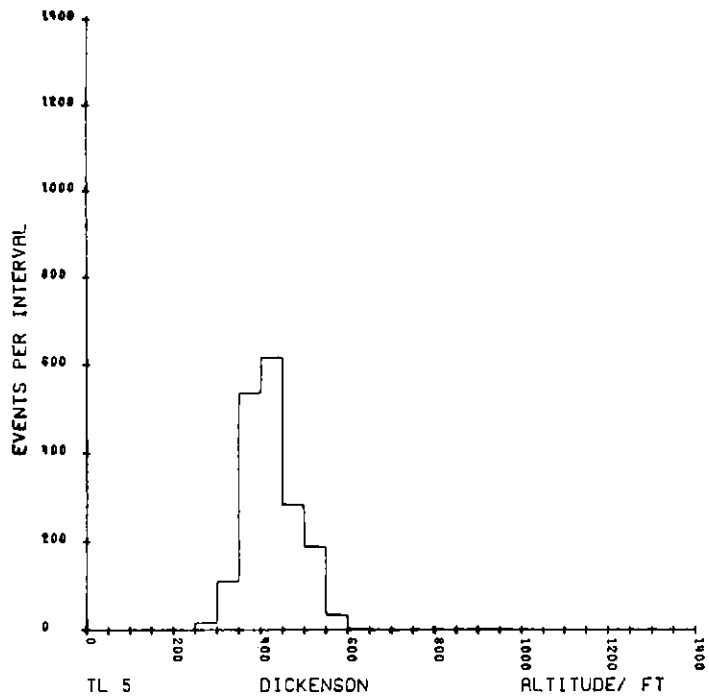
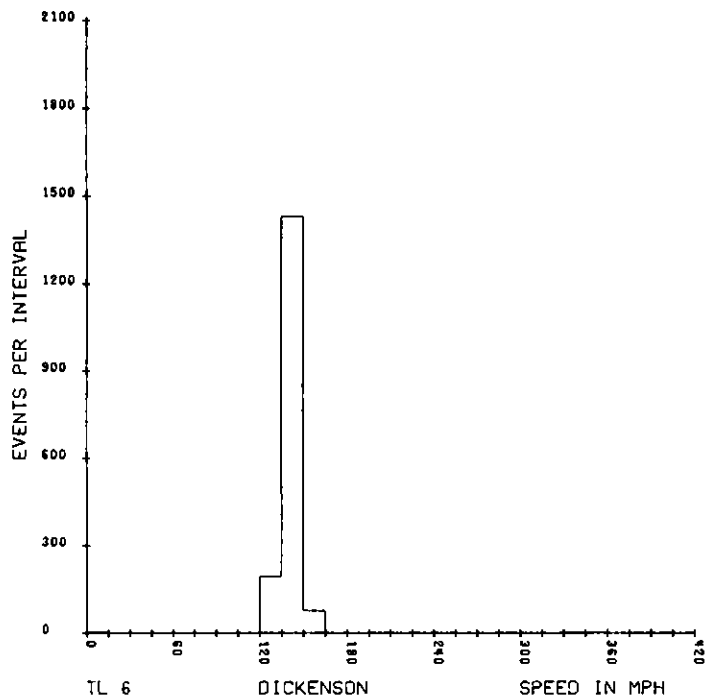
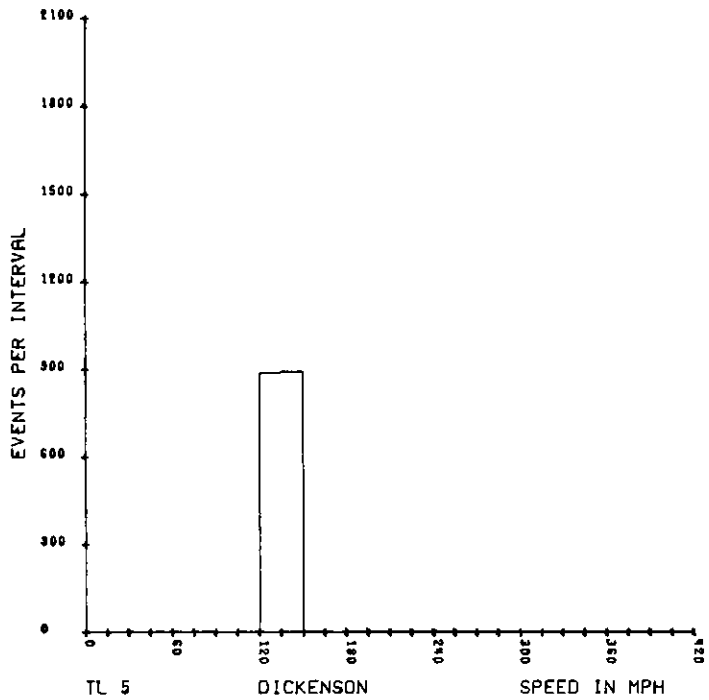












## REFERENCES

- Baker, C. L. (1952) Geology of Harding County. South Dakota Geol. Survey Rept. Inv. no. 68.
- Bauer, C. M. (1924) The Ekalaka lignite field, southeastern Montana. U. S. Geol. Survey Bull. 751-F, pp. 231-267.
- Collier, A. J. (1918) The Nesson anticline, Williams County, North Dakota. U. S. Geol. Sur. Bull. 691 G, pp. 211-217.
- Denson, N. M. (1959) Introduction to uranium in coal in the western United States. U. S. G. S. Bull. 1055-A, pp. 1-10.
- Denson, N. M. and Gill, J. R. (1955) Uranium-bearing lignite and its relation to volcanic tuffs in eastern Montana and North and South Dakota, U. S. G. S. Prof. Paper 300, pp. 413-418.
- Denson, N. M., Bachman, G. O., and Zeller, H. D. (1959) Uranium-bearing lignite in northwestern South Dakota and adjacent states. U. S. G. S. Bull. 1055-B, pp. 11-57.
- Fenneman, N. M. (1946) Map of physical divisions of the United States. U. S. Geol. Sur.
- Gill, J. R. (1962) Tertiary landslides, northwestern South Dakota and southeastern Montana. G. S. A. B., vol. 73, pp. 725-736.
- Hansen, M. (1954) Structural interpretations in southwestern North Dakota. North Dakota Geological Society Guidebook June 1954, pp. 16-17.
- Hares, C. J. (1928) Geology and lignite resources of the Marmarth Field, southwestern North Dakota. U. S. Geol. Sur. Bull. 775.
- King, J. W., and Young, H. B. (1955) High-grade uraniferous lignites in Harding County, South Dakota. U. S. G. S. Prof. Paper 300, pp. 419-430.
- Moore, G. W., Melin, R. E., and Kepferle, R. C. (1959) Uranium-bearing lignite in southwestern North Dakota. Geol. Sur. Bull. 1055-E, pp. 147-179.
- The Tertiary Committee of North Dakota Geological Society (1954) Description of the Tertiary Formations. North Dakota Geol. Soc. Guidebook, June 1954, pp. 9-13.
- Trimble, Donald E. (1979) Unstable ground in western North Dakota. Geological Survey Circular 798, pp. 1-19.
- Winchester, D. E., Hares, C. J., Lloyd, E. R., and Parks, E. M. (1916) The lignite field of northwestern South Dakota. U. S. Geol. Survey Bull. 627
- Zeller, H. D. and Schopf, J. M. (1959) Core drilling for uranium-bearing lignite in Harding and Perkins counties, South Dakota and Rowman county North Dakota. Geol. Sur. Bull. 1055-C, pp. 59-95.





